

STATUS OF THESIS

Title of thesis

NON-INVASIVE IMAGE DENOISING AND CONTRAST
ENHANCEMENT TECHNIQUES FOR RETINAL FUNDUS
IMAGES

I TOUFIQUE AHMED SOOMRO

hereby allow my thesis to be placed at the Information Resource Center (IRC) of Universiti Teknologi PETRONAS (UTP) with the following conditions:

1. The thesis becomes the property of UTP
2. The IRC of UTP may make copies of the thesis for academic purposes only.
3. This thesis is classified as

Confidential

Non-confidential

If this thesis is confidential, please state the reason:

The contents of the thesis will remain confidential for _____ years.

Remarks on disclosure:

Endorsed by

Signature of Author

Signature of Supervisor

Permanent address: HOUSE NO. 10
SOOMRA STREET VILLAGE RUK
DISTRICT SHIKARPUR SINDH
PAKISTAN

Name of Supervisor
Prof. Ir. Dr. Ahmad Fadzil M. Hani

Date : _____

Date : _____

UNIVERSITI TEKNOLOGI PETRONAS

NON-INVASIVE IMAGE DENOISING AND CONTRAST ENHANCEMENT
TECHNIQUES FOR RETINAL FUNDUS IMAGES

by

TOUFIQUE AHMED SOOMRO

The undersigned certify that they have read, and recommend to the Postgraduate Studies Programme for acceptance this thesis for the fulfillment of the requirements for the degree stated.

Signature:

Main Supervisor:

Prof. Ir. Dr. Ahmad Fadzil M. Hani

Signature:

Co-Supervisor:

Assoc.Prof . Dr. Ibrahima Faye

Signature:

Head of Department:

Assoc.Prof. Dr. Rosdiazli B Ibrahim

Date:

NON-INVASIVE IMAGE DENOISING AND CONTRAST ENHANCEMENT
TECHNIQUES FOR RETINAL FUNDUS IMAGES

by

TOUFIQUE AHMED SOOMRO

A Thesis

Submitted to the Postgraduate Studies Programme

as a Requirement for the Degree of

MASTER OF SCIENCE

ELECTRICAL AND ELECTRONIC ENGINEERING DEPARTMENT

UNIVERSITI TEKNOLOGI PETRONAS

BANDAR SERI ISKANDAR,

PERAK

JUNE 2014

DECLARATION OF THESIS

Title of thesis

NON-INVASIVE IMAGE DENOISING AND CONTRAST
ENHANCEMENT TECHNIQUES FOR RETINAL FUNDUS
IMAGES

I TOUFIQUE AHMED SOOMRO

hereby declare that the thesis is based on my original work except for quotations and citations which have been duly acknowledged. I also declare that it has not been previously or concurrently submitted for any other degree at UTP or other institutions.

Witnessed by

Signature of Author

Signature of Supervisor

Permanent address: HOUSE NO. 10
SOOMRA STREET VILLAGE RUK
DISTRICT SHIKARPUR SINDH
PAKISTAN.

Name of Supervisor
Prof. Ir. Dr. Ahmad Fadzil M. Hani

Date : _____

Date : _____

DEDICATION

This thesis is dedicated to my father Dr. Ghulam Akbar Ali.G.Soomro , who taught me that the best kind of knowledge to have is that which is learned for its own sake. It is also dedicated to my mother Hameeda Khatoon Soomro, who taught me that even the largest task can be accomplished if it is done one step at a time. I also dedicated this thesis to my sisters and adorable brother who have always encouraged me. Last but not least I dedicate this work and give special thanks to my supervisor Prof. Ir .Dr. Ahmad Fadzil M Hani for his kind supervision and guidance to accomplish this research work.

ACKNOWLEDGEMENTS

First and foremost, I would like to thank Allah, the one and only almighty God, the source and hope for everything in my life.

I would particularly like to thank my respectable and honorable supervisor, Prof. Ir.Dr. Ahmad Fadzil M. Hani, for his guidance in every step of my research works and his support and encouragement during my study. I have gained a great deal by learning from his greater experience. I would like to thank my co-supervisor AP.Dr.Ibrahima Faye for his guidance and encouragement during my study.

I would also like to express sincere gratitude to AP Dr. Nidal kamel, Miss Norashikin Yahya, AP Dr. Aamir Saeed Malik for their knowledge guidance and help during my research study.

I would also like to thank those with whom I have worked and discussed during the course of my study. Special thanks to Hermawan Nugroho , Essa Prakasa, Nauhman ul Haq, Dileep kumar for general sharing their time throughout this research. To my dearest friend in the intelligent signals and imaging lab,Aamir Shahzad, Syed Ayaz Ali Shah, Junaid Ahmed , Javid khan , Rishu Gupta and Vedpal Singh and others who have passed throughout this lab and neurosignal labmates, thanks for your kind friendship.

The financial support from Universiti Teknologi PETRONAS are always gratefully acknowledged.

Last but not least, I would like to thank my family members, my parents, Father Dr. Ghulam Akber Ali .G . Soomro and mother Hameeda Khatoon Soomro, my lovely brother Engr. Shafique Ahmed Soomro and adorables sisters for their prayers,their love ,their understanding ,their patience and their endless encouragement.

ABSTRACT

The analysis of retinal vasculature in digital fundus images is important for diagnosing eye related diseases. However, digital colour fundus images suffer from low and varied contrast, and are also affected by noise, requiring the use of fundus angiogram modality. The Fundus Fluorescein Angiogram (FFA) modality gives 5 to 6 times higher contrast. However, FFA is an invasive method that requires contrast agents to be injected and this can lead to other physiological problems. A reported digital image enhancement technique named RETICA that combines Retinex and ICA (Independent Component Analysis) techniques, reduces varied contrast, and enhances the low contrast blood vessels of model fundus images.

In this thesis the performance of RETICA has been investigated using real fundus images for two databases. The first database is the 35-Fundus database that contains 35 colour fundus images with their corresponding Fundus Fluorescein Angiogram (FFA) images. RETICA is found to give a better Contrast Improvement Factor (CIF) of 5.46 as compared to CIF of 5.12 for FFA images. The second database is the Fundus Image for Non-invasive Diabetic Retinopathy System (FINDeRS) database that contains 175 colour fundus images of various Diabetic Retinopathy (DR) stages. The cause for the lower CIF performance for RETICA in the case of FINDeRS database is due to lower Peak Signal-To-Noise Ratio (PSNR) of the images. Noise seems to be affecting the performance of RETICA. However, before attempting to improve PSNR by reducing noise in fundus images, it is necessary to identify the nature of noise in the images.

The identification of the noise in the fundus image (model fundus image or real fundus image) has been the focus in this research. The approach used to identify noise is based on 3 adaptive Wiener filters (additive, multiplicative, and additive plus multiplicative filters) and determining the highest PSNR improvement among three an

adaptive wiener filters. It is observed that fundus image contained additive and multiplicative noise and this is because of the image acquisition in Fundus camera. Various denoising methods are used to improve the Signal to Noise Ratio (SNR) of the fundus images before further image enhancement. Based on the performance of several techniques for denoising fundus images, it was found that the Time Domain Constraint Estimator (TDCE) gave a better performance in the PSNR improvement of retinal fundus images around 3dB.

The noise in fundus images of the FINDeRS database is reduced by applying the TDCE. The PSNR of the FINDeRS images (green band) are first improved by around 3dB using TDCE and after applying RETICA, higher contrast improvement factors have been achieved averaging around 5.56 compared to 5.46 for the normal fundus images and 5.12 for FFA images of 35-Fundus dataset. TDCE along with RETICA has a fair potential to reduce the need for FFA method in eye related disease assessment.

ABSTRAK

Analisis vaskular retina dari imej digital fundus adalah penting untuk mengdiagnosis penyakit yang berkaitan mata. Namun, imej warna fundus digital yang diambil mempunyai nilai kontras yang rendah dan berbeza, ditambah dengan kehadiran hingar, ia memerlukan penggunaan fundus angiogram sebagai modaliti. Fundus fluorescein angiogram (FFA) adalah modaliti yang meningkatkan nilai kontras pada vaskular retina kepada 5 hingga 6 kali ganda. Namun, FFA adalah teknik invasif (suntikan perwarna kontra) yang boleh memberi kesan kepada masalah fisiologi. Terdapat satu teknik untuk peningkatan imej secara digital yang dinamakan sebagai RETICA iaitu kombinasi daripada teknik Retinex dan ICA dimana ia mengurangkan nilai kontras yang tidak tetap dan meningkatkan nilai kontras yang rendah pada imej fundus pembuluh darah. RETICA telah diuji menggunakan imej fundus yang sebenar.

Dua pangkalan data dianalisis menggunakan teknik RETICA. Pangkalan data pertama 35-Fundus, mempunyai 35 imej warna fundus berserta imej FFA yang sepadan setiap satu. Faktor peningkatan kontra diukur dan RETICA memberi faktor peningkatan kontra (CIF) yang lebih baik iaitu 5.46 berbanding CIF imej FFA iaitu 5.12. Pangkalan data kedua adalah himpunan data Fundus Image for Non-invasive Diabetic Retinopathy System (FINDeRS) yang terdiri daripada 175 imej warna fundus dari pelbagai peringkat retinopati diabetik (DR). Faktor penurunan prestasi CIF untuk pangkalan data FINDeRS diselidiki. CIF yang rendah pada pangkalan data FINDeRS menggunakan teknik RETICA adalah disebabkan oleh nisbah signal ke hingar (SNR) imej tersebut adalah rendah. Hingar telah memberi kesan kepada prestasi RETICA. Namun, sebelum mencuba meningkatkan nilai puncak SNR (PSNR) dengan mengurangkan hingar pada imej retina fundus, adalah perlu untuk mengenalpasti sifat hingar dalam imej-imej tersebut.

Pengenalan hingar dalam imej fundus (model imej fundus atau imej fundus yang sebenar) adalah fokus dalam kajian ini. Pendekatan yang digunakan untuk mengenal pasti bunyi adalah berdasarkan pada tiga adaptive wiener filters (penapis penambahan, pendaraban, dan penambahan & pendaraban) dan menentukan peningkatan PSNR yang tertinggi di antara tiga adaptive wiener filters tersebut. Daripada kajian yang dibuat, didapati imej fundus retina mempunyai hingar penambahan dan pendaraban. Hingar penambahan dan pendaraban dijumpai di spektrum hijau pada imej kerana modaliti imej (kamera fundus). Pelbagai kaedah membuang hingar digunakan untuk meningkatkan SNR dalam imej fundus retina sebelum peningkatan kualiti imej dilakukan. Berdasarkan prestasi teknik membuang hingar imej fundus, didapati bahawa Time Domain Constraint Estimator (TDCE) menunjukkan prestasi yang bagus dalam meningkatkan PSNR pada imej fundus retina.

Hingar pada imej fundus daripada pangkalan data FINDeRS dikurangkan dengan menggunakan TDCE. Teknik ini digunakan untuk membuang hingar pada imej fundus retina. TDCE adalah teknik linear sub-space yang berfungsi keatas isyarat condong dan membuang hingar pada imej. PSNR pada imej FINDeRS (spektrum hijau) akan ditingkatkan sebanyak 3dB dengan menggunakan TDCE dan setelah mengaplikasikan RETICA, faktor peningkatan kontras yang tinggi telah dicapai dengan purata sebanyak 5.56 berbanding 5.46 pada imej fundus yang biasa dan sebanyak 5.12 pada set data 35-Fundus. TDCE bersama-sama dengan Retina mempunyai potensi yang adil Mengurangkan keperluan untuk kaedah FFA dalam penyakit berkaitan penilaian mata.

In compliance with the terms of the Copyright Act 1987 and the IP Policy of the university, the copyright of this thesis has been reassigned by the author to the legal entity of the university,

Institute of Technology PETRONAS Sdn Bhd.

Due acknowledgement shall always be made of the use of any material contained in, or derived from, this thesis.

© Toufique Ahmed Soomro, 2014

Institute of Technology PETRONAS Sdn Bhd

All rights reserved.

TABLE OF CONTENT

ABSTRACT.....	vii
ABSTRAK.....	ix
LIST OF FIGURES	xv
LIST OF TABLES	xviii
CHAPTER 1 INTRODUCTION	1
1.1 Background Study	1
1.2 Medical Imaging Modalities.....	3
1.2.1 Ionizing Radiation Imaging Modalities.....	3
1.2.2 Non-Ionizing Radiation Imaging Modalities	4
1.3 Problems in Medical Images	4
1.4 Problems in Retinal Fundus Images	6
1.4.1 Low Contrast in Retinal Colour Fundus Images	6
1.4.2 Varied Contrast Problem in Retinal Fundus Images	10
1.4.3 Noise in Retinal Fundus Images.....	11
1.5 Medical Image Enhancement Techniques for Retinal Fundus Images	12
1.5.1 Invasive Image Enhancement Techniques	16
1.5.2 Non-Invasive Image Enhancement Techniques	16
1.6 Problem Statement and Formulation	17
1.7 Research Objectives.....	19
1.8 Contribution.....	19
1.9 Scope of Work	20
1.10 An Overview of Thesis Structure	20
CHAPTER 2 LITERATURE REVIEW	22
2.1 Introduction to Diabetic Retinopathy	22
2.2 Anatomy of Fundus image of Normal Retina	23
2.3 Abnormalities in Fundus Images	24
2.3.1 Microaneurysms	25
2.3.2 Blot and Dot Haemorrhages	26
2.3.3 Hard and Soft (Cotton wool spot) Exudates.....	26
2.3.4 Foveal Avascular Zone (FAZ)	27

2.4 Severity Level of Diabetic Retinopathy	28
2.5 Computerised Analysis for the Detection of Diabetic Retinopathy	30
2.5.1 Microaneurysm and Haemorrhage Detection	30
2.5.2 Hard and Soft Exudate Detection.....	33
2.5.3 Analysis of FAZ for Grading of Diabetic Retinopathy.....	35
2.6 Image Enhancement Techniques for Varied and Low Contrast Images	36
2.6.1 Image Normalisation for Varied Contrast Medical Images	37
2.6.2 Image Enhancement for low contrast Medical Images	38
2.6.3 Image Normalisation and Enhancement Technique.....	39
2.6.3.1 Retinex for contrast Normalisation.....	40
2.6.3.2 Independent Component Analysis for Contrast Enhancement	47
2.7 Noise in the Medical Images	48
2.7.1 Image Noise Models.....	49
2.7.2 Noise in Retinal Fundus Image	53
2.7.3 Image Denoising Methods	54
2.7.3.1 Singular Value Decomposition (SVD)	59
2.7.3.2 Signal and Noise Model.....	67
2.7.3.3 Time-Domain Constrained (TDC) Estimator	69
2.8 Summary.....	73
CHAPTER 3 METHODOLOGY	78
3.1 Analysis of Fundus Images.....	78
3.2 Problem Formulation	80
3.3 Design of Experimental Work	81
3.3.1 Implementation of RETICA on a Real Fundus Image	81
3.3.2 Measurement of the Contrast and the Contrast Improvement Factor of Fundus Images.....	83
3.3.3 Measurement of the Signal to Noise Ratio of the Fundus Images	85
3.3.4 Measurement of the Signal Energy of the Fundus Image	86
3.3.5 Noise Identification in the Fundus Image	86
3.3.5.1 Study 1	88
3.3.5.2 Study 2	89
3.3.5.3 Study 3	90

3.4 Denoising Methods for Retinal Fundus Images	91
3.5 Improving the SNR of the Fundus Image.....	91
3.6 Summary.....	96
CHAPTER 4 RESULTS AND DISCUSSION.....	98
4.1 Performance Analysis of RETICA Method on Real Fundus Images	98
4.2 Results and Analysis of Identification of Noise Approach	106
4.2.1 Study 1.....	106
4.2.2 Study 2.....	109
4.2.3 Study 3.....	112
4.3 Results and Analysis of Denoising Methods for Fundus Image	115
4.4 Results and Analysis of Improving the SNR of the Fundus Image.....	121
4.4.1 Comparison of the Improved RETICA with other Algorithms.....	127
4.5 Summary.....	128
CHAPTER 5 CONCLUSION AND FUTURE WORK	131
5.1 Conclusion	131
5.2 Suggestion for Future Works.....	133
REFERENCES	135
APPENDIX A 35-FUNDUS DATABASE	145
APPENDIX B ANALYSIS OF FINDERS DATABASE	152
APPENDIX C LISTS OF PUBLICATIONS AND EXHIBITIONS	154
APPENDIX D 35-FUNDUS IMAGE AND FINDERS DATABASE.....	156

LIST OF FIGURES

Figure 1.1 Incidence of DR in Malaysia [5]	2
Figure 1.2 Examples of Ionizing Radiation Imaging Modalities.....	3
Figure 1.3 Examples of Non- Ionizing Radiation Imaging Modalities	4
Figure 1.4 Examples of Medical Images Problem of Contrast Obtained From Different Medical Imaging Device	5
Figure 1.5 Example of Low contrast Images	7
Figure 1.6 Illustration of Low contrast in Retinal colour fundus Images.....	8
Figure 1.7 Example of varied contrast in Fundus Images	9
Figure 1.8 Example of varied contrast in Fundus Images	10
Figure 1.9 Illustration of noise in Fundus Images	11
Figure 1.10 Principle of indirect ophthalmoscopy [4]	13
Figure 1.11 Principle of Fundus Camera [2]	13
Figure 1.12 Fundus illumination and imaging path from optic fundus camera.....	14
Figure 1.13 Colour Fundus Image vs FFA Image	15
Figure 2.1 FFA and Digital Colour Fundus Image	24
Figure 2.2 MAs in Colour Fundus image and FFA image	25
Figure 2.3 Haemorrhages in colour Fundus Image.....	26
Figure 2.4 Hard and Soft Exudates in Retinal Fundus Images	27
Figure 2.5 FAZ in Colour Fundus Image and FFA Image	27
Figure 2.6 Retinal Fundus Image [1]	28
Figure 2.7 Retinal Images Contained Pathologies.....	29
Figure 2.8 RETICA – Image enhancement for varied and low contrast fundus images	40
Figure 2.9 Image Formation Model	41
Figure 2.10 Image Pyramid.....	43
Figure 2.11 Ratio-Product-Reset-Average Operations	44
Figure 2.12 McCann99 Retinex Algorithm	46
Figure 2.13 Linear ICA model.....	47
Figure 2.14 Noise in the Medical Images	49

Figure 2.15 Model of Image degradation and Restoration process [3].....	50
Figure 2.16 Illustration of Salt and Pepper Noise in Image.....	51
Figure 2.17 Illustration of Gaussian noise	52
Figure 2.18 Illustration of Speckle noise	53
Figure 2.19 Noise in the Retinal Fundus Images	53
Figure 2.20 Time-Frequency Representation of Fourier Transform	55
Figure 2.21 STFT Representation.....	56
Figure 2.22 Time-Frequency Representation of Wavelet Transform.....	56
Figure 2.23 TDCE on Signal [6].....	72
Figure 2.24 TDCE on Standard Test Images	73
Figure 3.1 Illustration of noise in Fundus Images	78
Figure 3.2 Illustration of noise varying contrast in Fundus Images	79
Figure 3.3 RETICA Method	82
Figure 3.4 Selection of intensity data points (blood vessel and background) for Green band, FFA and RETICA images.....	84
Figure 3.5 Modelling of Adaptive Wiener Filter.....	87
Figure 3.6 Study 1.....	88
Figure 3.7 Study 2.....	89
Figure 3.8 Study 3.....	90
Figure 3.9 Noise reduction.....	91
Figure 3.10 Implementation of TDCE in MATLAB	92
Figure 3.11 Illustration of TDCE on Retinal Fundus Image	93
Figure 3.12 Proposed Non-Invasive Image Enhancement Techniques (TDCE+RETICA).....	95
Figure 4.1 Comparison of selected FFA and RETICA images	100
Figure 4.2 Contrast Improvement Factor of RETICA and FFA.....	101
Figure 4.3 Contrast Improvement Factor of FINDeRS Database.....	102
Figure 4.4 Contrast Improvement Factor Comparison between Images from FINDeRS and 35-Fundus Databases	102
Figure 4.5 PSNR Comparisons between FINDeRS Database and 35 Fundus Image Database.....	103

Figure 4.6 Average signal energy of fundus images for the two databases (35-Fundus and FINDeRS Database) for various DR stages	104
Figure 4.7 Analysis of Green Band Image and RETICA Image of FINDeRS Database	105
Figure 4.8 Study 1	107
Figure 4.9 Results of Study 1 of Model Fundus Images.....	107
Figure 4.10 Results of Study 1 on Green Band Fundus Image.....	108
Figure 4.11 PSNR Improvement of Proposed Study 1 on FINDeRS Database	108
Figure 4.12 Study 2.....	109
Figure 4.13 Results of proposed Method 2 on Model Fundus Image.....	110
Figure 4.14 Results of Study 2 on Retinex Fundus Image	111
Figure 4.15 PSNR Improvement of Proposed study 2 on FINDeRS Database	111
Figure 4.16 Study 3.....	112
Figure 4.17 Results of proposed study 3 on Model Fundus Image	113
Figure 4.18 Results of study 3 on Retinex Fundus Image	114
Figure 4.19 PSNR Improvement of Proposed Method 3 on FINDeRS Database	114
Figure 4.20 Green bands is denoised by using TDCE.....	115
Figure 4.21 Analysis based on TDCE.....	116
Figure 4.22 Analysis based on Wiener Filter.....	116
Figure 4.23 Analysis based on SWT.....	117
Figure 4.24 PSNR Analysis based on LSE.....	117
Figure 4.25 Analysis based on MVE	118
Figure 4.26 PSNR Improvement of Different Denoising Methods on Green band Fundus Images	119
Figure 4.27 Analysis of Selected Images.....	120
Figure 4.28 Modified RETICA.....	121
Figure 4.29 Comparison of RETICA Image and Modified RETICA.....	122
Figure 4.30 Comparisons between PSNR of Improved FINDeRS Database and PSNR of 35-Fundus Database	124
Figure 4.31 Comparison between CIF of Improved FINDeRS Database and CIF Of 35- Fundus Database.....	125
Figure 4.32 Comparison of Contrast Improvement factor among different methods	127

LIST OF TABLES

Table 2.1 International DR Grading Scale [44]	28
Table 2.2 Performances of Proposed Micro aneurysms	32
Table 2.3 Performances of Proposed Haemorrhages	33
Table 2.4 Performances of Proposed Microaneurysms and Haemorrhages	33
Table 2.5 Reported Performances of Soft Exudates	34
Table 2.6 Performances of Proposed hard Exudates	35
Table 2.7 Varied Contrast Normalisation Techniques	37
Table 2.8 Low Contrast Enhancement Techniques	38
Table 2.9 Comparison among Image denoising methods	58
Table 3.1 Formula of Contrast Improvement Factor	85
Table 4.1 Contrast and CIF of 35–Fundus database	99

CHAPTER 1

INTRODUCTION

1.1 Background Study

Analysis of biomedical images is one of emergent research area that is related to the study and analysis of digital images based on the image processing techniques with computation tools that assist in analysis of clinical problems [7]. In recent years, the progress of research in biomedical images analysis has proven significantly important in order to provide the solution of digital analysis while reducing the use invasive approaches.

Eye related disease such as Diabetic Retinopathy is the impediment of diabetes mellitus which is caused by damage to retinal vasculature and is the leading cause of blindness. It is a silent disease that is only realised by the patient when they have vision problems. However, this occurs when the changes in the retina have progressed to a level where treatment is complicated and there is a greater chance of vision loss [8].

The prevalence of diabetic retinopathy has increased with an increase in life expectancy of diabetics. In world healthcare challenges, the diabetes is one of the major issues [9]. World Health Organization (WHO) forecasted that number of people with diabetics is to increase from 130 million to 350 million over the next 25years [9]. In Malaysian National Eye database 2007, among 10,856 cases with diabetes 36.8% had any form of DR, from which 7.1% comprises of proliferative

diabetic retinopathy [5]. The incidences of diabetic and diabetic retinopathy (DR) are shown in Figure 1.

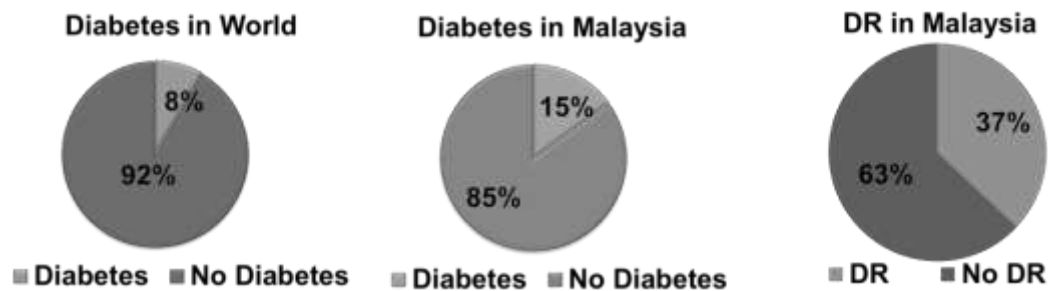


Figure 1.1 Incidence of DR in Malaysia [5]

Diabetic retinopathy generally has two categories, Non-Proliferative Diabetic Retinopathy (PDR) and Proliferative Diabetic Retinopathy (NPDR), characterised by presence of pathologies namely micro aneurysms, dot and blot haemorrhages, cotton wool spots, exudates and changes of veins. NPDR is further classified into Mild, Moderate and Severe NPDR stages. Eye screening is important in detecting of DR. The main purpose of eye screening is to identify patients with sight-threatening DR so that essential treatment could be given for prevention of vision loss [8].

It has been observed that a retinal vasculature feature analysed in DR cases is loss of retinal capillaries in the perifoveal capillary network resulting in the enlargement of the Foveal avascular zone (FAZ). The area of FAZ can be observed in colour fundus image and fundus fluorescein angiograms (FFA). Previous research by Fadzil *et al* [10, 11] on analysis of fundus images found that size of fovea avascular zone increases with severity level of DR

The retinal photography known as FFA is carried out after an arterial injection of fluorescein dye which takes place in a rapid sequence. Three main characteristics are given by the FFA: Firstly, First, the characteristic of how the dye flows through blood vessels to reach the retina and choroid, and its circulation when it gets there. Secondly, fine details of the pigment epithelium and retinal circulation are recorded which might be invisible. Thirdly, the retinal blood vessels are clear in the resulting

image and their functional integrity is assessed [8]. Most of research work on determination of FAZ is evaluated based on the FFA images.

1.2 Medical Imaging Modalities

Medical imaging modalities are the source of medical images. Medical image contain information that can be used to ascertain or grade severity of diseases and monitor diseases during treatments. Medical imaging modalities enable investigations into the anatomical structure, function and pathologies of the human organs. There are two types of the medical image modalities namely, Ionizing radiation (Invasive) imaging and Non-ionizing radiation (Non-Invasive) imaging [12].

1.2.1 Ionizing Radiation Imaging Modalities

Due to the use of radiation in Ionizing radiation imaging modalities, living tissues are damaged by destruction of individual cells at molecular level.



Fluoroscopy



Computed Tomography



Single Photon Emission Computed Tomography (SPECT)



Positron Emission Tomography (PET)

Figure 1.2 Examples of Ionizing Radiation Imaging Modalities

Figure 1.2 shows an example of ionizing radiation imaging modalities such as Radiography and Fluoroscopy, Computed Tomography (CT), Radionuclide imaging (Nuclear Medicine), Single photon emission computed tomography (SPECT), Positron emission tomography (PET) [13].

1.2.2 Non-Ionizing Radiation Imaging Modalities

Non-ionizing radiation imaging modalities use radio frequency (RF) waves that can be low frequency, infrared and visible light. Figure 1.3 shows image modalities that use non-ionizing radiation such as fundus camera, magnetic resonance imaging (MRI), ultrasound, and optical 3D scanner [13].



Magnetic Resonance Imaging (MRI)



Mammography Machine



Fundus Image

Figure 1.3 Examples of Non- Ionizing Radiation Imaging Modalities

There are some technical confines in these medical imaging modalities due to improper acquisition processes including poor focus and uneven illumination which produces noise and artefacts in the image.

1.3 Problems in Medical Images

Three main problems are identified when using imaging modalities; these are low contrast, varied contrast and noise in the medical images. Referring to the Figure 1.4, as an example, such problems could be observed in retinal images from fundus camera [14], images obtained from magnetic resonance imaging (MRI) [1],

mammography images obtained by x-rays [15] and ultrasound images obtained by CT angiography [16].

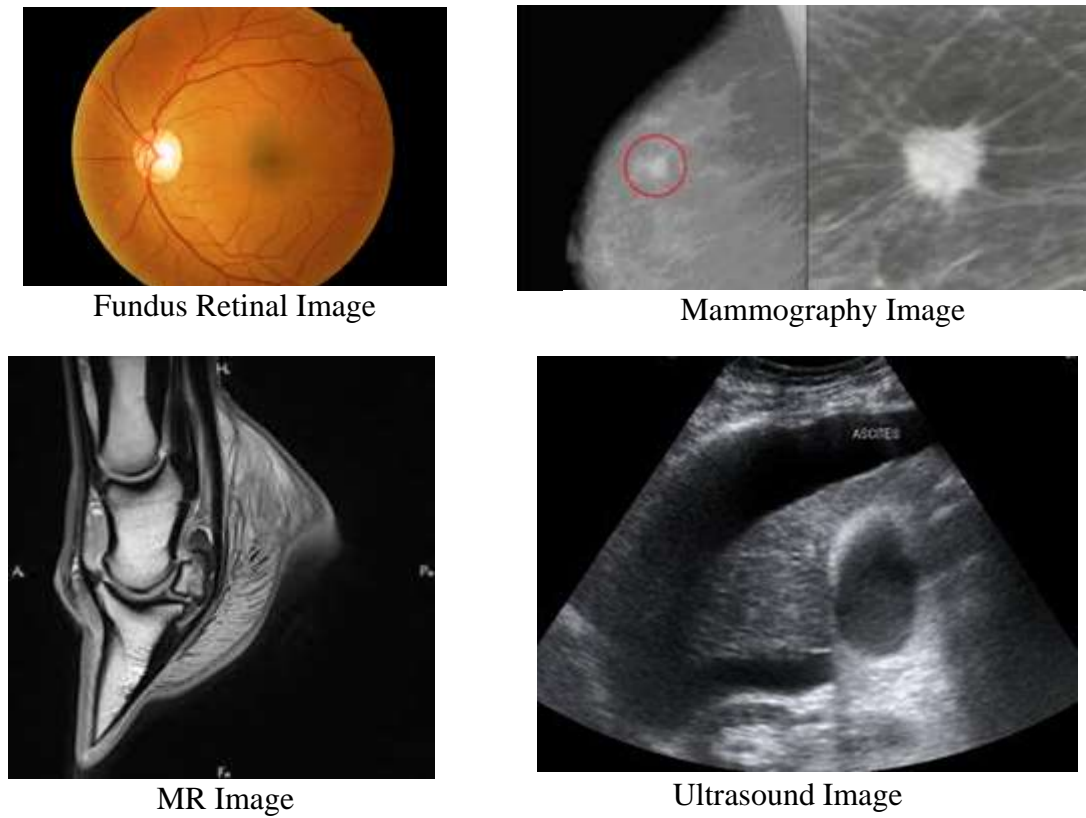


Figure 1.4 Examples of Medical Images Problem of Contrast Obtained From Different Medical Imaging Device

The different medical images are shown in Figure 1.4. The Retinal fundus image is captured by using fundus camera and it suffers from low and varied contrast and occurrence of noise also as elaborated in the next section.

1.4 Problems in Retinal Fundus Images

Retinal images are obtained from fundus cameras and suffer from problems of varied contrast, low contrast and noise. To obtain a good image, it depends upon the acquisition process and the illumination variation on the different parts of the retina. In spite of making the proper acquisition process with the fundus camera, the retinal fundus image suffers from varied and low contrast [17]. A detailed explanation on these three factors is given below.

1.4.1 Low Contrast in Retinal Colour Fundus Images

The image of the retina captured by using advanced fundus cameras has become a standard imaging modality in many ophthalmologic clinics. The digital retinal images can be analysed by using digital image processing techniques for diagnosis of eye related diseases. The diagnostics of eye related diseases from a digital colour fundus image depends upon the image quality. The quality of a digital retinal fundus image depends upon three factors, i.e., the image resolution (determined by the camera resolution), contrast of the objects on the retina (bloods vessels against their background and the optic disc) and proper illumination. It is very important to uniform and enhance the contrast of the retinal fundus image. There are two different definitions of contrast found in the literature. First, Michelson Peli *et al* [18] defined the contrast as a relation between the luminous intensity values in an image or selected specified region of the image. This is mathematically shown in Equation 1-1.

(1-1)

$$C = \frac{I_{max} - I_{min}}{I_{max} + I_{min}}$$

Where I_{max} and I_{min} are the largest and smallest luminous intensity values of an image. The second definition of contrast was given by Weber's law. He defined the contrast as the ratio of intensities between the most intense (brightest) and least intense (darkest) elements of a scene. This is mathematically as given in Equation 1.2.

$$C = \frac{I - I_b}{I_b} \quad (1-2)$$

Where I and I_b are the luminance of specified objects or the image and the background. Contrast is the dimensionless ratio between the absolute luminance difference of an object and the average background luminance. An image's information is distributed in terms of its intensity values and its contained specified range, and an image may appear in low contrast. The aim of image enhancement is to increase image intensity values of low contrast objects to be observed clearly. The digital retinal color fundus image suffers from low contrast between the blood vessels against their surrounding background. Due to the low contrast between the retinal blood vessels and their surrounding background in retinal fundus images, it becomes difficult to determine the retinal vasculature [6]. Consider Figure 1.5, a macular region of a colour fundus image is shown to suffer from low contrast.

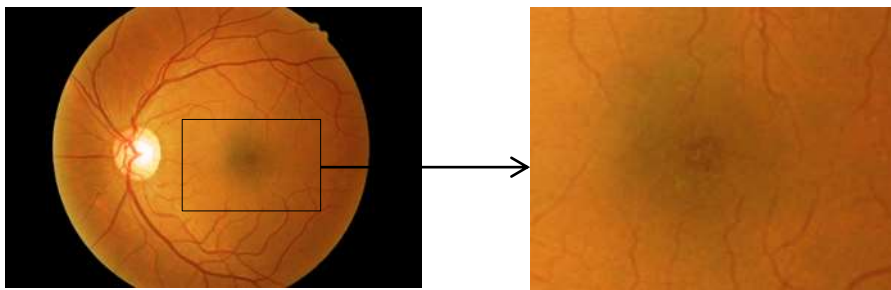


Figure 1.5 Example of Low contrast Images

Consider Figure 1.6, the colour retinal fundus image is shown and its green channels. The yellow circles are shown in which the intensity values of the blood vessels are low against the surrounding background. Due to this low contrast issue, the tiny blood vessels cannot be observed clearly; that makes it difficult to analysis the retinal fundus image properly.

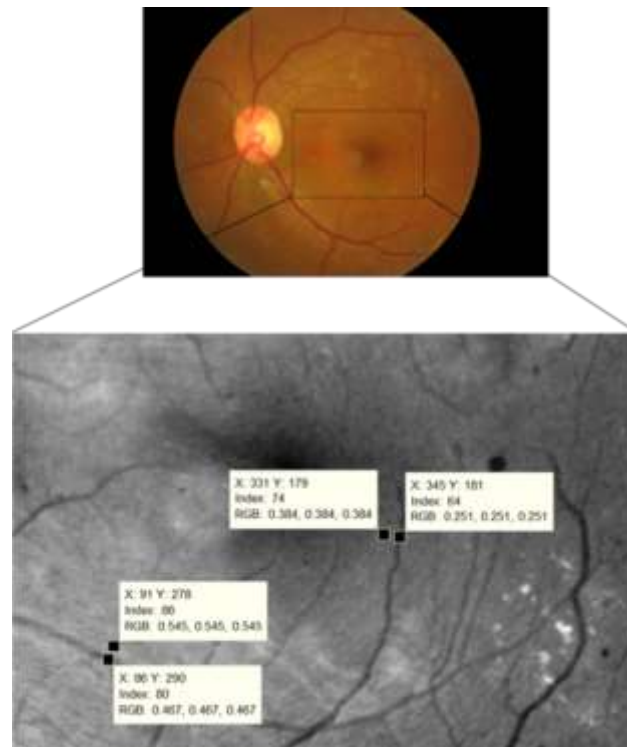
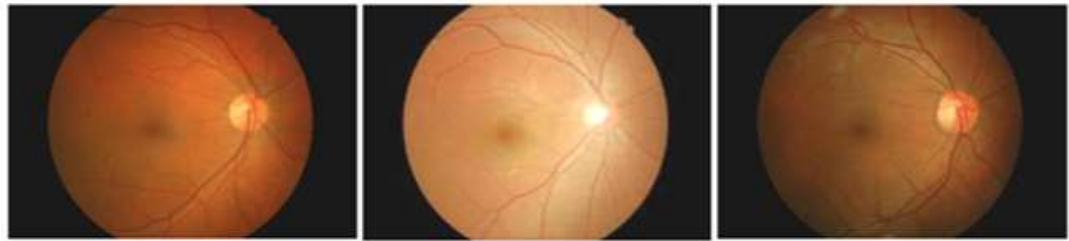


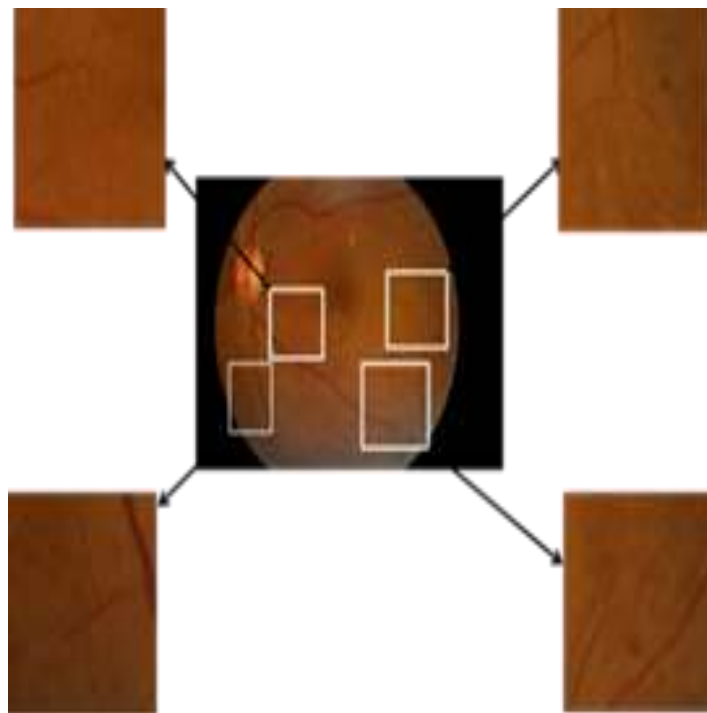
Figure 1.6 Illustration of Low contrast in Retinal colour fundus Images

1.4.2 Varied Contrast Problem in Retinal Fundus Images

Varied contrast occurs due to the configuration of the light source and the uneven illumination of the retinal surfaces that are irregularly curved [19]. There are two types of varied contrast in the retinal fundus image, i.e., inter-varying and intra-varying contrast.



(a) Inter- Varying contrast



(b) Intra- Varying contrast

Figure 1.7 Example of varied contrast in Fundus Images

Retinal fundus images of different eyes have different contrasts; this is known as inter-varying contrast and is shown in Figure 1.7a. This can occur when the retinal image is obtained from the same eye but at different times. Intra-varying contrast is when the contrast varies within the retinal fundus image and this is shown in Figure 1.7b.

The macular regions of the two fundus images shown also suffered from the varied contrast because some regions are dark and some regions are brighter due to the variation of the illumination. Consider Figure 1.8, a green band macular region of the fundus images are shown and different regions are marked with yellow circles within the macula of the green band. Due to the varying contrast, the image cannot be analysed properly.

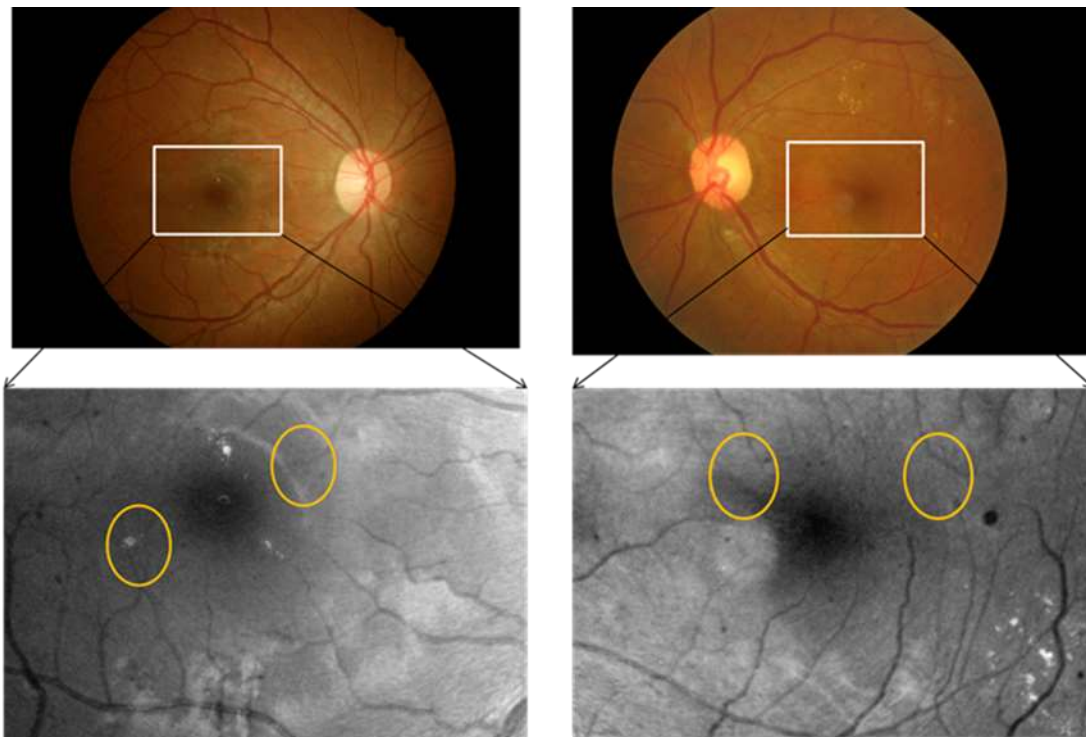


Figure 1.8 Example of varied contrast in Fundus Images

1.4.3 Noise in Retinal Fundus Images

Noise is any unwanted data that occurs in the image due to the improper acquisition process of imaging modalities and imaging process methods that could decrease the contrast and details of the image. There are three basic noise models, additive, multiplicative and additive plus multiplicative. Multiplicative noise, which is commonly known as speckle noise, is dependent on the image properties; on the other hand, additive noise is naturally systematic and can be easily modelled [20]. The additive plus multiplicative noise models contain both types of noise. The Retinal fundus images (FFA images and digital colour fundus images) contain noise due to which the blood vessels in the fundus images cannot be observed clearly as shown in Figure 1.9.

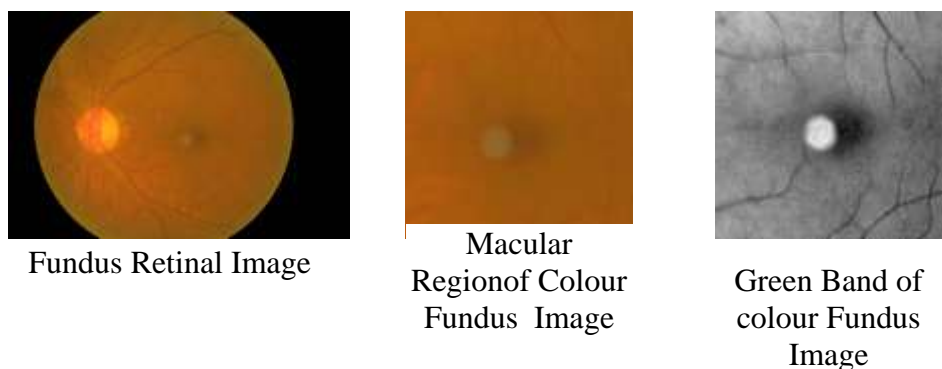


Figure 1.9 Illustration of noise in Fundus Images

Referring to Figure 1.9, colour fundus images contain noise due to which the blood vessels against their background cannot be observed clearly but the green band image of colour also contains noise due to which the details of the image are lost. The source of the noise in the digital fundus image was the image modality (Fundus camera) and during the acquisition process, it was observed that the fundus image contained additive noise because of the camera electronics and multiplicative noise due to the flash of the fundus camera. The filter-based approach has been developed in this thesis for the identification of noise in the fundus image. It has been proved that the fundus image contained additive and multiplicative noise [21]. Further

identification of noise in digital colour fundus images are elaborated in chapter 3 and 4.

1.5 Medical Image Enhancement Techniques for Retinal Fundus Images

Image enhancement is an important pre-processing step to improve the quality of the image for the purpose of better analysis. The quality of medical images obtained from the medical imaging devices depends on three factors; they are, spatial resolution, illumination and signal to noise ratio [22].

Spatial resolution gives the information about the sharpness of the image and its detailed features thus, sufficient resolution is needed to analyse, objectively, the image features of interest; in this work, and this is the retinal blood vessels and related pathologies, such as the FAZ area. The different fundus cameras have different resolutions depending upon the manufacturers but in this research work, the fundus camera Kowa 7 is used to capture the colour retinal fundus images. However, in this research work, the image resolution used is 1296×1936 pixels and the selected macular region has a resolution of 390×582 pixels. The resultant contrast of an image is related to the illumination of the scene. Thus, a proper acquisition process with the fundus camera is required, which provides an even illumination and will produce a good quality image.

A fundus camera contains a specialised low power microscope with an attached camera to capture the interior surface of the eye (Fundus), which contains the retina, optic disc, macula and posterior pole [2]. The ophthalmologists use the fundus camera to capture fundus images to analyse the progression of eye related diseases, such as diabetic retinopathy.

A digital fundus camera obtains retinal fundus images by capturing the illumination reflected from the retinal surface. The principle of the fundus camera is similar to that of indirect ophthalmoscopy in which illumination and imaging systems follow a dissimilar path surface [2]. The only difference is that the observed eye in the indirect ophthalmoscopy, as shown in Figure 1.10, is now replaced by a camera as

a sensor to photograph and capture the image digitally. An optical diagrammed of the fundus camera is shown in Figure 1.11.

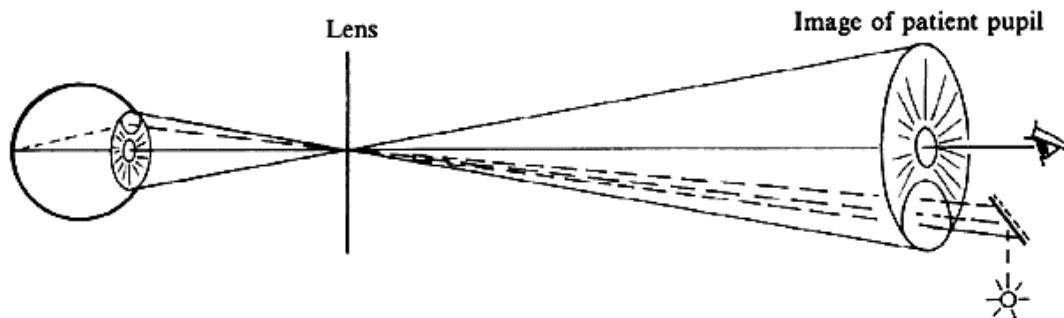


Figure 1.10 Principle of indirect ophthalmoscopy [4]

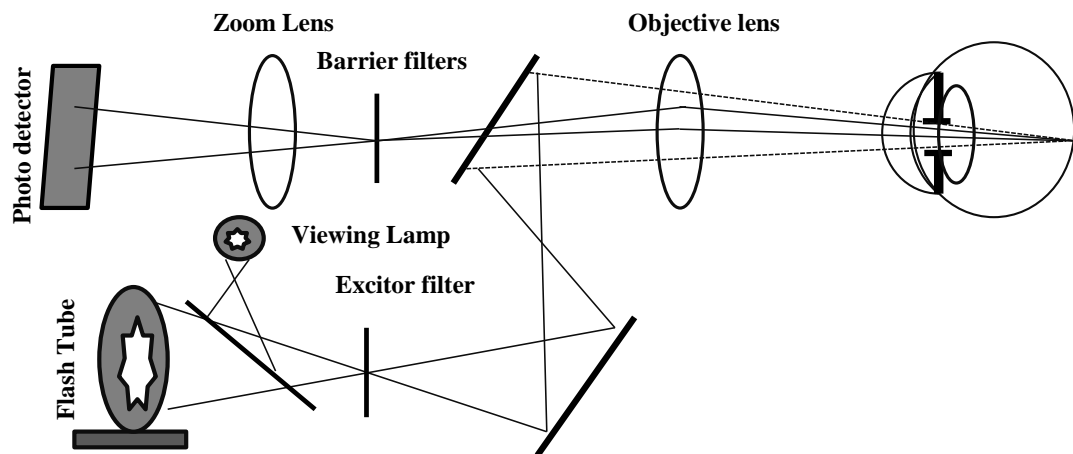


Figure 1.11 Principle of Fundus Camera [2]

The fundus camera is one of the complex optical systems that give a magnified view of the retina of the eye. The fundus camera contains two illumination systems, a flash tube for flash photography and a viewing lamp for the observation; whilst, the indirect ophthalmoscope contains only one illumination system. The source of these two illumination systems is required since the intensity of the light used for the visual observation of the retinal surface is not sufficient for photographing the image of the retinal surface. The use of one illumination system in the indirect ophthalmoscope is one of its drawbacks because of prolonged exposure to high intensity indirect ophthalmoscope illumination. Moreover, it causes discomfort

to patients and possibly leads to damage of the retina. In the fundus camera, the illumination system passes the light from the source to the retinal surface through a condensing lens [2].

The condensing lens has two main functions. First, it projects the illuminated light to form a ring, such as the illumination at the pupil, allowing the retinal surface to be illuminated through the outer part of the pupil. The ring like illumination is shown in Figure 1.13. It has the imaging pupil and contains the imaging path and illumination path to the exit and entrance of the aperture.

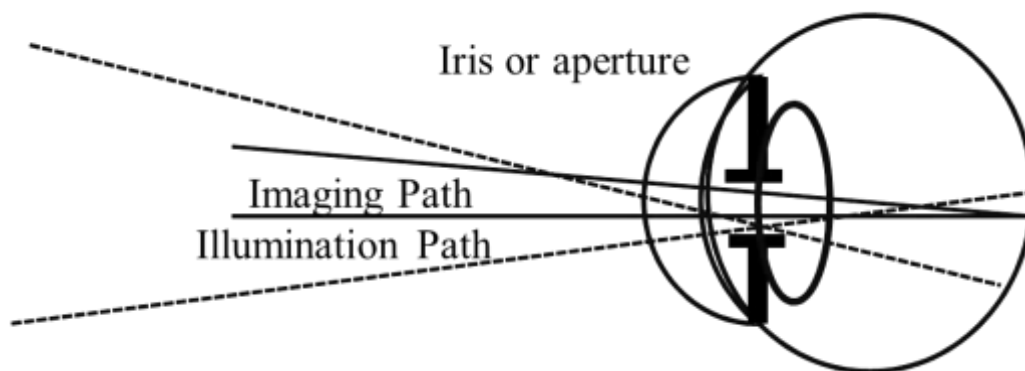


Figure 1.12 Fundus illumination and imaging path from optic fundus camera

Second, the converging lens collects the reflected diverging light from the retinal surface and passes it to further optics to form an image. The field of view of the retinal surface is determined by the ratio of the condensing lens and its focal length. An optic fundus camera normally has a field of view (FOV) of the retinal area from 20 to 60 degrees with a magnification of around 2.5times. The modification can be possible in the fundus camera with inserting the additional zoom lens with the FOV of around 15 to 140 degrees with a magnification of around five times.

Noise contains undesired objects that deteriorate an image's contrast and its quality. A good quality medical image is required for the analysis of pathologies. Due to the contrast injecting agent in the blood vessel of a patient in the invasive method, it gives good contrast of the image and the pathologies in the FFA image can be observed. However, in a colour fundus image, due to the presence of noise from

uneven illumination, the tiny blood vessels against the background cannot be observed clearly nor can the pathologies. Consider Figure 1.13, the colour fundus image and FFA is shown. Due to the contrast injecting FFA, a more clear observation of the blood vessels and pathologies is given as shown in the white circle as compared to the colour fundus image. But, the invasive method is not preferred due to injecting the contrast agent that causes other physiological problems. It is challenging to achieve a well contrasted colour fundus such as with FFA. In this research work, novel image enhancement techniques have been developed to handle noise levels in fundus images, and normalise and enhance the contrast of the images.

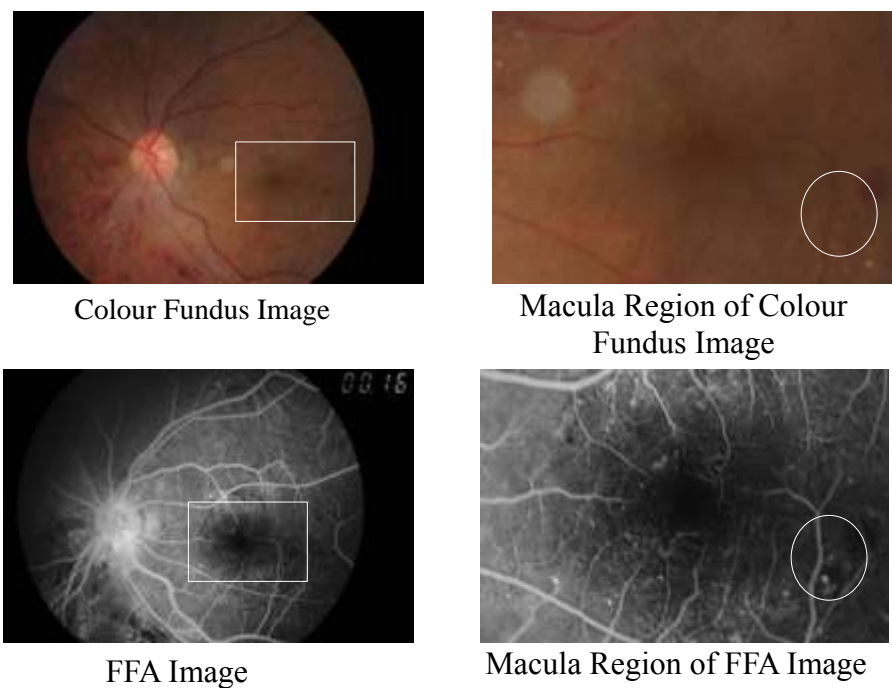


Figure 1.13 Colour Fundus Image vs FFA Image

Technically, in overcoming the above issues, medical image enhancement offers two approaches, namely, invasive and non-invasive image enhancement methods [23].

1.5.1 Invasive Image Enhancement Techniques

The invasive enhancement method is related to injecting a contrast agent into the human body to capture an image through image modalities. In ophthalmology, the fluorescein angiography is used as an invasive method to capture retinal images. It gives a better contrast of the retinal blood vessels against their background. Due to injecting the contrast agent into the patient's blood vessels, this method leads to physiological problems, such as nausea, vomiting and dizziness. In the worst case, death can occur as well. It was reported by Yanmuzzi *et al* [24] that there is a 1:222,000 frequency rate of deaths due to fundus fluorescein angiography so it is not recommended for daily routine use other than the fact that it gives good contrast of the image. For this issue, the safety of the patient is a priority whilst acquiring medical images. Whilst FFA gives a good contrasted image but needs an injecting contrast agent. The non-invasive image enhancement technique provides safety of the patient and good quality of images without any injection for improving the contrast of the blood vessels against their background [25].

1.5.2 Non-Invasive Image Enhancement Techniques

This approach is based on a digital image processing method which gives better quality images without the injection of a contrast agent and provides a solution for the automatic analysis of an image and its grading severity. The main purpose of the implementation of non-invasive image enhancement techniques is to improve the image quality without using any contrast agent in the human body [26]. Many image enhancement techniques are used to improve the image quality and remove noise; moreover, it is very necessary to enhance the contrast of the image, normalise the contrast and reduce noise in order to improve the image quality for the visual perception of the human observation [27]. Different enhancement techniques are used for different problem related applications. In medical images, there are problems of varied contrast, low contrast and noise. The main challenge of a non-invasive image enhancement technique is to determine the object of interest in the image and

distinguish the object of interest from other objects, such as noise and artefacts, to obtain a better enhanced image.

1.6 Problem Statement and Formulation

Digital colour fundus images suffer from noise and varying low contrast problems. Due to an improper acquisition process, noise is observed in the image, which degrades the image quality. Due to uneven illumination, the colour fundus image suffers from varied contrast. The colour fundus image also suffers from low contrast due to the biological structure of the objects in the image and the amount of light being absorbed. These low contrast objects of the retinal fundus image, especially in the macular region, need to be enhanced properly to observe the tiny blood vessels against the background.

A digital image enhancement technique developed by Hanung.A.Nugroho *et al* [28] called RETICA reduces the varied contrast and enhances the low contrast blood vessels and the technique was investigated on model fundus images. The RETICA method applies the Retinex algorithm [29] for contrast normalisation to overcome the varied contrast followed by the Independent Component Analysis [30] for contrast enhancement to overcome the low contrast. RETICA was tested on the model fundus image. RETICA successfully achieved a good contrast improvement factor of 5.38 on model images as compared to the standard contrast improvement factor of 5.79 of the FFA method. However, Hanung.A.Nugroho *et al* [28] did not extensively investigate the performance of RETICA on real fundus images in FiNDeRs database and more importantly the effects of noise in fundus images on RETICA.

To address the issues related with the analysis of fundus images, it is important to understand the nature of the noise in fundus images and to develop a suitable noise reduction technique to address noise prior to any contrast enhancement. Noise that arises from the image acquisition by fundus camera will have to be investigated thoroughly in order to identify the type(s) of noise. Available noise

reduction schemes should be investigated to obtain the most effective noise reduction for the type(s) of noise in fundus images.

In improving the contrast of the fundus images, it is clear that the RETICA method has the potential to address varied and low contrast effectively as described from Hanung *et al* [28]. However, there is a need to ascertain its performance with real fundus images.

RETICA is based on the two hypotheses as follows:-

1. First, the digital colour fundus images are taken with a fundus camera and these images suffer from a varied contrast problem. The colour fundus image has a problem of uneven illumination. According to the image formulation model, the image intensity is the product of illumination and reflectance. Due to uneven illumination, the image has a varied contrast which affects its quality. Therefore, in order to achieve a uniform contrast image, it is necessary to normalise the image contrast and separate the illumination from the reflectance. Retinex makes this possible by separating the illumination from the reflectance part of the image to give a contrast normalised image.
2. Secondly, the objects of interest (macular region of the fundus image) suffer from low contrast because it is related to the reflectance. The independent component analysis is used to enhance the objects without introducing noise or any artefacts.

The above two problems of varied and low contrast were formulated and addressed on statistical models of fundus image by Hanung *et al* [28]. The performance of RETICA was evaluated in terms of the contrast improvement factor and it successfully achieved an average of 5.38 contrast improvement factor on the model fundus images. However, RETICA was not validated on the real fundus image.

In this research, it is hypothesised that noise affects the performance of RETICA and that RETICA can be improved with better SNR of fundus images. The

noise in fundus images is therefore studied and its effect on the performance of RETICA with real colour fundus image is investigated.

1.7 Research Objectives

Initially, the objective of this research work was to validate and improve the earlier developed non-invasive image enhancement technique named RETICA on the real colour fundus image instead of the model fundus image. The improved non-invasive image enhancement technique can normalise the varied contrast, enhance low contrast objects and remove noise to achieve a better image in terms of contrast and visualisation as compared to FFA images. This research addresses three main objectives as follows:-.

1. To validate and analyse the performance of RETICA on the real fundus image instead of the model fundus image.
2. To investigate noise in fundus images in order to identify noise type(s) and propose appropriate noise reduction schemes.
3. To investigate the performance of proposed noise reductions in terms of SNR in fundus images and determine the improvement to the contrast improvement factors in RETICA.

1.8 Contribution

The main contribution of this thesis is the validation and modification of the earlier proposed non-invasive image enhancement technique RETICA (it is combination of Retinex and ICA) on real fundus image instead of model fundus image. RETICA has been improved by using a denoised technique before Retinex algorithm. Now, image enhancement technique is based on denoised techniques (TDCE), Retinex for contrast normalisation and ICA for enhanced digital colour fundus image to obtain from fundus camera as imaging modality. One of the main contributions of this thesis is the achievement of the almost same contrast

improvement factor 5.56 as compared to contrast improvement factor 5.79 of FFA (Referred Chapter 4).

Another contribution of this thesis is also the development of an approach to identify the nature of noise in Fundus image (Referred Chapter 4) which can be used for identification of noise in any image processing application and other contribution is also study of different denoised methods on fundus and observed the limitation of different denoised methods on fundus image.

1.9 Scope of Work

It is important to analysis the digital colour fundus image to analysis the eye related disease such as diabetic retinopathy. In ophthalmology, the fluorescein angiography is used as an invasive method to capture retinal images. It gives a better contrast of the retinal blood vessels against their background. Due to injecting the contrast agent into the patient's blood vessels, this method leads to physiological problems. For this issue, the safety of the patient is a priority whilst acquiring medical images. Whilst fundus fluorescein angiography (FFA) gives a good contrasted image but needs an injecting contrast agent. The non-invasive image enhancement technique provides safety of the patient and good quality of images without any injection for improving the contrast of the blood vessels against their background. The non-invasive image enhancement technique is improved in this research work , it can normalise the varied contrast, enhance low contrast objects and remove noise to achieve a better image in terms of contrast and visualisation as compared to FFA images. The improved non-invasive image enhancement technique can be played significant role to reduce the use of invasive modality.

1.10 An Overview of Thesis Structure

This thesis consists of five chapters. First chapter of this thesis provides the introduction of our research work and give a brief knowledge of medical image modalities and problems occurred due to medical imaging modalities. A detailed

explanation of problems occurred in medical imaging such as varied contrast, low contrast and noise is also provided. It outlines the motivation, research objectives and problem formulation.

Second chapter of this thesis is about critical literature review of the eye related disease such as diabetic retinopathy in terms of medical science and critical literature of computerised automatic detection of diabetic retinopathy and is divided into three main parts. First part is related to computerised detection of diabetic retinopathy based on pathologies, second part provides an analysis of retinal blood vessels and fovea for grading diabetic retinopathy and the third part is related to non-invasive image enhancement techniques of retinal fundus for grading diabetic retinopathy. The last section of this chapter provides comparison of our work with other researcher's works in the field of computerised analysis of diabetic retinopathy.

Third chapter is related to the proposed methodology. It is related to analysis of retinal fundus images, implementation of RETICA on real fundus image instead of model fundus image. The method of measuring contrast and contrast improvement for evaluation of RETICA performance is elaborated in this chapter. The approach is proposed to identify the nature of noise in retinal fundus and method of measuring PSNR of fundus image and method of improve of SNR of fundus image is also explained in third chapter.

Fourth chapter is related to results and analysis of proposed experimental work in third chapter. RETICA is validated on real fundus image and performance evaluation of RETICA is evaluated in terms of contrast improvement factor and performance comparison of the RETICA on real colour fundus images with FFA images. The proposed approach to identify the nature of noise in retinal fundus is successfully tested on real fundus image and model fundus. The modification of RETICA by inserting denoised method (Time Domain Constraint Estimator (TDCE)) before Retinex, validation of modified methods is also elaborated in fourth chapter.

The fifth chapter of this thesis concludes the research including the brief summary of authentication of RETICA and overcome limitations and analysis results of improved RETICA and future contribution to research work in this area.

CHAPTER 2

LITERATURE REVIEW

This chapter presents a literature review on diabetic retinopathy, an eye related disease due to diabetes mellitus, and clinical methods to detect and grade the disease. This chapter also contains a critical review on a computerised analysis of digital colour fundus images for the detection and grading of diabetic retinopathy. The varied and low contrast issues, and noise problems in fundus images are also discussed. In addition, a discussion on noise reduction techniques is presented.

2.1 Introduction to Diabetic Retinopathy

Diabetic Retinopathy is damage of the retinal vasculature that is a common complication of the diabetes mellitus disease. It is the leading cause of blindness in the working age population. The vision loss problem is due to high blood sugar level and hypertension that damage tiny blood vessels which affects the Retina of eye. According to the National Eye Institute Database of United States, diabetes is the leading cause of blindness among adults aged 20 to 74 years[5]. Diabetes is regarded as one of the world healthcare challenges [31]. The World Health Organization (WHO) expects the number of people with diabetes to increase from 130 million to 350 million over the next 25years[9].

The rate of diabetes is higher in developed countries than undeveloped countries. It is estimated that 75% of people with diabetic retinopathy are living in developing countries[9]. This situation occurs due to inadequate treatment and improper management of health care, so proper treatment is essential because patient may identify it before treatment is complicated and nearly impossible. Eye screening is important for the detection of the diabetic retinopathy [32]. The main purpose of

the screening is to recognize patients with sight-threatening DR so that essential treatment would be given for prevention of vision loss [8]. It has been observed that retinal vasculature features analysed in DR are the loss of retinal capillaries in the perifoveal capillary network due to the increase in the size of Foveal Avascular Zone (FAZ) [33]. Recent research on the analysis of fundus images found that the size of the fovea avascular zone increased with the severity level of DR.

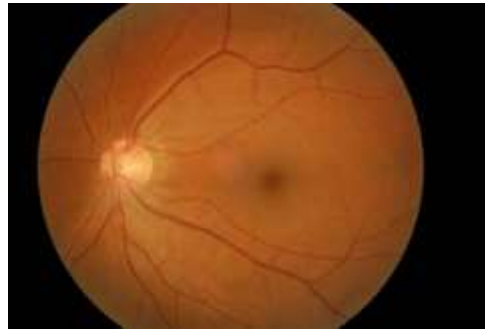
The area of the FAZ can only be observed in colour fundus images and can only be seen in fundus fluorescein angiograms (FFA) [28]. The retinal photography known as FFA is carried out after an arterial injection of fluorescein dye which takes place in a rapid sequence. Three main characteristics are given by the FFA: First, the characteristic of the dye flow through the blood vessels to reach the retina and choroid, and its circulation when it gets there. Second, fine details of the pigment epithelium and retinal circulation are recorded which might be invisible otherwise. Third, the retinal blood vessels are clear in the resulting image and their functional integrity is assessed [34]. The research related to analysis the retinal fundus image to diagnosis eye related disease such diabetic retinopathy is a challenging area for medical image processing.

2.2 Anatomy of Fundus image of Normal Retina

Fundus image is digital colour retinal image of the eye that can be obtained using a fundus camera. Many eye related diseases can be diagnosed through analysis of fundus image. There are two ways to capture the fundus image i.e. Fundus fluorescein angiogram image (invasive method) and digital colour fundus image (non-invasive method). Fundus fluorescein angiogram is injection based method in which fluorescein dye is injected into patient blood vessel to increase the contrast level of retinal vasculature (Retinal vasculature is network of vessel in the retinal layer) of it [35]. The digital colour fundus is captured by fundus camera without injecting the contrast agent into patient's blood vessels. Figure 2.1 shows the FFA and digital Colour image.



Fundus fluorescein Angiogram



Digital Colour Fundus Image

Figure 2.1 FFA and Digital Colour Fundus Image

Two retinal images of the same eye are shown in Figure 2.3 using FFA (invasive) and normal fundus (non-invasive). With the use of contrast agents, the retinal vessels appear brighter in the higher contrast FFA image compared to low contrast colour fundus image. Contrast of retinal vasculature of a colour fundus image can be enhanced to similar level or better than FFA image and this is discussed in the later sections. The main components of the fundus image are optic disc, macula and retinal blood vessels. The macula is a centre part of retinal that provides visual acuity. Oxygen and nutrients are supplied to retina cells by retinal blood vessels. The retinal blood vessels grow from central retinal artery and vein in optic nerve to nourish the inner part of the retina.

2.3 Abnormalities in Fundus Images

The abnormalities observed clinically in fundus images are also known as pathologies. These pathologies indicate DR severity levels or disease severity level [36]. Pathologies that occur in retinal fundus image such as micro aneurysms, haemorrhages and exudates are described in the following sub sections.

2.3.1 Microaneurysms

Microaneurysms (MAs) are the first clinical signs of DR in the fundus image. Referring to the colour fundus image and FFA image of Figure 2.2, MAs that appear as small dark red lesions in colour fundus images (in white circles) are clearly seen as small around lesions with sharp edges and irregularly brighter rim in the FFA images. The colour and inundation of MA vary according to the oxygenation of the blood from brighter red to deep red [37]. MA can be observed as small in size around 15-100 μ m in diameter in high quality images. MAs are mostly fairly circular, dark red spots with relatively sharp edges. MAs are appeared as tiny dilations of the blood vessels and their occurrences correspond to progression of DR [38]. They are mostly occurred in the area near to the macula [39].

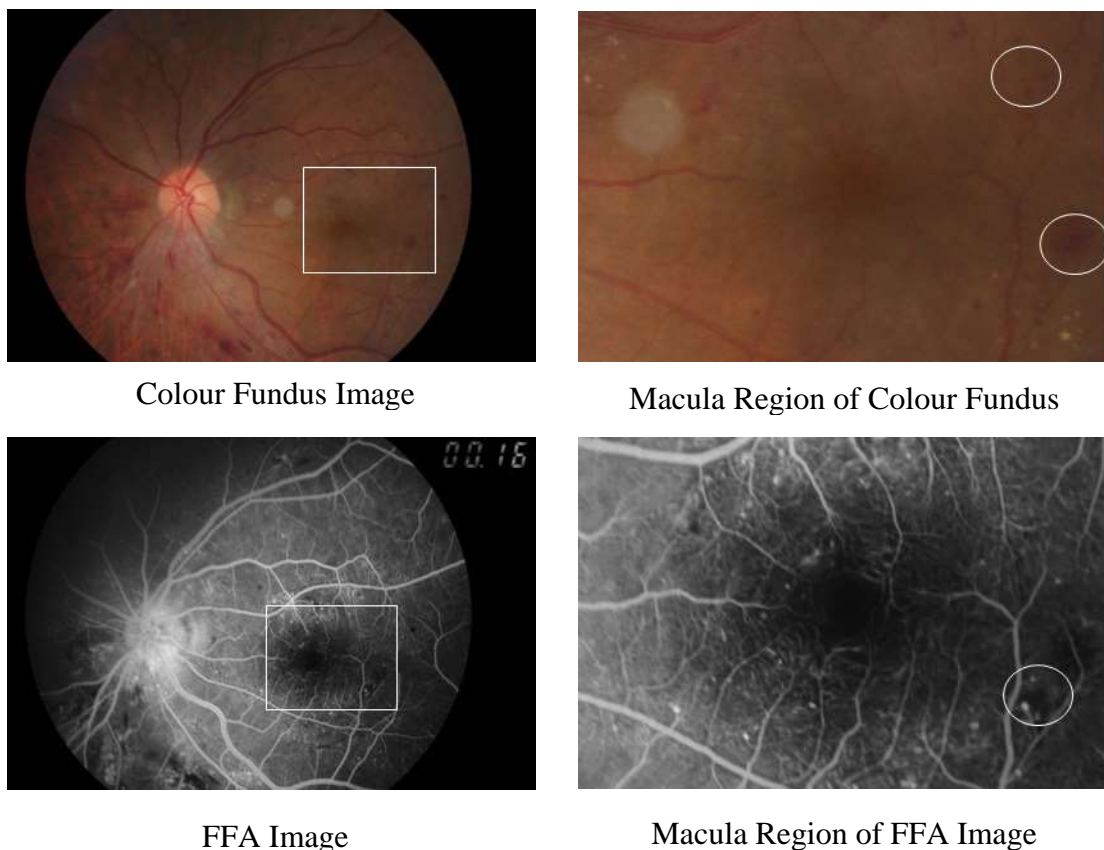


Figure 2.2 MAs in Colour Fundus image and FFA image

2.3.2 Blot and Dot Haemorrhages

A haemorrhage appears as round shaped or irregular shaped sharped or diffusely delineated and deep red (colour of intravenous blood) in fundus images. Red cells are the main source of haemorrhages formation as the cells leak out from damaged blood vessels. There are two types of haemorrhages blot and dot haemorrhages. Mostly, blot haemorrhages are larger than dot haemorrhages [36]. Haemorrhages (dot or blot) appear with irregular margins that may occur deeper in the retina. The haemorrhages are found in fundus images shown in Figure 2.3 (see marked areas).

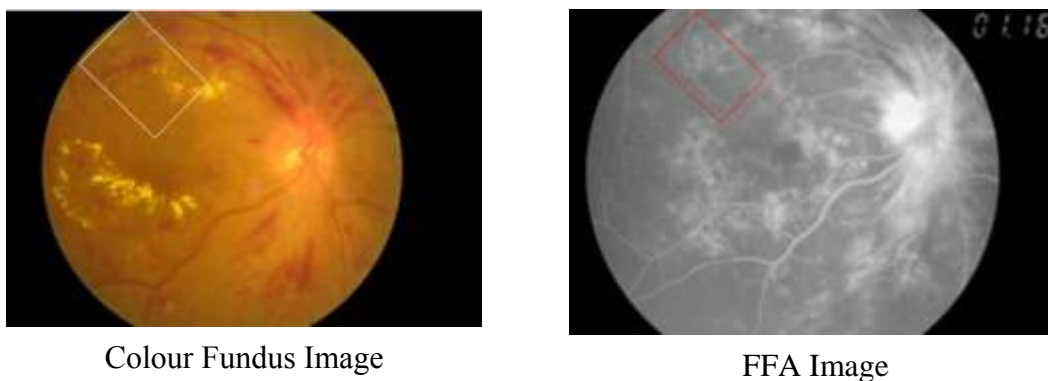
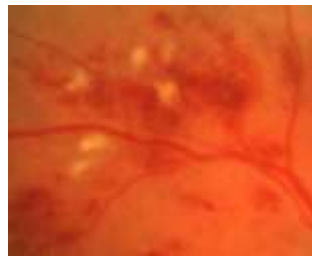


Figure 2.3 Haemorrhages in colour Fundus Image

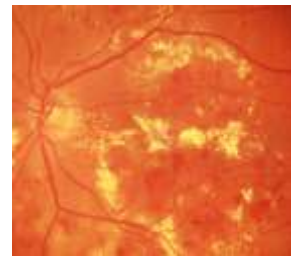
2.3.3 Hard and Soft (Cotton wool spot) Exudates

In DR, exudates are the second clinical sign appearing after MAs in the fundus image. Exudates are random whitish or yellowish patches found in the retinal fundus image with different sizes, shapes and at different locations [40]. There are two types of exudates i.e. soft exudates and hard exudates. Hard Exudates are formed by serum lipoproteins that outflow from MA and dump in the retina [38]. Exudates are also formed as individual circulate pattern by accumulation of lipids that leak from surrounding capillaries and micro- aneurysms (MA). The soft exudates are also known as cotton wool spots. In the areas where blood vessels are blocked and damaged, soft exudates appear as the brighter areas. They are white, fluffy lesions in

the nerve fibre layer. Fluorescein angiography shows no capillary perfusion in the area of the soft exudate [41]. They are very common in eye related disease especially if the patient is also hypertensive. Figure 2.4 shows the image containing hard and soft exudates.



(a) Hard Exudates
Retinal Image



(b) Soft Exudates
Retinal Image

Figure 2.4 Hard and Soft Exudates in Retinal Fundus Images

2.3.4 Foveal Avascular Zone (FAZ)

The FAZ is the central region of the fovea that is usually free of capillaries [42]. FAZ is usually has a diameter of ranging from 500μ to 1500μ [43]. The enlargement of FAZ is often observed in the eye with diabetic retinopathy progresses with DR severity as the diabetic condition causes capillary loss in the perifoveal capillary network [28]. Figure 2.5 depicts FAZ in colour fundus image and FFA image.



(a) FAZ (white circle) in Colour
Fundus Image



(b) FAZ (red circle) in FFA
Image

Figure 2.5 FAZ in Colour Fundus Image and FFA Image

2.4 Severity Level of Diabetic Retinopathy

The main purpose of the screening of eye is to recognise subjects (patients) with sight-threatening DR so that essential treatment would be given to prevent vision loss. The international clinical diabetic retinopathy disease severity scale is defined in Table 2.1 [44-45]. From Table 2.1, it can be seen that the appearance of pathologies increases with increase in DR severity. There are four quadrants of retinal fundus and pathologies can occur in any of quadrants depending upon the level of severity of DR as shown in Figure 2.6.

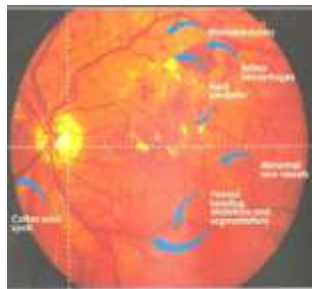


Figure 2.6 Retinal Fundus Image [1]

Table 2.1 International DR Grading Scale [44-45]

DR-Stage	Indicator
No_DR	Normal image, there is no any abnormalities.
Mild NPDR	Micro- aneurysms only.
Moderate NPDR	Extensive MA, Haemorrhages, hard and soft exudates.
Severe NPDR	Any of the below. <ul style="list-style-type: none"> • Micro-aneurysms in all 4 quadrants • Venous beading in at least 2 quadrants • Prominent intra-retinal micro avascular abnormalities (MRA) in 1 quadrant.
PDR	Any of the following <ul style="list-style-type: none"> • New blood vessels formation either at disc (NVD) or elsewhere (NVE) • Vitreous/Pre-retinal haemorrhages

Referring Figure 2.7, in which all DR stages of retinal fundus images are shown according to appearance of pathologies as mentioned in Table 2.1.

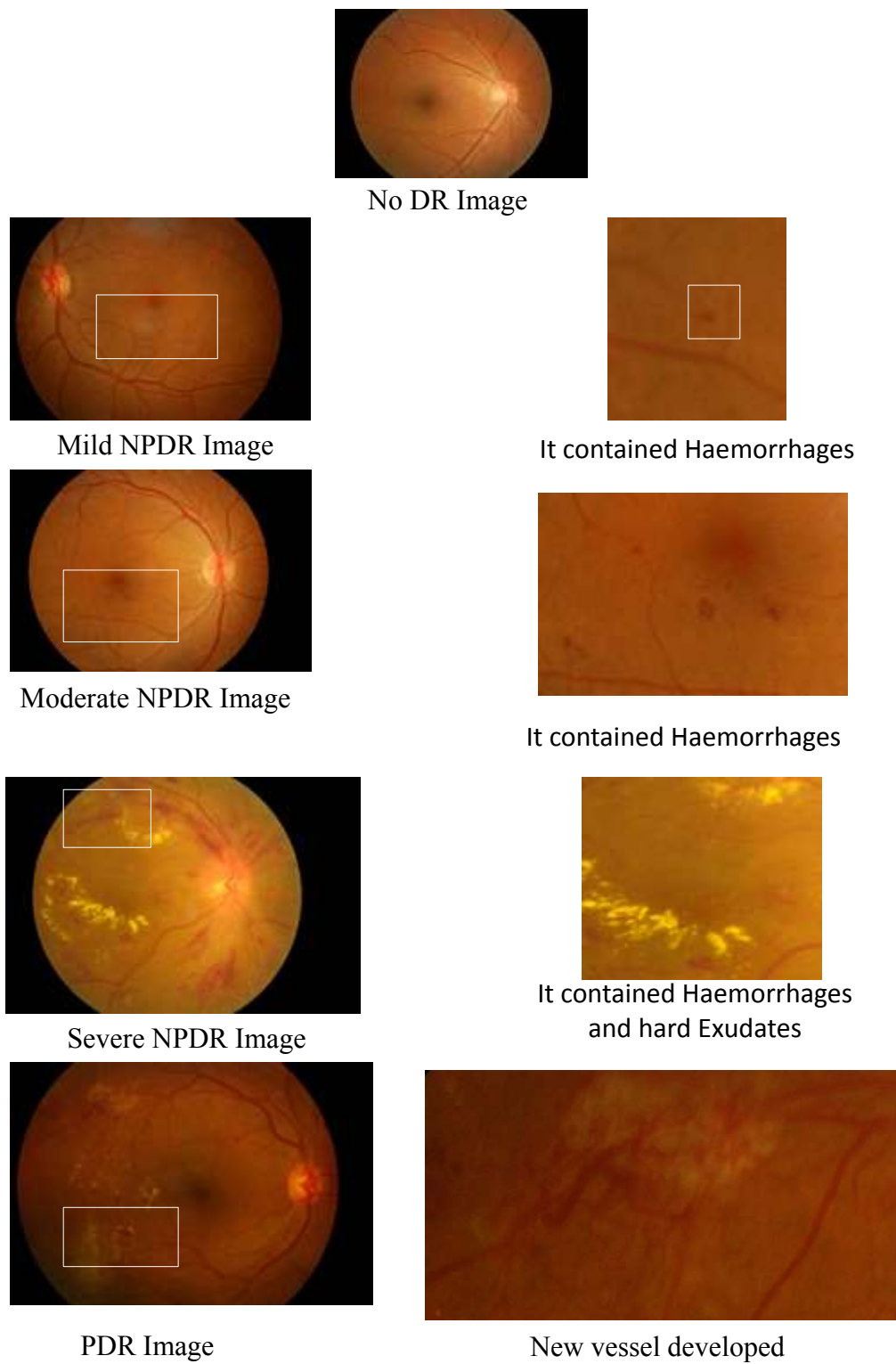


Figure 2.7 Retinal Images Contained Pathologies

2.5 Computerised Analysis for the Detection of Diabetic Retinopathy

Interest in computerised analysis of Diabetic Retinopathy pathologies has been rapidly increasing and the review of related works is divided into three parts. The first part is related to computerised analysis of micro aneurysms and haemorrhages, followed by, computerised analysis of soft and hard exudates and finally, computerised analysis of FAZ for grading of diabetic retinopathy. Analysis of retinal fundus image is difficult because colour fundus images suffer from varied and low contrast.

Many researchers worked on the detection of DR on the basis its pathologies detection. Researchers have developed various computerised methods for the detection of Diabetic Retinopathy based on pathologies. Microaneurysms can be automatically detected as the early signs of DR as reported by Kahai *et al* [46]. The automatic detection of DR using the microaneurysm count was improved using other DR-related pathologies. Sinthanayothin *et al* [47] proposed a method for the automatic detection of DR by determining the number of hard exudates. Larsen *et al.* [48] and Hansen *et al* [49] proposed a method for the detection of microaneurysms and haemorrhages. Usher *et al* [50] proposed a method for the detection of diabetic retinopathy to count microaneurysms, haemorrhages and exudates.

2.5.1 Microaneurysm and Haemorrhage Detection

The first automatic detection method for diabetic retinopathy was developed by Baudoin and kelin *et al* [51] to detect the microaneurysms from fluorescein angiograms. They used a morphological top hat transform with linear structuring elements with different orientations. The round shaped micro-aneurysms were connected by elongated structures, such as vessels, but it gave many false detections. Spencer *et al* [52] used the top hat transform to produce the candidate microaneurysms with an extension of the earlier work of Baudoin *et al* [51]. The candidate microaneurysm segmentation was performed by using a combination of the

top hat transform and match filtering along with the region growing technique. The Spencer *et al* [52] method did not give so many false results of the microaneurysm detection. Spencer *et al* [52] method improved the sensitivity of the microaneurysm detection by introducing the pre-processing steps. These pre-processing steps were based on the rule-based classifier with a number of shapes and intensities of features. The difference between the Spencer *et al* [52] method and the earlier proposed method was the classification steps of the different features.

Another morphological-based technique for the detection of micro-aneurysms was studied by Walter *et al.* [53] to overcome the inadequacy of the top hat-based methods. Walter *et al.* [53] used the bounding box closing was applied with the top hat transform instead of the linear structuring element with the top hat transform.

There are many techniques used for the detection of microaneurysms that are not based on morphological operations. Gardner *et al.* [54] proposed a method for the detection of microaneurysms and haemorrhages based on neural networks. The neural network and supervised learning have been used to detect microaneurysms and haemorrhages for the screening of DR. The colour fundus images contain pathologies, such as microaneurysms and haemorrhages. Many methods [36, 55, 56] have assumed that the dark parts in the colour fundus contained blood vessels. Sinthanayothin *et al* [36] and Usher *et al.* [50] used the recursive region growing to cluster the dark areas in the image and classify the vessels. The vessel segment region growing resulted from using a neural network. Enrico and Grisan *et al* [57] gave another suitable method instead of using the neural network; they detected the dark parts of the colour fundus image by clustering similar pixels with a local spatial density.

Further, Garcra *et al.* [58] improved the method by modification with the use of an automatic feature selection and classification steps. Further, Xiahui and Chutatape *et al* [59, 60] proposed a method for the detection of haemorrhages by using the principal component analysis. The features were extracted by using the support vector machine to classify the image patch. To detect the different sizes of haemorrhages, a pyramid of images was created to compute the changing image resolution. Quellec *et al* [61, 62] also used image templates for the detection of

microaneurysms based on template matching in the wavelet domain. Tables 2.2, 2.3 and 2.4 summarise the reported performances of the microaneurysm and haemorrhage-based detection algorithms for the screening of diabetic retinopathy.

Table 2.2 Performances of Proposed Micro aneurysms Automatic Detection Algorithms

Method	Sensitivity	Specificity
Bhalerao <i>et al</i> [63]	0.83	0.80
Ege <i>et al</i> [64]	0.69	–
Pallawala <i>et al</i> [65]	0.93	–
Spencer <i>et al</i> [52]	0.82	–
Cree <i>et al</i> [66]	0.82	0.84
Frame <i>et al</i> [67]	0.84	0.85
Hipwell <i>et al</i> [68]	0.43	–
Yang <i>et al</i> [69]	0.80	0.90
Walter and Klein <i>et al</i> [70]	0.86	–
Quellec <i>et al</i> [62]	0.88	0.96
Quellec <i>et al</i> [61]	0.90	0.90
Quellec <i>et al</i> [61]	0.94	0.92
Quellec <i>et al</i> [61]	0.90	0.89
Walter <i>et al</i> [71]	0.89	–
Hipwell <i>et al</i> [68]	0.81	0.93
Fleming <i>et al</i> [72]	0.85	0.83

Table 2.3 Performances of Proposed Haemorrhages
Automatic Detection Algorithms

Method	Sensitivity	Specificity
Gardner <i>et al</i> [54]	0.74	0.74
Ege <i>et al</i> [73]	0.83	–
Zhang <i>et al</i> [59]	0.90	–
Hatanaka <i>et al</i> [74]	0.85	0.21
Hatanaka <i>et al</i> [75]	0.80	0.80

Table 2.4 Performances of Proposed Microaneurysms and Haemorrhages
Automatic Detection Algorithms

Method	Sensitivity	Specificity
Sinthanayothin <i>et al</i> [47]	0.78	0.89
Niemeijer <i>et al</i> [76]	0.30	–
Grisan and Ruggeri <i>et al</i> [57]	0.94	–
Niemeijer <i>et al</i> [76]	1.00	0.87
Garcia <i>et al</i> [58]	1.00	0.60

2.5.2 Hard and Soft Exudate Detection

Thresholding-based detection was initially used to detect hard and soft exudates. Ward *et al* [77] introduced the semi-automatic exudate detection based on the thresholding and shade correction method but user interaction is required to apply the thresholding. Philips *et al* [78] and Zheng *et al* [79] improved the previous system by introducing the dynamic method of thresholding. The Philips *et al* [78] method was

the based on the detection of large high intensity areas of colour fundus image by using global thresholding techniques. On the other hand, the block-wise local threshold method has been used to segment the smaller exudates. Philips' method was better at detecting the exudate pixels but it gave many false positives. To overcome the false positive detection, Zheng *et al* [79] introduces the exudate detection system based on the local neighbouring along with the dynamic block-wise thresholding method. Goldbaum *et al* [80] proposed a method of exudate detection algorithm based on the template matching and edge detection approach. Goldbaum *et al* [80] applied the template matching on the image and located bright lesions of all sizes.

The outlined edges of the located bright lesions were identified by using the edge detection method. The Goldbaum *et al* [80] method was improved by Wang *et al* [77] and it was based on the supervised statistical pixel-based lesion classification. Wang *et al* [77] applied the minimum distance discriminant classifier to classify image pixels into two classes (hard and soft exudates) according to their pixel values. The true hard exudate pixels were then detected by using the contrast information of the local neighbourhood. Sanchez *et al* [81] further improved the method using the alternative approaches for the non-uniform illumination correction factor. The reported algorithms for the detection of hard and soft exudates along with their performances are summarised in Tables 2.5 and 2.6.

Table 2.5 Reported Performances of Soft Exudates
Automatic Detection Algorithms

Method	Sensitivity	Specificity
Ege <i>et al</i> [82]	0.80	–
Niemeijer <i>et al</i> [83]	0.70	0.93
Zhang <i>et al</i> [60]	0.88	0.84

Table 2.6 Performances of Proposed hard Exudates Automatic Detection Algorithms

Method	Sensitivity	Specificity
Phillips <i>et al</i> [78]	0.87	–
Walter <i>et al</i> [84]	0.93	0.95
Walter <i>et al</i> [85]	0.93	0.92
Osareh <i>et al</i> [86]	0.90	0.89
Osareh <i>et al</i> [87]	0.94	0.92
Sivaswamy and Ram <i>et al</i> [88]	0.72	–
Ravishankar <i>et al</i> [89]	0.95	0.91
Gardner <i>et al</i> [90]	0.93	0.93
Ege <i>et al</i> [82]	0.99	–
Sinthanaya <i>et al</i> [47]	0.89	1.00
Xu and Luo <i>et al</i> [91]	0.88	0.80

2.5.3 Analysis of FAZ for Grading of Diabetic Retinopathy

Foveal avascular zone (FAZ) is the most accurate vision zone on the retina devoid of capillaries in the macular region [42]. Ibanez and Simo [92] showed the detection of the foveal avascular zone using eye fundus angiographies. In diabetic retinopathy, an enlargement of the FAZ occurs as a result of a loss of capillaries in the peritoneal capillary network [31, 43, 93]. Due to higher hemodynamic stress (increase in heart rate and blood flow) the small capillaries surrounding the FAZ possibly tend to be blocked or damaged. A rapid loss in visual acuity may occur as a result of the defect of the peritoneal area [42]. Due to the problem in the visual observation of FAZ, the diabetic patient may suffer from an abnormally enlarged FAZ compared to the normal vision patient [94]. The effect of an enlargement of FAZ has now been observable in colour fundus images [28], which was previously observed in FFA images [94], for both PDR and NPDR. The FAZ area has been determined in the FFA image by using the Bayesian statistical methods or

thresholding techniques based on the morphological operators and Sobel edge detectors [95]. H.A.Nugroho and Lila Izhar *et al* [28, 96] and his team worked on the determination of the FAZ area in the colour fundus image to reduce the use of the invasive method, FFA. Lila Izhar *et al* [96] developed the method for analysis of FAZ in a colour fundus image based on the vessel extraction and reconstruction for grading of DR and achieved a 92.2% accuracy. Later Ahmad Fadzil and H.A.Nugroho *et al* [28] developed RETINO, an automated determination of FAZ for DR grading achieving an accuracy of 95%.

2.6 Image Enhancement Techniques for Varied and Low Contrast Images

Analysis of retinal fundus images is a difficult task because the colour fundus images suffer from the problem of varied and low contrast. Many researchers have worked on the detection of diabetic retinopathy without firstly addressing the problem of low and varied contrast. Image enhancement is one of the important tasks in the field of image processing to improve the quality of the processed image for human visual observation. To obtain a good enhanced image, it is necessary that the enhancement technique contains the required application operations because every image dataset has different problems. Most medical images need contrast normalisation, contrast enhancement and noise removing image processing operation to achieve a good enhancement. Contrast normalisation is a very important step for medical images because medical images have a problem of varying contrast because of the variation of the illumination and tiny objects in the medical images are difficult to recognise. Therefore, contrast enhancement techniques have played a vital part to enhance the tiny low contrast objects. Noise affects image quality, therefore, in order to obtain a better image quality, it is very important to remove noise and achieve more detailed information of the image. In clinical application, the medical images are analysed to diagnosis the disease at early stage such as analysis of retinal images [11], MR images [97], fluoroscopic images [98], and microscopic images [99]. It is important to help the doctors for the accurate analysis of the image data through a digital image analysis system. Many digital image enhancement techniques have been proposed by different researchers for the improved or enhanced quality of

medical images. All techniques are proposed for a solution to most of the common problems of varied and low contrast images. Due to these two issues, medical image enhancement technique can be divided into three categories, medical image normalisation for varied contrast images, image enhancement for low contrast images and medical image enhancement for both low and varied contrast images.

2.6.1 Image Normalisation for Varied Contrast Medical Images

Medical image normalisation for varied contrast is categorised into two types [100]:-

1. Prospective Contrast Normalisation
2. Retrospective Contrast Normalisation

The prospective contrast normalisation techniques require an acquisition protocol for the adjustment of the varied contrast correction. It is also known as the calibration method. Whereas, retrospective types depend upon the details in the processed image and make certain assumptions about the image setting, and are able to be used for required applications [101]. In general, prospective methods can only handle the varied contrast problem for machine failures. But, most techniques for contrast normalisation are intensively developed in retrospective methods. Most retrospective techniques can be classified into the filtering, surface filtering, segmentation based, statistical model and all of the varied contrast techniques. These are listed in Table 2.7.

Table 2.7 Varied Contrast Normalisation Techniques

Techniques	Advantages	Disadvantages
Filtering [102]	Simple Implementation. Fast operation and well performed.	Produce artefacts(creation of edge effects)
Surface Fitting [103]	Well performed if homogenous areas of the image are distinctive and large.	Estimation of a varied contrast area using intensities of one dominant region may cause some adverse information

		during the extrapolation.
Segmentation based [97]	Give better contrast normalisation through selection of the explicitly modelled objects classes.	Assumption that the distribution of image intensity is achieved by a mixture of normal distribution for selection of explicitly modelled classes is often invalid for pathological image data.
Statistical Model [104]	Its insensitiveness to pathological data and fully automatic process require no model of object classes.	Computation time and convergence performance due to its iterative optimisation.
Retinex [105]	Detail of image is increased. Increase contrast of image with uniform illumination and Reduce noise also.	Size of the image must be in the power of two.

2.6.2 Image Enhancement for low contrast Medical Images

The main task of contrast enhancement is to increase the image intensity difference to improve the image quality. Image enhancement techniques for low contrast images are divided into two categories, namely, spatial domain and frequency domain for low contrast images. The spatial domain techniques involve a process of the contrast enhancement by adjusting the luminous intensity histogram of the processed image and subsequently, it performs the enhancement process in the frequency domain of the image [3]. Some of the most used image enhancement techniques for low contrast images are shown in Table 2.8.

Table 2.8 Low Contrast Enhancement Techniques

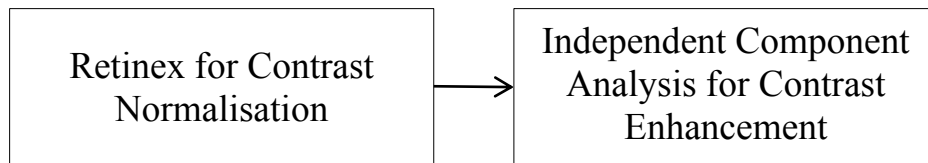
Techniques	Advantages	Disadvantages
Linear Contrast Stretching Techniques[3]	Easy to implementation, well performed enhancement by stretching certain values of histogram but must be bimodal	Losing correct value in the processed image due to possibility of having various values in output image.

Global Histogram Equalisation [106]	Effective to enhance low contrast image if the image contains one or two distinctive objects.	Over-enhanced image leading to an unwanted loss of objects visibility with presence of high peak in the histogram.
Local Histogram Equalisation [107]	Improve image local contrast and produce more detail image.	Produce noise and artefacts.
Spatial Filtering [106]	The use of more local information of image enables to enhance image details.	Ringling artefacts and noise over enhancement caused by amplification of noise and high contrast image.
Wavelet based Multi Scale [108]	Selectively enhance or degrade image features of importance in different resolution level.	The results of wavelet transform are no longer shift invariant.
Independent Component Analysis (ICA)[30]	ICA determines hidden variables which are called as the independent components of the processed data that are both non – Gaussian and statistically independent	The number of determine sources are not in the order.

2.6.3 Image Normalisation and Enhancement Technique

The non-invasive digital enhancement technique has been required to overcome the problem of varied and low contrast. The Retinal fundus images suffer from varying low contrast. These above techniques were analysed by the different researchers on different medical images but most of researchers' work contained the enhancement techniques on the retinal fundus image or any medical image. But, the colour fundus image suffered from varied contrast due to varying illumination; so, the retinal fundus image needed to be normalised first and then enhancement was performed to overcome the contrast problem in the image. Ahmad Fadzil and H.A.Nugroho *et al* [28] incorporated a non-invasive image enhancement technique called RETICA based on both normalisation and enhancement of the retinal fundus image into the computerised DR grading system (RETINO). But, RETICA has been applied on the model retinal fundus images as shown in Figure 2.8. RETICA is applied to overcome the problem of the varied and low contrast of the colour fundus

retinal images. RETICA contains two stages: Retinex for contrast normalisation and Independent component analysis for contrast enhancement. RETICA successfully achieved a good contrast improvement factor of 5.38 on retinal model images as compared to the standard contrast improvement factor of 5.79 of the FFA method. In this research, RETICA has been further studied and validated with real fundus images and analysed to improve the performance of RETICA. The Retinex and ICA algorithms are explained in the following sub-sections.



RETICA

Figure 2.8 RETICA – Image enhancement for varied and low contrast fundus images

2.6.3.1 Retinex for contrast Normalisation

The Retinex algorithm has been proposed to reduce variations that exist in the illumination in order that the observed image is entirely due to the image reflectance. Retinex theory has four rules to follow. First, three kinds of lightness are used to obtain colour; they are lightness sensation, perceived reflectance and physical reflectance. Measuring the sensation of light from the physical reflectance which will be averaged using a specific colour channel to get the perceived reflectance found in the human vision system result is the key goal of Retinex. A measurement of the ratios of intensity for the image that has been processed is taken from the surrounding area of the estimated changes in the illumination found in the event. A measurement of the lightness in that particular channel (Green, Red, and Blue) of the processed image is taken from a large area because the total of the local ratio is used to ascertain the lightness of channel that was measured over a large area. The lightness with highest value is to be calculated from a particular place in each channel (Green, Red and Blue) of the processed image, which is considered to be maximum reflectance for

that particular channel. Unlike traditional image enhancement algorithm, such as linear, non-linear transformation, image sharpening, etc. can only be enhanced to a certain type of image features, such as compression of the dynamic range of the image, or to enhance the edges of the image, Retinex can be in the dynamic range compression, edge enhancement and colour constancy achieve balance, and therefore can be performed in a variety of different types of image adaptively enhanced. Because of Retinex have many good properties, the Retinex algorithm widely used in many ways in different applications [109]. In the many applications, the Retinex-core algorithms used such as the single-scale (Single-Scale Retinex SSR) algorithm [110], multi-scale (Multi-Scale Retinex, MSR) algorithm [111] are used. In the Retinex algorithm, it is assumed that perceived reflectance depends upon the relative measure of lightness is called the lightness sensation. The Retinex intensity image has some wavelength so it is the product of illumination and reflectance at some specific wavelength as shown in Equation 2-1 and Figure 2.9.

$$I(x, y, \lambda) = L(x, y, \lambda) \cdot R(x, y, \lambda) \quad (2-1)$$

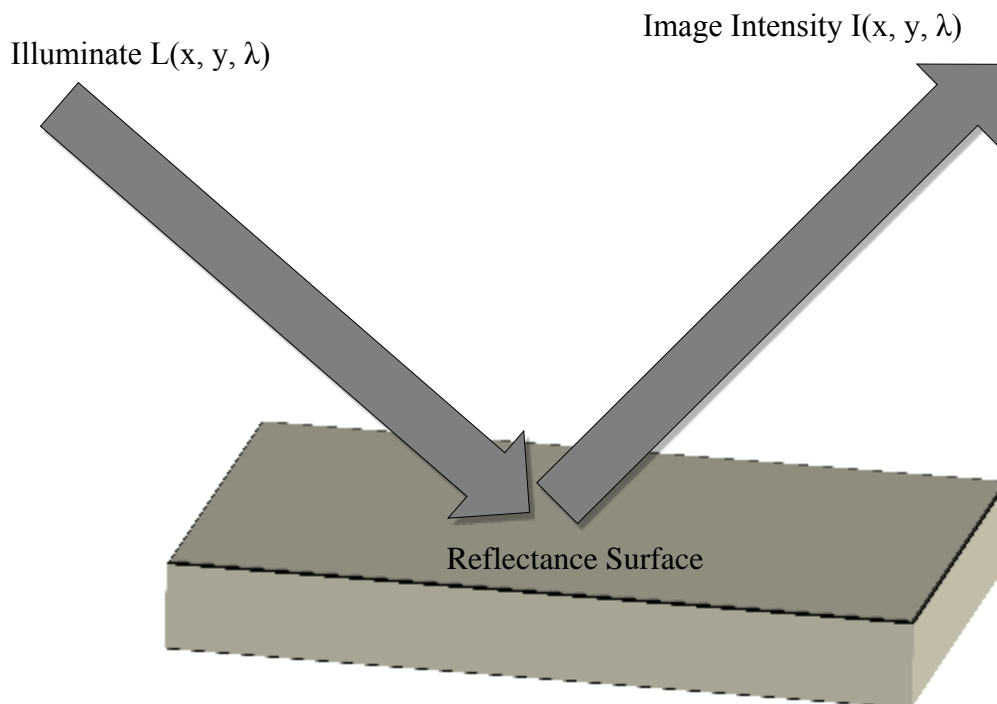


Figure 2.9 Image Formation Model

McCann *et al* [112] improved the random walk Retinex algorithm by developing the multilevel one dimensional Retinex algorithm [109]. The algorithm is based on multi-resolution pyramids and an iteration process through a ratio-product-reset-average operation. A fundamental concept behind the Retinex computation of lightness is the comparison of pixel values to that of other pixels of the image. In a multi-resolution pyramid, pixel comparison starts at the most averaged top level of the pyramid.

After computing the lightness of the image at a reduced resolution (top level pyramid), the resulting lightness values are propagated down, by pixel replication to the pyramid's next level as the initial lightness estimates at that level. The pixel comparison process continues to refine lightness estimates down to the next level as the initial lightness estimate until the new product or refined estimated lightness is computed at the bottom level of the pyramid (original image resolution).

An image pyramid is shown in Figure 2.9 [29]. The iterative Retinex algorithm processes image data according to a multi-resolution pyramid but the process depends upon the number of iterations. This iterative Retinex calculates the long distance iterations then gradually moves to short distance iterations. At each step, the spacing between the pixels being compared decreases with a one-shift pixel distance. The direction among the pixels also alters at each step in a clockwise direction. At each step, the pixel comparison is implemented to estimate the reflectance part using a ratio-product-reset-average operation [110], which is iteratively computed a certain number of times. The number of iterations is a very important parameter of the Retinex algorithm. The implementation of the McCann Retinex algorithm contains four steps described below. The flow chart of the McCann Retinex algorithm is shown in Figure 2.11 [29].

1. The input images must have dimension of $w \cdot 2^n \times h \cdot 2^n$. Where $w \geq h$ and w and h are integers in the range. This limitation arises because of different levels of image pyramid with factor of 2 as shown in Figure 2.10

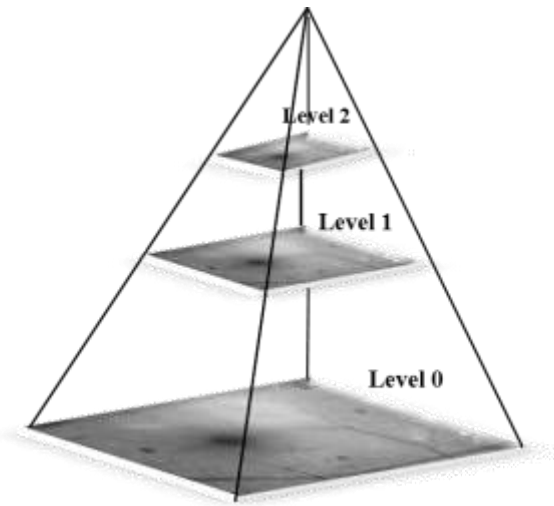


Figure 2.10 Image Pyramid

2. In first step, the log image is averaged down to the lowest resolution level. At each step, resolution level will be doubled. The number of layers in the pyramid depends on the size of the input image. The number of layers will be the greatest power of 2 as shown in Figure 2.10, dividing both the width and height of input images as calculated by the function Compute Steps in the MATLAB.
3. When the results (called new products) at one level of dimension $n \times m$ have been computed, the values are then replicated to form an old product result of image with the dimensions of $2n \times 2m$.

At all levels of pyramid, the new products are calculated for computed estimated lightness and each pixel is computed by visiting each of its (image) eight immediately neighbouring pixels in clockwise order. Each visit involves a ratio-product-reset-average operation, which is implemented by the function “CompareWithNeighbor” in MATLAB and ratio-product-reset-average operation is the main implementation of Retinex to achieve normalised image. It subtracts the neighbour’s log luminance (the ratio step) and then adds the result to the old product (the product step). If the result exceeds the maximum defined by Maximum, it is reset to Maximum (the reset step) finally, the new product for the pixel obtained by comparison to its neighbour is averaged with previous old product (average steps).

The flow chart of comparison with neighbour function is shown in Figure 2.11. Mathematically, ratio-product-reset and average operation is represented by Equation 2-2.

$$\log R * (x, y) = \frac{\text{Reset}([\log I(x,y) - \log L(x,y)] + \log R(x,y)) + \log R(x,y)}{2} \quad (2-2)$$

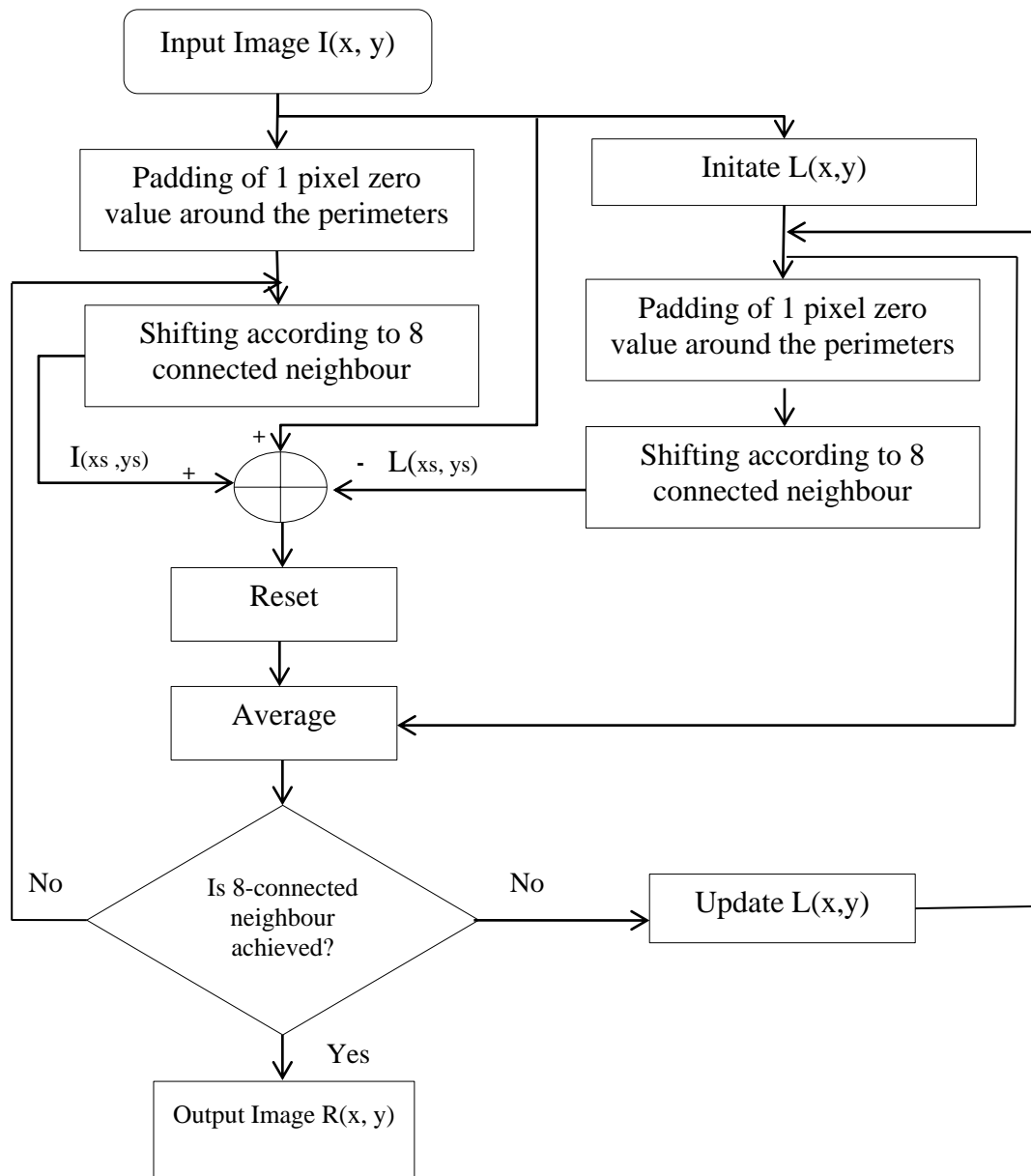


Figure 2.11 Ratio-Product-Reset-Average Operations

The term $[\log I(x,y) - \log L'(x,y)]$ represents the ratio of image with estimated illumination and the term $([\log I(x,y) - \log L'(x,y)] + \log R'(x,y))$ represents the product of ratio with initially estimated reflectance of image in the log domain. Reset operation updates the maximum intensity according to number iteration. The outcome, $\log R(x,y)^*$ is a result of averaging with $\log R'(x,y)$ and $\log R^*(x,y)$ is an updated output produced in each iteration that will be used as an input for next iteration till the final reflectance is obtained at given last iteration.

A fundamental parameter of the McCann Retinex algorithm is the number of times a pixel's neighbours are to be visited. The number of times the neighbours are cycled through each pixel, as a result, affects the distance at which pixels influence one another. This happens because new product values for all pixels are being computed in parallel, for second iteration, all neighbouring pixels have had their new products update values. In second iteration, these update values or new values contain information propagated from beyond pixels immediate neighbours. This process is continued with given number of iterations and output image is obtained that is simply the input image scaled by the image maximum value. The flow chart of whole process is shown in the Figure 2.12.

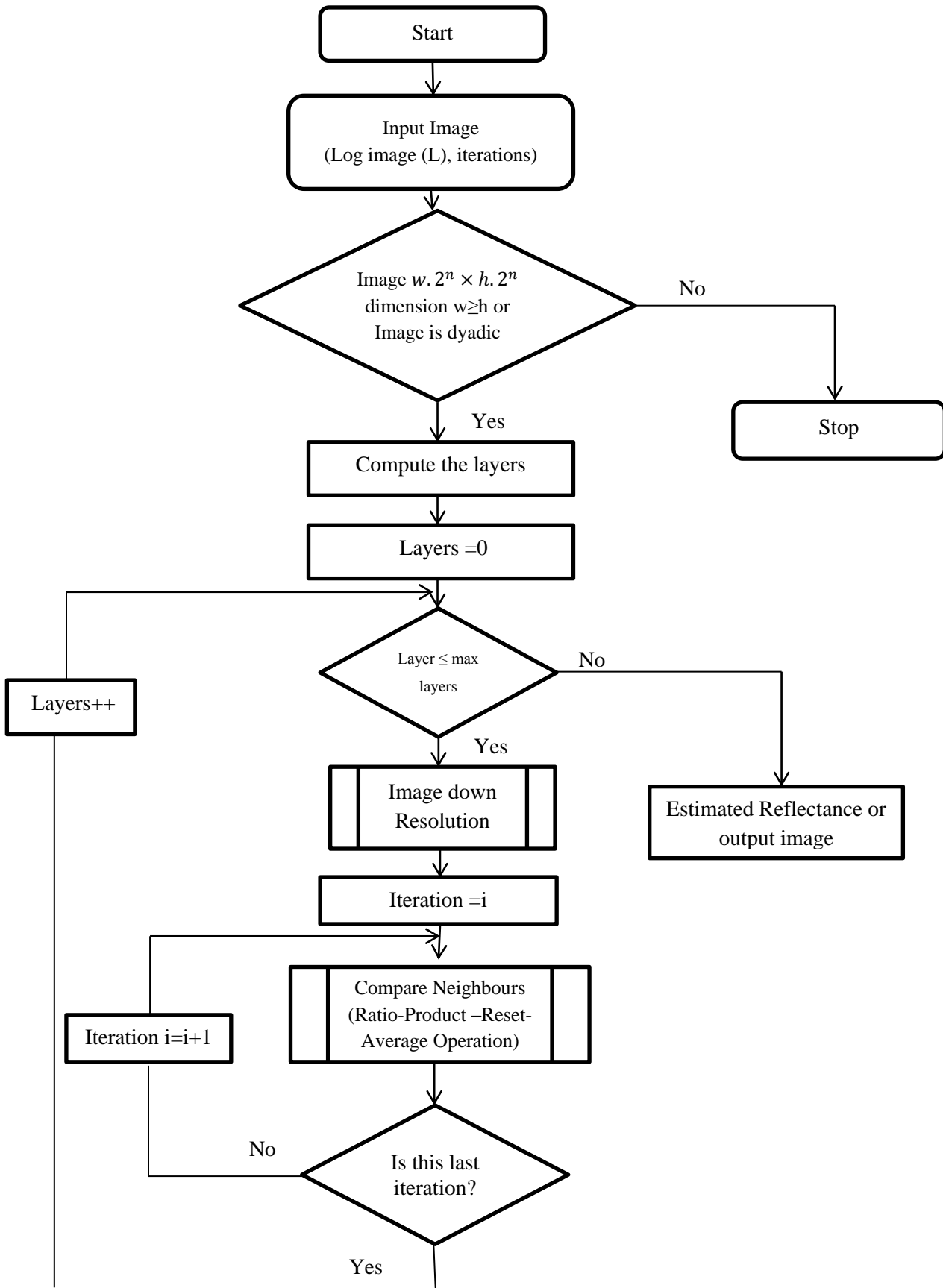


Figure 2.12 McCann99 Retinex Algorithm

2.6.3.2 Independent Component Analysis for Contrast Enhancement

Independent component analysis is used for contrast enhancement in this research work. Independent component analysis (ICA) is a blind statistical and computational technique that belongs to a class of the blind source separation for separating the mixed signals and determines the independent components from the mixed signals. ICA is a general model defined for observed multivariate data generally obtained from a large number of samples. Multivariate data consider are to be linear or non-linear mixture of some unknown hidden variables or source while the mixing process or the distribution of source is unknown as shown in Figure 2.13. A given signal (v) is generated by linear mixing (A) of independent components(s). ICA is a statistical analysis method to estimate those independent components (\hat{s}) and mixing matrix (W). The uniqueness of ICA from other methods is that it determines hidden variables which are called as the independent components of the processed data that are both non Gaussian and statistically independent [30].

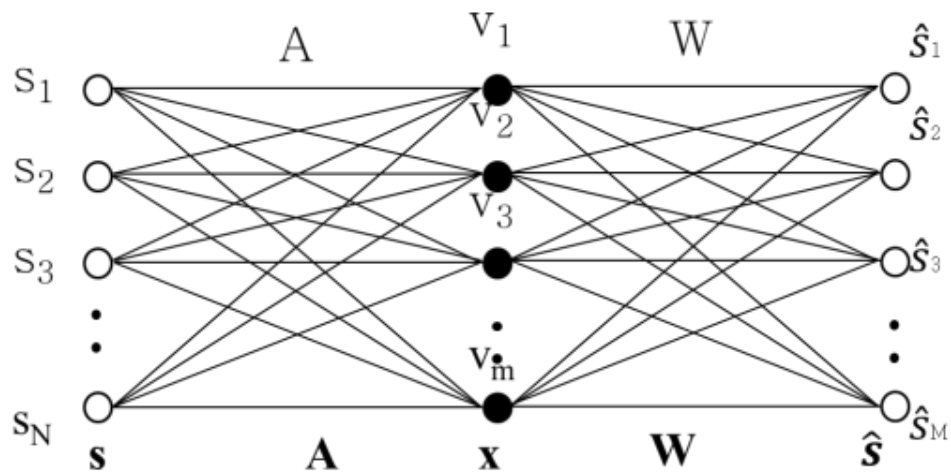


Figure 2.13 Linear ICA model

The FastICA algorithm with the symmetrical orthogonalisation is commonly used to achieve estimated independent components because of its precise accuracy and high computational speed for high dimensional data [112]. The ICA is a

technique used to determine the original signals from the mixtures of several independent sources.

In the case of retinal fundus image, the enhancement of the low contrast of the retinal blood vessels in the digital fundus image is performed by determining the retinal pigment make-up, namely Haemoglobin I_H Melanin I_M and Macular I_{MC} pigment using the ICA. The independent component due to haemoglobin exhibits higher contrast of retinal blood vessels and background (melanin and macular components).

2.7 Noise in the Medical Images

Image noise is a variation of brightness or colour information in image, and is usually an aspect of electronic noise. It can be produced by the circuitry of digital camera. In image processing, noise reduction and restoration of an image is expected to improve the qualitative inspection of an image and the performance criteria of the quantitative image analysis techniques. A digital image is inclined to a variety of noise which affects the quality of the image.

The main purpose of denoising the image is to restore the details of the original image as much as possible [2]. The criteria of the noise removal problem depend on the noise type by which the image is corrupted. In the field of reducing the image noise, several types of linear and non-linear filtering techniques have been proposed.

Different approaches for the reduction of noise and image enhancement have been considered, each of which has their own limitations and advantages. Especially, medical images are captured through imaging modalities which give noise. Due to the noise, the image details cannot be analysed properly [113]. The nature of the noise presented in the medical image modality depends upon the operation principle of the image modality as shown in Figure 2.14. Consider Figure 2.14, different medical images like X-ray images, ultrasound images and MRI (brain) images are shown. The noise affects the X-ray images due to which details of the image cannot be observed clearly; similarly, ultrasound and MRI images are affected due to noise.

But identification of these images are based on the sources of the acquisition process of the devices; like the ultrasound image that contains speckles or multiplicative noise due to the inherent characteristics of coherent imaging like ultrasound imaging.

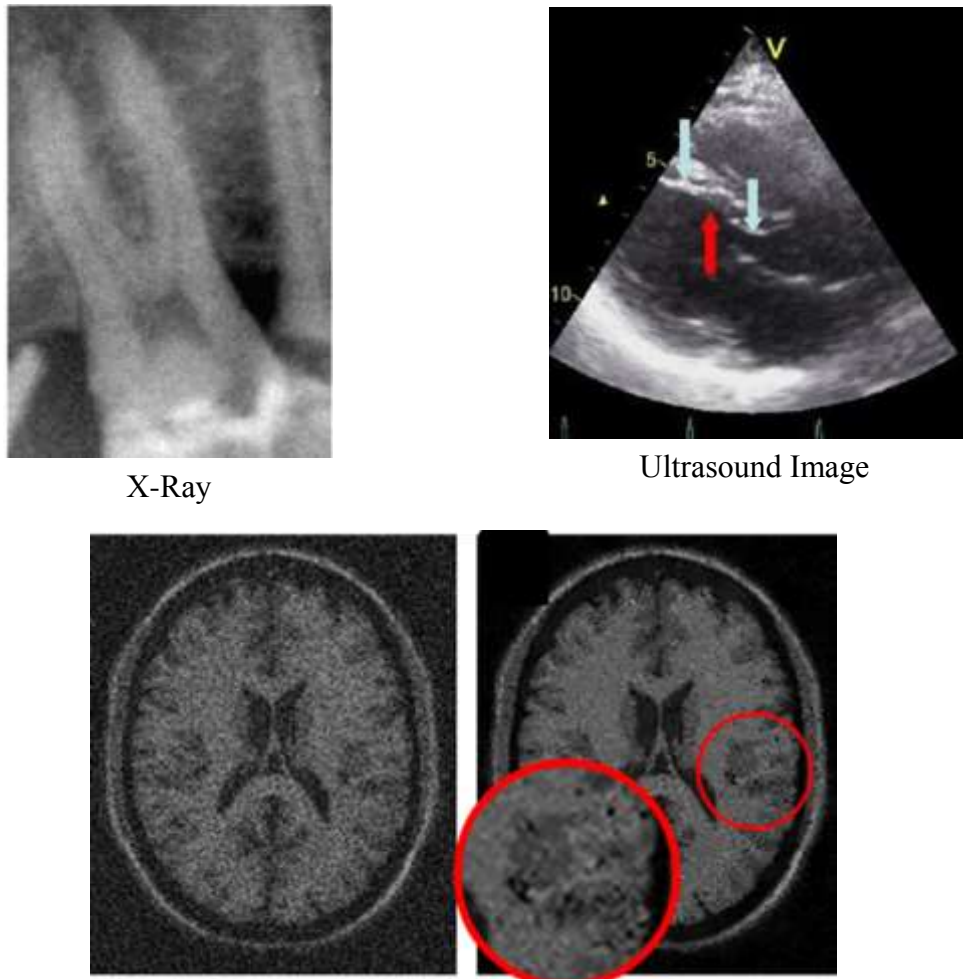


Figure 2.14 Noise in the Medical Images

2.7.1 Image Noise Models

Image restoration concerns the removal of degradation which has become a concern during the acquisition of the image. Such degradation may include noise, which are errors in the pixel values or optic effects, such as out of focus blurring. The degradation process is modelled in the Figure 2.15 as degradation function that

together with additive noise term. It contained input image $f(x, y)$ to produce degrade image $g(x, y)$. Given (x, y) , some knowledge about degradation function H and some knowledge about the additive noise term $\eta(x, y)$. The objective of restoration is to obtain an estimate $\hat{f}(x, y)$ of the original image. We want the estimate to be as close as possible to original image and in general, the more we know about H and η , the closer $\hat{f}(x, y)$ will be to $f(x, y)$. If H is a linear, position-invariant process then the degraded image is represented by Equation 2-3.

$$g(x, y) = h(x, y) * f(x, y) + \eta(x, y) \quad 2-3$$

Where $h(x, y)$ spatial representation of the degradation is function and $*$ indicates the convolution. The convolution in spatial domain is analogous to multiplication in the frequency domain, so Equation 2-3 equivalent frequency domain representation as Equation 2-4.

$$G(u, v) = H(u, v)F(u, v) + N(u, v) \quad 2-4$$

Where the term with capital letters are Fourier transform of corresponding terms in Eq 2-3. These are two basic equation image restoration processes. The degradation function $F(u, v)$ sometimes is known as the optical transfer function (OTF), it is term derived from the Fourier analysis of optical systems. In spatial domain $h(x, y)$ is referred to as the point spread function (PSF), a term that arises from letting $h(x, y)$ operate on a point of light to obtain the characteristics of the degradation for any type of input. The degradation due to linear space-invariant degradation function H can be modelled as convolution, sometimes the degradation process is referred to as “convolving the image with a PSF”. Similarly, the restoration process is sometimes referred to as deconvolution [3].

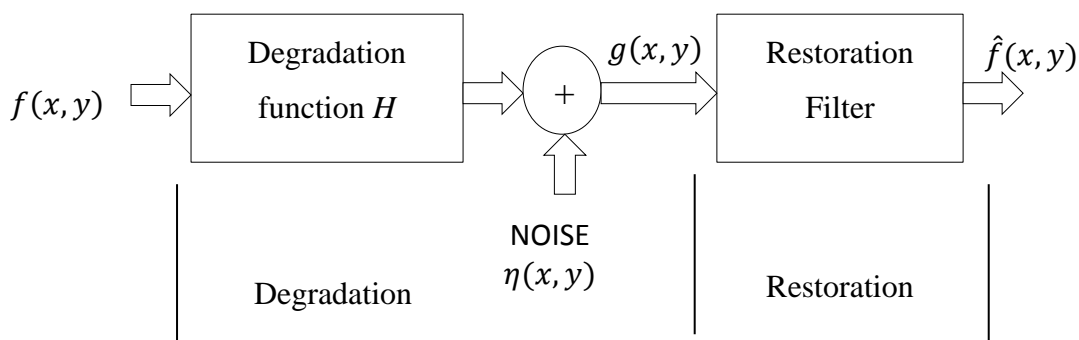


Figure 2.15 Model of Image degradation and Restoration process [3]

The main sources of noise in digital images arise during image acquisition process. The performance of imaging sensors is affected by a variety factors, such as environmental conditions during image acquisition process and by quality of the sensing elements themselves. For example in acquiring images with CCD camera, light levels and sensors temperature are major factors affecting the amount of noise in resulting image[3]. The basic noise models are defined below.

Salt and pepper noise is also known as impulse noise or shot noise or binary noise. This degradation can be caused by a sharp, sudden distribution in the image and its appearance is randomly scattered white or black pixels over the image as the example shown in Figure 2.16. Salt and pepper noise is modelled as Equation 2-5 [3]

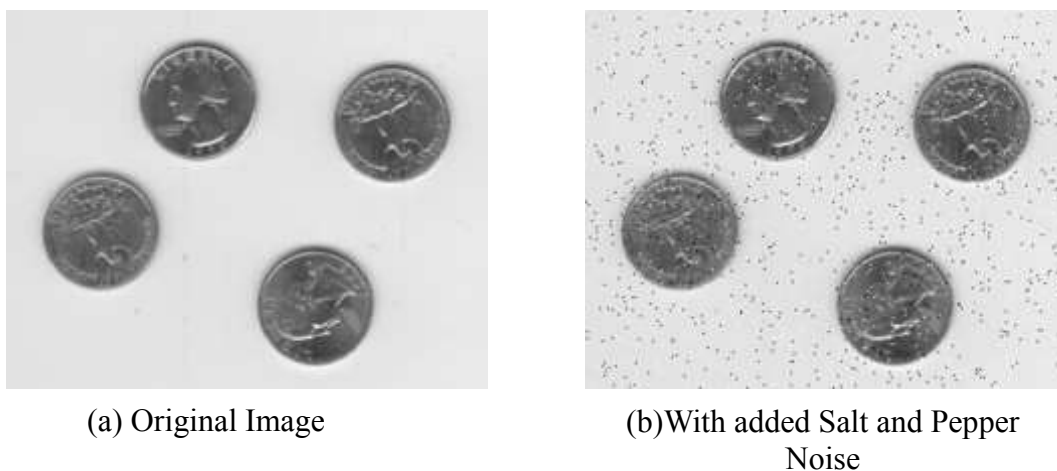


Figure 2.16 Illustration of Salt and Pepper Noise in Image

$$p(z) = \begin{cases} P_a & \text{for } a = z \\ P_b & \text{for } z = b \\ 0 & \text{otherwise} \end{cases} \quad 2-5$$

If $z > a$, intensity b will appear as light dot in the image and a will appear as a dark dot. If either P_a and P_b is zero the impulse (salt-and-pepper) noise is called unipolar. If neither probability is zero and especially if they are approximately equal to impulse noise values will resembles salt-and-pepper granules randomly distributed over the image.

Gaussian noise is an idealised form of white noise, which is caused by the random fluctuation in the signals. One can observe the white noise by watching a TV

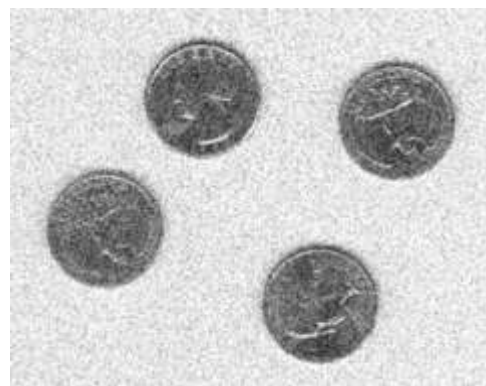
which is slightly mistuned to a particular channel. Gaussian noise is white noise which is normally disturbed. If the image is presented as I and the Gaussian noise by N, it can be modelled as a noise image by simply adding the two, I and N. Gaussian noise is also called additive noise, the Probability Density Function (PDF) of Gaussian noise is shown mathematically [3].

$$p(z) = \frac{1}{\sqrt{2\pi}\sigma} e^{-\frac{(z-\bar{z})^2}{2\sigma^2}}$$

Where z represents intensity of image or signal, \bar{z} is the mean value of z and σ is the standard deviation of image or signal. As an example the effect of Gaussian noise is shown in Figure 2.17.



(a) Original Image



(b) With Gaussian Noise

Figure 2.17 Illustration of Gaussian noise

Whereas, Gaussian noise can be modelled by random values added to an image and speckle noise can be modelled by random values multiplied by the pixel values; hence, it is also known as speckle noise. As an example, the effect of speckle noise on the image is shown in Figure 2.18.

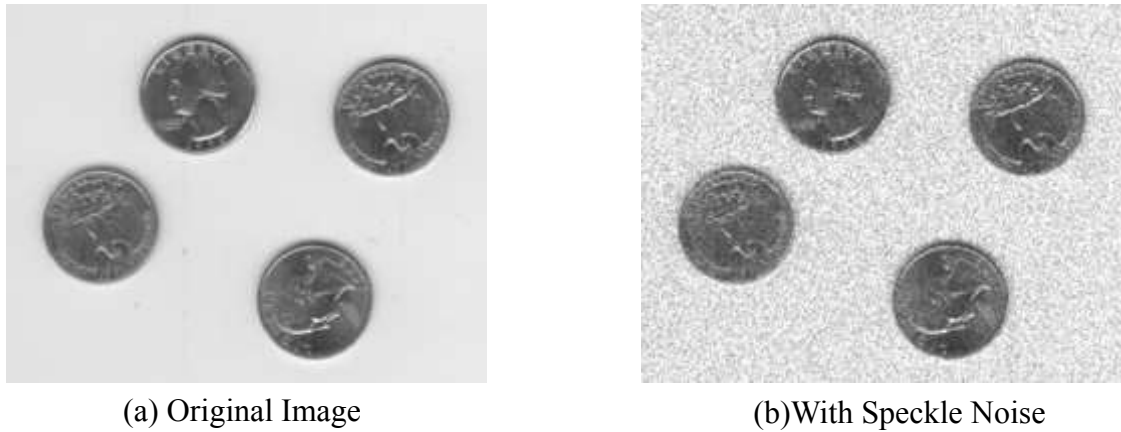


Figure 2.18 Illustration of Speckle noise

2.7.2 Noise in Retinal Fundus Image

Retinal fundus images were captured by using a fundus camera and they contained noise as shown in the Figure 2.19. When the Retinal fundus image contained noise, it was very difficult to analysis the tiny blood vessels against the surrounding background in the selected RGB macular region. The green band also contained noise. The different regions of the green band image were cropped for observation and it was clearly observable that due to the noise, the blood vessels could not be observed. This observation has been proved that without reducing the noise from the colour fundus image any enhancement and extraction of the blood vessel technique is affected. Moreover, the performance of the enhancement techniques and the extraction of the blood vessels of the retinal image technique are affected.

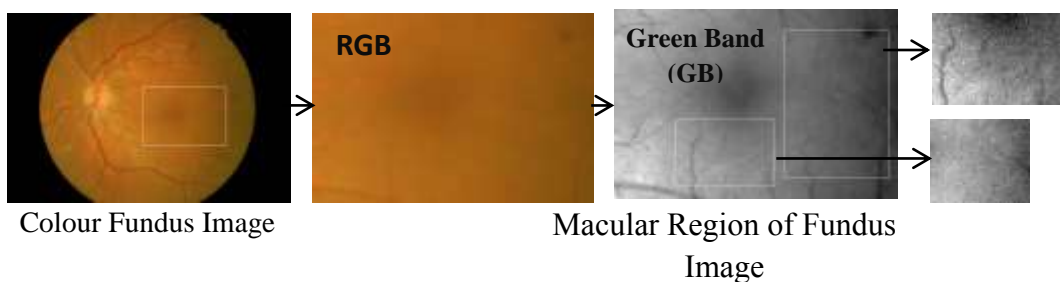


Figure 2.19 Noise in the Retinal Fundus Images

A fundus camera has a complex optical design system and according to the principle operation of the fundus camera, it contains two illumination systems: the flash tube and photo detector (camera circuitry) [4]. Noise in the retinal fundus image may be multiplicative due to the speckle flash or iteration of the patient's eye and the flash of the fundus camera. Additive noise is also present due to the circuitry of the camera electronics because no digital image is a free additive as it is captured with cameras and camera circuitry produces noise. The study of noise in the fundus image was first explained by Timothy *et al* [114]. Timothy *et al* [114] explained the effect of noise in Fundus auto fluorescence imaging. The noise occurred due to the varying illumination during the acquisition process. But Timothy also analysed the FFA image, and these images were obtained through invasive methods. For those, Timothy *et al* [114] indicated only the appearance of noise but Timothy *et al* [114] did not elaborate on the nature of the noise in the FFA images. From the literature survey, it is observed that many researchers have worked on the retinal fundus but they are working only on enhancement and detection of pathologies. However, it is very important to handle the noise first to make a better performance of the image enhancement technique. The noise issue in colour fundus images has been studied in this thesis. No one had proposed any method to identify the noise in the fundus image. However, identification of the noise type in the retinal fundus image gave significance to applying a suitable denoising method to improve the Retinal fundus image quality. It is elaborated in the chapter 4.

2.7.3 Image Denoising Methods

Image denoising problem is still a challenge for the researchers because removal of noise causes the artefacts and image blurring. Image denoising is classified into two types i.e., spatial domain filtering and transform domain filtering methods. A spatial filter is an image operation where each pixel value $I(x,y)$ is changed by a function of the intensities of pixels in a neighbourhood of (x,y) . Spatial filters can be further classified into non-linear and linear filters. A filtering method is linear when the output is a weighted sum of the input pixels such as mean filter, average filter, Wiener and Lee filter. Non-linear spatial filters cannot be calculated using just a weighted sum. Other operations (e.g. square root, log, sorting, and

selection) are involved in calculation of non-linear filters. Examples of non-linear filters are median filter and weighted median filters. Non-linear filters are not easy to implement as compared to linear spatial filters such as non-linear Lee filter, Roberts filter, and Kirsch's template filter. Non-linear filters can smooth with less blurring edges compared to linear filters and can detect edges at all orientations simultaneously, but can be slow to compute. Some of transform domain filtering are specifically used to remove the noise [24]. The purpose of transform domain filtering is to find a domain where signal can be more easily separated from noise. Transform domain filtering has three main techniques namely frequency transform, short frequency transform and wavelet transform and these techniques can be used for image denoising purpose. Wavelet transform is one of most popular method in image denoising [24]. The Fourier transform analysis is the main technique for frequency domain analysis. However, Fourier transform cannot provide any information of spectrum changes with respect to time. To overcome this limitation of Fourier transform, the Short time Fourier transform (STFT) was introduced. The short time Fourier transforms (STFT) allows representing the signals in both time and frequency domains through time windowing function. The window lengths in the STFT determine the constant time and frequency resolution. In the Short Time Fourier Transform (STFT) the fixed time-frequency resolution is used [115] to overcome this limitation of Short Time Fourier Transform (STFT) then the wavelet transform was introduced. Wavelet transform is used to analyse the signal at different frequencies with different resolutions. Figure 2.20 represents the Fourier transform and it can be observed that very good frequency localization has occurred, however, non-existing time localization has happened.

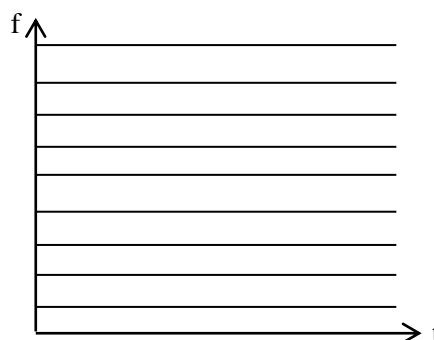


Figure 2.20 Time-Frequency Representation of Fourier Transform

Figure 2.21a and 2.21b represent the time-frequency localization of the Short-Time Fourier Transform (STFT). The operations of STFT depend upon the window size and due to fixed window size and it gives the fixed frequency localization. The fixed time –frequency resolution is one of disadvantage of STFT. STFT based on Heisenberg principle [116]. It is stated that the time and frequency localization are limited to certain bounds which lead to the fact that time-frequency elements will be equal to surface. In Figure 2.20a and 2.20b, the rectangles represent time –frequency elements. Figure 2.19a represents STFT but with better localized in frequency while Figure 2.19b represents STFT with better time localization.

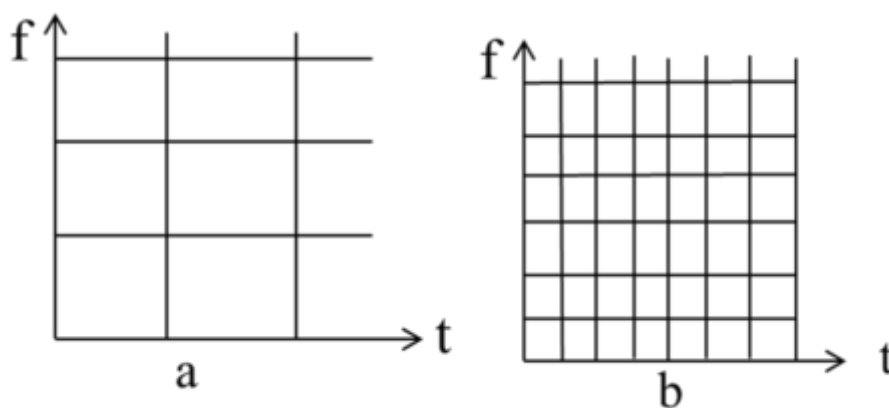


Figure 2.21 STFT Representation

In order to achieve the uniform splitting of time-frequency localisation the wavelet transform is introduced because STFT did not give uniform splitting of time-frequency localisation. Wavelet transform is shown in Figure 2.22. This particular approach is suited for most signals and images applications.

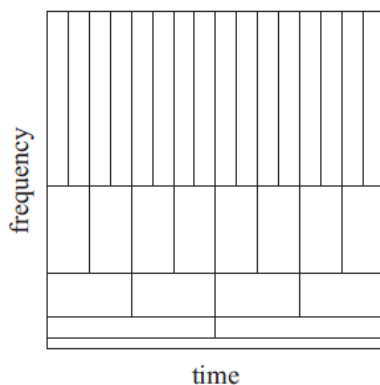


Figure 2.22 Time-Frequency Representation of Wavelet Transform

Many researchers worked on the spatial domain and transform domain to solve the problem of removal of noise from the image. Chang. *et.al* [25] highlight on an image-de-noising filter that his proposed method is based on the median filter with thresholding. In Chang *et al* [25] proposed method median filter is used to remove the noise. Authors also focused on comparative study of image de-noising techniques relying on spatial filters and transform domain filters. Subjective and objective evaluation methods are used for judging the efficiency of different types of spatial filters and transform filters applied to different types of noise. Folke *et al* [26] proposed de-noising technique that is based on combination of median and wavelets filter [26]. Image is usually corrupted by two or more different type of noise simultaneously can be denoised. But it is one of drawback of cascaded two filters for one task (removal of noise) because it takes more time and median filters [117] gave smoothness in images and wavelet produce artefacts due to its higher frequency coefficient and details of image are lost due to smoothness of median filter [22, 27].

Denoising techniques based on the subspace structure of the image have been proposed over the last decade, among them are the Least Squares (LS) and the Minimum Variance (MV) [118]. These two techniques depend on the Singular Values Decomposition (SVD) of the original image or the Eigen Decomposition (ED) of the covariance in segregating the signal subspace from the noise subspace and use this information in minimizing the distance between the noisy image and the signal subspace. The least squares and the minimum variance do achieve significant improvement in image denoising but at the expense of signal distortion. Recently a novel subspace technique is proposed that take care of signal distortion and noise reduction. This technique is an extension of the time-domain constraints estimators of Ephraim and Van Trees *et al* [119] and towards two-dimension signal (image). The technique is proposed by Nidal Kamel *et al* [120]. This technique is used for retina image denoising in this research.

The signal subspace approach was originally proposed by Ephraim and Van Trees [15] for speech enhancement applications. Extensive research works in speech enhancement had been done by different researchers by using Time-Domain

Constrained (TDC) estimators. The principle is based on to decompose the vector space of the noisy signal into a signal subspace. The noise removal is achieved by nulling the noise subspace and controlling the noise distribution in the signal (signal + residual noise) subspace. It is observed that signal distortion and residual noise (Once denoised image or signal sub-space is obtained, it is also possible that it contained noise so that noise is known residual noise and its effect the details of image, it is possible also to calculate the noise residual or residual image as it is difference between the original and denoised image [121]) cannot minimized simultaneously. Linear estimation of the clean image is performed using TDC estimator to keep residual noise energy below the threshold while minimizing the signal distortion. The method involved decomposition of noisy images into two orthogonal subspaces, signal (signal+ residual noise) subspace and noise subspace. The signal (signal+ residual noise) subspace is predominated by eigenvalues of clean image so it is termed as signal subspace.

In this research, the TDC estimator is used in retinal colour fundus image to improve the SNR of image because TDC estimator can control signal distortion and reduce the noise also. TDC estimator is based on the singular value decomposition. The Singular Value Decomposition (SVD) is used to determine the signal sub-space; the SVD is defined in below sub-section. The underlying principle of subspace denoising is to null the noise subspace and control the noise contribution in the signal subspace. Hence, the methods try to achieve a trade-off between the amount of reduced noise and signal distortion. This can be achieved by optimisation criteria which seek to minimize signal distortion while setting a user-defined upper bound on the residual noise via a control parameter and this can be achieved by using TDC estimator. The below sub-section defined SVD, description of signal and noise model with TDC estimator. Consider the Table 2.9 contained description of different denoising methods along with its strength and weakness

Table 2.9 Comparison among Image denoising methods

No	Denoising method	Description	Strengths	Weaknesses
1	Mean Filter	The value of each pixel is replaced by the	Easy to implement.	Lose the details of

		average of all the values in the local neighbourhood.		image due to blurring in the image.
2	Median Filter [19]	Replace each pixel value with the median of the gray values in the local neighborhood.	Easy to implement	Lose the details of image due to blurring in the image.
3	Wiener Filter [20]	Wiener filter is based on statistical measurement of basic parameters like standard deviation, mean and window size.	Local filtering is performed and it remove the noise while maintain the contrast also.	Wiener filter makes the image smooth and due to its smoothness image details are lost.
4	Wavelet Transform [122]	Uniform localisation of the time-frequency. Wavelet transform give good image then spatial filtering and other frequency domain filtering.	Removed the noise and give good information about the edges of image.	Produce the artifacts. The results of wavelet transform are no longer shift invariant.
5	Least Squares Estimator (LSE) [22]	It minimises the distance between noisy vectors and signal sub space and to give denoised image.	LSE is good technique to handle noise level.	LS estimator cannot control the signal distortion that affects the details of image.
6	The Minimum Variance Estimator (MVE) [23]	MVE is used to minimize the variance according to rank of matrix	MVE is much better technique to handle the noise level then LSE.	MVE estimator cannot control the signal distortion that affects the details of image.

2.7.3.1 Singular Value Decomposition (SVD)

The Singular Value Decomposition (SVD) is one strong mathematical tool for factorizing data [123]. SVD is robust orthogonal matrix decomposition method [124]. Due to SVD conceptual and stability reasons, it becomes more commonly used in signal and image processing applications. SVD is a good technique of algebraic transformation of image. SVD has many useful properties in image processing. SVD

have many properties and some properties are highly advantageous for images such as; its maximum energy packing, solving of least squares problem, computing pseudo- inverse of a matrix and multivariate analysis [125, 126]. A key property of SVD is its relation to the rank of a matrix and its ability to approximate matrices of a given rank. Digital images are often represented by low rank matrices and, therefore, able to be described by a sum of a relatively small set of Eigen values. This concept rises the manipulating of the signal as two distinct subspaces [127, 128]. SVD is constituted from two orthogonal subspaces. This property of SVD is mostly used in noise filtering to determine the signal sub-space and noise sub-space [129, 130].

SVD is based on a theorem from linear algebra which says that a rectangular matrix A can be broken down into the product of three matrices - an orthogonal matrix U, a diagonal matrix S, and the transpose of an orthogonal matrix V and this theorem is shown in Equation 2-6.

$$A_{mn} = U_{mm} S_{mn} V_{nn}^T \quad (2-6)$$

Where

$$U_{mm} = [u_1, u_2 \dots \dots \dots u_m], V_{nn} = [v_1, v_2 \dots \dots \dots v_n] \text{ and } S_{mn} = \begin{bmatrix} \sigma_1 & & \\ & \sigma_2 & \\ & & \sigma_n \end{bmatrix} \text{ here}$$

Where $U^T U = I$, $V^T V = I$; the columns of U are orthonormal eigenvectors of AA^T , the columns of V are orthonormal eigenvectors of $A^T A$ and S is a diagonal matrix containing the square roots of eigenvalues ($[\sigma_1, \sigma_2 \dots \dots \sigma_n]$) from U or V in descending order [131]. For example, consider matrix A

$$A = \begin{bmatrix} 3 & 1 & 1 \\ -1 & 3 & 1 \end{bmatrix}$$

In order to find U we have to start with AA^T . The transpose of A is

$$A = \begin{bmatrix} 3 & -1 \\ 1 & 3 \\ 1 & 1 \end{bmatrix}$$

$$AA^T = \begin{bmatrix} 3 & 1 & 1 \\ -1 & 3 & 1 \end{bmatrix} \begin{bmatrix} 3 & -1 \\ 1 & 3 \\ 1 & 1 \end{bmatrix} = \begin{bmatrix} 11 & 1 \\ 1 & 11 \end{bmatrix}$$

Next, we have to find the eigenvalues and corresponding eigenvectors of AA^T . We know that eigenvectors are represented by the equation $Au = \lambda u$. Where A is a square matrix of data, λ is a scalar value known as eigenvalue also, and v is the eigenvector and applying this to AA^T gives us

$$Au = \lambda u = \begin{bmatrix} 11 & 1 \\ 1 & 11 \end{bmatrix} \begin{bmatrix} u_1 \\ u_2 \end{bmatrix} = \lambda \begin{bmatrix} u_1 \\ u_2 \end{bmatrix}$$

This represents the system of equations

$$11u_1 + u_2 = \lambda u_1 = (11 - \lambda)u_1 + u_2 = 0 \quad 2-7$$

$$u_1 + 11u_2 = \lambda u_2 = u_1 + (11 - \lambda)u_2 = 0 \quad 2-8$$

Solve for λ by setting the determinant of the co-efficient matrix to zero,

$$\begin{vmatrix} (11 - \lambda) & 1 \\ 1 & (11 - \lambda) \end{vmatrix} = 0$$

It work out as

$$(11 - \lambda)(11 - \lambda) - 1.1 = 0 \quad (2-9)$$

$$(\lambda - 10)(\lambda - 12) = 0 \quad (2-10)$$

$$\lambda = 10, \lambda = 12 \quad (2-11)$$

It gives us two eigenvalues $\lambda = 10, \lambda = 12$. Plugging λ back in to the original Equation 2-7 and 2-8 and it gives us eigenvectors u_1 and u_2 . For $\lambda = 10$ we get

$$(11 - \lambda)u_1 + u_2 = 0$$

$$(11 - 10)u_1 + u_2 = 0$$

$$u_1 + u_2 = 0$$

$$u_1 = -u_2$$

Which is true for lots of values, so we'll pick $u_1 = 1$ and $u_2 = -1$ since those are small and easier to work with. Thus, we have the eigenvector $[1, -1]$ corresponding to the eigenvalue $\lambda = 10$. For $\lambda = 12$ we have

$$\begin{aligned}u_1 + (11 - \lambda)u_2 &= 0 \\u_1 + (11 - 12)u_2 &= 0 \\u_1 - u_2 &= 0 \\u_1 &= u_2\end{aligned}$$

For the same reason as before we'll take $u_1 = 1$ and $u_2 = 1$. Now, for $\lambda = 12$ we have the eigenvector $[1, 1]$. These eigenvectors become column vectors in a matrix ordered by the size of the corresponding eigenvalue. In other words, the eigenvector of the largest eigenvalue is column one, the eigenvector of the next largest eigenvalue is column two, and so forth and so on until we have the eigenvector of the smallest eigenvalue as the last column of our matrix. In the matrix below, the eigenvector for $\lambda = 12$ is column one, and the eigenvector for $\lambda = 10$ is column two.

$$\begin{bmatrix} 1 & 1 \\ 1 & -1 \end{bmatrix}$$

Finally, we have to convert this matrix into an orthogonal matrix which we do by applying the Gram-Schmidt orthonormalisation process to the column vectors[132]. Below Equations are used for orthogonal matrix conversion.

$$u_1 = \frac{u_1}{|u_1|} = \frac{[1, 1]}{\sqrt{1^2 + 1^2}} = \frac{[1, 1]}{\sqrt{2}} = \left[\frac{1}{\sqrt{2}}, \frac{1}{\sqrt{2}} \right]$$

Similarly u_2

$$u_2 = \frac{u_2}{|u_2|} = \frac{[1, -1]}{\sqrt{1^2 + (-1)^2}} = \frac{[1, -1]}{\sqrt{2}} = \left[\frac{1}{\sqrt{2}}, \frac{-1}{\sqrt{2}} \right]$$

It gives

$$U = \begin{bmatrix} \frac{1}{\sqrt{2}} & \frac{1}{\sqrt{2}} \\ \frac{1}{\sqrt{2}} & -\frac{1}{\sqrt{2}} \end{bmatrix}$$

The calculation of V is similar. V is based on $A^T A$, so we have

$$A^T A = \begin{bmatrix} 3 & -1 \\ 1 & 3 \\ 1 & 1 \end{bmatrix} \begin{bmatrix} 3 & 1 & 1 \\ -1 & 3 & 1 \end{bmatrix} = \begin{bmatrix} 10 & 0 & 2 \\ 0 & 10 & 4 \\ 2 & 4 & 4 \end{bmatrix}$$

Find the eigenvalues of $A^T A$ by

$$A v = \lambda v = \begin{bmatrix} 10 & 0 & 2 \\ 0 & 10 & 4 \\ 2 & 4 & 2 \end{bmatrix} \begin{bmatrix} v_1 \\ v_2 \\ v_3 \end{bmatrix} = \lambda \begin{bmatrix} v_1 \\ v_2 \\ v_3 \end{bmatrix}$$

This represents the system of equations

$$10v_1 + 2v_3 = \lambda v_1$$

$$10v_2 + 4v_3 = \lambda v_2$$

$$2v_1 + 4v_2 + 2v_3 = \lambda v_3$$

These equations can rewrite as

$$(10 - \lambda)v_1 + 2v_3 = 0 \tag{2-12}$$

$$(10 - \lambda)v_2 + 4v_3 = 0 \tag{2-13}$$

$$2v_1 + 4v_2 + (2 - \lambda)v_3 = 0 \tag{2-14}$$

This can be solved as

$$\begin{vmatrix} (10 - \lambda) & 0 & 2 \\ 0 & (10 - \lambda) & 4 \\ 2 & 4 & (2 - \lambda) \end{vmatrix} = 0$$

This will be solve as

$$(10 - \lambda) \begin{vmatrix} (10 - \lambda) & 4 \\ 4 & (2 - \lambda) \end{vmatrix} + 2 \begin{vmatrix} 0 & (10 - \lambda) \\ 2 & 4 \end{vmatrix} = 0$$

$$(10 - \lambda)[(10 - \lambda)(2 - \lambda) - 16] + 2[0 - 2(10 - \lambda)] = 0$$

$$\lambda(\lambda - 10)(\lambda - 10)$$

so $\lambda = 0$, $\lambda = 10$, $\lambda = 12$ are the eigenvalues for $A^T A$. Substituting λ back into the original Equations 2-7 to find corresponding eigenvectors yields for $\lambda = 12$

$$(10 - \lambda)v_1 + 2v_3 = 0$$

$$(10 - 12)v_1 + 2v_3 = 0$$

$$-2v_1 + 2v_3 = 0$$

$$v_1 = v_3$$

$$v_1 = 1, v_3 = 1$$

Put v_1 and v_3 in Equation 2-9.

$$2v_1 + 4v_2 + (2 - 12)v_3 = 0$$

$$2 + 4v_2 - 10 = 0$$

$$4v_2 = 8$$

$$v_2 = 2$$

So for $\lambda = 12$, $V_1 = [1, 2, 1]$. For $\lambda = 10$ we have

$$(10 - \lambda)v_1 + 2v_3 = 0$$

$$(10 - 10)v_1 + 2v_3 = 0$$

$$v_3 = 0$$

Put v_3 in Equation 2-9

$$2v_1 + 4v_2 + (2 - \lambda)v_3 = 0$$

$$2v_1 + 4v_2 + (2 - \lambda) * 0 = 0$$

$$2v_1 + 4v_2 = 0$$

$$2v_1 = 4v_2$$

$$v_1 = -2v_2$$

$$v_1 = 2, v_2 = -1$$

Which means for $\lambda = 10$, $V_2 = [2, -1, 0]$. For $\lambda = 0$ put in Equation 2-6.

$$(10 - 0)v_1 + 2v_3$$

$$10v_1 = -2v_3$$

$$v_3 = -5$$

Put $v_3 = 5$ and $\lambda = 0$ in Equation 2-8

$$(10 - 0)v_2 + 4 * 5 = 0$$

$$10v_2 - 20 = 0$$

$$v_2 = 2$$

Put $v_3 = 5$, $v_2 = 2$ and $\lambda = 0$ in Equation 2-9

$$2v_1 + 4v_2 + (2 - \lambda)v_3 = 0$$

$$2v_1 + 4 * 2 + (2 - 0) * (-5) = 0$$

$$2v_1 = 2$$

$$v_1 = 1$$

Which means for $\lambda = 0$, $V_3 = [1, 2, -5]$. Order V_1, V_2, V_3 as column vectors in a matrix according to the size of the eigenvalue to get

$$V = \begin{bmatrix} 1 & 2 & 1 \\ 2 & -1 & 2 \\ 1 & 0 & -5 \end{bmatrix}$$

Finally, we have to convert this matrix into an orthogonal matrix which we do by applying the Gram-Schmidt orthonormalisation process to the column vectors [132]. Below Equations are used for orthogonal matrix conversion.

$$v_1 = \frac{v_1}{|v_1|} = \frac{[1, 2, 1]}{\sqrt{1^2 + 2^2 + 1^2}} = \frac{[1, 2, 1]}{\sqrt{6}} = \left[\frac{1}{\sqrt{6}}, \frac{2}{\sqrt{6}}, \frac{1}{\sqrt{6}} \right]$$

$$v_2 = \frac{v_2}{|v_2|} = \frac{[2, -1, 0]}{\sqrt{2^2 + (-1)^2}} = \frac{[2, -1, 0]}{\sqrt{5}} = \left[\frac{2}{\sqrt{5}}, \frac{-1}{\sqrt{5}}, 0 \right]$$

$$v_3 = \frac{v_3}{|v_3|} = \frac{[1, 2, -5]}{\sqrt{1^2 + 2^2 + (-5)^2}} = \frac{[1, 2, -5]}{\sqrt{30}} = \left[\frac{1}{\sqrt{30}}, \frac{2}{\sqrt{30}}, \frac{-5}{\sqrt{30}} \right]$$

The V matrix is

$$V = \begin{bmatrix} \frac{1}{\sqrt{6}} & \frac{2}{\sqrt{5}} & \frac{1}{\sqrt{30}} \\ \frac{2}{\sqrt{6}} & \frac{-1}{\sqrt{5}} & \frac{2}{\sqrt{30}} \\ \frac{1}{\sqrt{6}} & 0 & \frac{-5}{\sqrt{30}} \end{bmatrix}$$

According to SVD theorem (Equation 2-2) , V matrix is transpose V^T is

$$V^T = \begin{bmatrix} \frac{1}{\sqrt{6}} & \frac{2}{\sqrt{6}} & \frac{1}{\sqrt{30}} \\ \frac{2}{\sqrt{5}} & \frac{-1}{\sqrt{5}} & 0 \\ \frac{1}{\sqrt{6}} & 0 & \frac{-5}{\sqrt{30}} \end{bmatrix}$$

For S we take the square roots of the non-zero eigenvalues and populate the diagonal with them, putting the largest in S_{11} , the next largest in S_{22} and so on until the smallest value ends up in S_{mn} . The non-zero eigenvalues of U and V are always the same, so that's why it doesn't matter which one we take them. The diagonal entries in S are the singular values of A, the columns in U are called left singular vectors, and the columns in V are called right singular vectors as shown in below matrix.

$$S = \begin{bmatrix} \sqrt{12} & 0 & 0 \\ 0 & \sqrt{10} & 0 \end{bmatrix}$$

We have SVD equation

$$A_{mn} = U_{mn} S_{mn} V_{nn}^T$$

$$A_{mn} = \begin{bmatrix} \frac{1}{\sqrt{2}} & \frac{1}{\sqrt{2}} \\ 1 & -\frac{1}{\sqrt{2}} \\ \frac{1}{\sqrt{2}} & -\frac{1}{\sqrt{2}} \end{bmatrix} \begin{bmatrix} \sqrt{12} & 0 & 0 \\ 0 & \sqrt{10} & 0 \end{bmatrix} \begin{bmatrix} \frac{1}{\sqrt{6}} & \frac{2}{\sqrt{6}} & \frac{1}{\sqrt{6}} \\ \frac{2}{\sqrt{5}} & \frac{-1}{\sqrt{5}} & 0 \\ \frac{1}{\sqrt{30}} & \frac{2}{\sqrt{30}} & \frac{-5}{\sqrt{30}} \end{bmatrix}$$

$$A_{mn} = \begin{bmatrix} \sqrt{12} & \sqrt{10} & 0 \\ \frac{1}{\sqrt{2}} & \frac{1}{\sqrt{2}} & 0 \\ \sqrt{12} & -\sqrt{10} & 0 \\ \frac{1}{\sqrt{2}} & -\frac{1}{\sqrt{2}} & 0 \end{bmatrix} \begin{bmatrix} \frac{1}{\sqrt{6}} & \frac{2}{\sqrt{6}} & \frac{1}{\sqrt{6}} \\ \frac{2}{\sqrt{5}} & \frac{-1}{\sqrt{5}} & 0 \\ \frac{1}{\sqrt{30}} & \frac{2}{\sqrt{30}} & \frac{-5}{\sqrt{30}} \end{bmatrix}$$

$$A_{mn} = \begin{bmatrix} 3 & 1 & 1 \\ -1 & 3 & 1 \end{bmatrix}$$

A_{mn} is required singular value decomposition matrix. A_{mn} is also known as signal sub-space and TDC estimator is defined in next section because TDC estimator is used to to keep residual noise energy below the threshold while minimizing the signal distortion and TDC estimator give image without noise, well contrast image and maintain image details. It is very important to understand the signal and noise model before explain the TDC estimator and the both section (Signal and noise model and TDC estimator) are explained in following sub-sections.

2.7.3.2 Signal and Noise Model

An image signal is short window, can be considered as wide sense stationary process, and thus can be represented by a linear stochastic model of the form as Equation 2-15.

$$X = H\theta \quad (2-15)$$

Where $X \in \mathbb{R}^{m \times n}$ a matrix of random samples is whose rank is $n < m$, $H \in \mathbb{R}^{m \times m}$ is a model matrix and $\theta \in \mathbb{R}^{m \times n}$ is zero mean random co-efficient matrix

drawn from multivariate distribution. Let consider an image is corrupted by additive independent white noise, N and uncorrelated with the clean signal, the $m \times n$ matrix of noisy image Y is given by Equation 2-16.

$$Y = X + N \quad (2-16)$$

Where $N \in \mathbb{R}^{m \times n}$ is the noise matrix and $X \in \mathbb{R}^{m \times n}$ is the clean image. Given the observed noisy signal, we wish to estimate the clean signal, X as accurate as possible according to some criteria. This is a classical problem in estimation theory. If H is the $m \times m$ filter matrix, then the linear estimator of the clean image given Y is equal to

$$\hat{X} = YH \quad (2-17)$$

The discussed noisy signals are realization of stochastic processes, which mean that the analysis of subspace methods is based on correlation matrices. First, consider the correlation matrix of the original image defined by the linear model of Equation 2-15, i.e.

$$R_X = E\{XX^T\} = E\{H\theta\theta^T H^T\} = HR_\theta H^T$$

Where $R_\theta = E\{\theta\theta^T\}$. The rank of R_X is r and this matrix has $(m - r)$ zero eigenvalues. Similarly, let the correlation matrix of the noise vector be denoted by $R_N = E\{NN^T\}$. When considering second order statistics, it is useful to assume the following two assumptions.

1. The element of X and N are uncorrelated ,i.e. $R_{XN} = 0, R_{NX} = 0$.
2. The noise is white with variance ϑ_n^2 i.e $R_N = \vartheta_n^2 I$.

The second assumption is based on the fact that the correlation matrix of noise is known and the mathematical approach of the estimators makes use of eigenvalue-decomposition (EVD) of covariance matrices R_Y , R_X and R_N given by Equation 2-18.

$$R_Y = R_N + R_X \quad (2-18)$$

It is clear that the noise power is uniformly distributed in the entire Euclidean space, while the image signal is confined to r dimensional subspace. In practical

scenario, the exact knowledge of the second-order statistic R_X is not available, but it is estimated from the noisy signal.

2.7.3.3 Time-Domain Constrained (TDC) Estimator

A novel subspace technique is proposed that take care of signal distortion and noise reduction and it is known as Time-Domain Constrained (TDC) Estimator. This technique is an extension of the time-domain constraints estimators of Ephraim et [119] towards two-dimension signal (image). Consider the estimated signal, \hat{X} in Equation 2-16. The error signal obtained in this estimation is given by

$$\epsilon = \hat{X} - X$$

The estimated signal according Equation 2-17 is $\hat{X} = YH$ then error signal become

$$\epsilon = YH - X$$

According to Equation 2-16, $Y = X + N$

$$\epsilon = (X + N)H - X$$

$$\epsilon = XH + NH - X$$

$$\epsilon = (H - I)X + HN \quad (2-19)$$

Where $(H - I)X$ is signal distortion and it is represented as ϵ_X and HN is residual noise and it is represented as ϵ_N [119]. The energy of $m \times n$ matrix of signal distortion and residual noise is equal to Frobenius norm given as,

$$\epsilon_X^2 = \|\epsilon_X\|_2^2 = \text{tr}\{\epsilon_X \epsilon_X^T\} = \text{tr}\{(H - I)R_s(H - I)^T\} \quad (2-20)$$

$$\epsilon_N^2 = \|\epsilon_N\|_2^2 = \text{tr}\{\epsilon_N \epsilon_N^T\} = \text{tr}\{H(NN^T)H^T\} = \text{tr}\{HR_NH^T\} \quad (2-21)$$

Where tr is matrix trace and it is defined as sum of diagonal elements of matrix.

Now, assuming known value of R_N , a TDC estimator [119] keeps the residual noise energy, below some threshold while minimizing the signal distortion energy. The optimum linear estimator can be obtained by solving a constrained optimization problem

$$\min_H \varepsilon_X^2 \text{ subject to } \frac{1}{m} \varepsilon_N^2 \leq \sigma^2 \quad (2-22)$$

where σ^2 is a positive constant and m is the rank of matrix. The constrained minimization described in Equation 2-22 can be solved using the method of Lagrange multipliers [133]. This means that, H is a stationary feasible point if it satisfies the gradient equation of Lagrangian [133],

$$\begin{aligned} \mathcal{L}(H, \lambda) &= \varepsilon_s^2 + \lambda(\varepsilon_N^2 - m\sigma^2) \\ \mathcal{L}(H, \lambda) &= \text{tr}\{(H - I)R_x(H - I)^T\} + \lambda(\text{tr}\{HR_nH^T\} - m\sigma^2) \end{aligned} \quad (2-23)$$

where $\lambda \geq 0$ is the Lagrangian multiplier, where λ is the Lagrangian multiplier

$$\lambda(\varepsilon_N^2 - m\sigma^2) = \lambda(\text{tr}\{HR_nH^T\} - m\sigma^2) = 0 \text{ for } \lambda \geq 0 \quad (2-24)$$

From $\nabla_H \mathcal{L}(H, \lambda)$ we obtained

$$\nabla_H \mathcal{L}(H, \lambda) = 2(H - I)R_x + 2\lambda HR_n = 0 \quad (2-25)$$

It gives

$$H_{TDC} = R_x(R_x + \lambda R_N)^{-1} \quad (2-26)$$

In the case of N being white, $R_N = \vartheta_n^2 I$, where ϑ_n^2 is the noise variance, and I , is the identity matrix, the optimal estimator H , can be written as

$$H_{TDC} = R_x(R_x + \lambda \vartheta_n^2 I)^{-1} \quad (2-27)$$

Also from Equation 2-123 and 2-25, it can be shown that σ^2 should satisfy

$$\sigma^2 = \frac{1}{m} \text{tr}(R_x((R_x + \lambda R_N)^{-1} R_N (R_x + \lambda R_N)^{-1} R_x)) \quad (2-28)$$

Equation 2-21 indicates that if λ varies from 0 to ∞ then it causes the σ^2 to vary from $\frac{1}{m} \text{tr}(R_N)$ to 0. This means that the estimator does not add noise to the estimated signal. Note that the value of λ depends on image and noise level. Now, Equation 2-27 can be simplified using the singular value decomposition of $R_x = U\Delta_X U^T$ to

$$H_{TDC} = U\Delta_X(\Delta_X + \lambda \vartheta_n^2 I)U^T \quad (2-29)$$

Where the U is the unitary eigenvectors matrix and Δ_X is the diagonal eigenvalue matrix of R_x . TDC is successfully applied and as example consider matrix A ,

$$A = \begin{bmatrix} 3 & 1 & 1 \\ -1 & 3 & 1 \end{bmatrix}$$

Perform the SVD on the matrix and achieved SVD components are given below (Referred section 2.7.3.1 for SVD calculation).

Where

$$U = \begin{bmatrix} \frac{1}{\sqrt{2}} & \frac{1}{\sqrt{2}} \\ 1 & -1 \\ \frac{1}{\sqrt{2}} & -\frac{1}{\sqrt{2}} \end{bmatrix}, V = \begin{bmatrix} \frac{1}{\sqrt{6}} & \frac{2}{\sqrt{6}} & \frac{1}{\sqrt{6}} \\ 2 & -1 & 0 \\ \frac{1}{\sqrt{5}} & \frac{1}{\sqrt{5}} & 0 \\ 1 & 2 & -5 \\ \frac{1}{\sqrt{30}} & \frac{2}{\sqrt{30}} & \frac{-5}{\sqrt{30}} \end{bmatrix} D = \begin{bmatrix} \sqrt{12} & 0 & 0 \\ 0 & \sqrt{10} & 0 \end{bmatrix}$$

According to the Equation 2-23 $H_{TDC} = U\Delta_X(\Delta_X + \lambda\theta_n^2 I)U^T$ and Δ_X is diagonal value of R_x and R_x is equal to $R_x = AA^T$.

$$R_x = \begin{bmatrix} 3 & 1 & 1 \\ -1 & 3 & 1 \end{bmatrix} \begin{bmatrix} 3 & -1 \\ 1 & 3 \\ 1 & 1 \end{bmatrix} = \begin{bmatrix} 11 & 1 \\ 1 & 11 \end{bmatrix}$$

But Δ_X is the diagonal matrix of its Eigen value of R_x and its Eigen values are 12 and 10 then Δ_X becomes

$$\Delta_X = \begin{bmatrix} 12 & 0 \\ 0 & 10 \end{bmatrix}$$

The transpose of U is

$$U^T = \begin{bmatrix} \frac{1}{\sqrt{2}} & \frac{1}{\sqrt{2}} \\ 1 & -1 \\ \frac{1}{\sqrt{2}} & -\frac{1}{\sqrt{2}} \end{bmatrix}$$

According to Equation 2-23 to determine the TDC estimated image H_{TDC}

$$H_{TDC} = U\Delta_X(\Delta_X + \lambda\theta_n^2 I)U^T$$

$$H_{TDC} = \begin{bmatrix} \frac{1}{\sqrt{2}} & \frac{1}{\sqrt{2}} \\ \frac{1}{\sqrt{2}} & -\frac{1}{\sqrt{2}} \end{bmatrix} \left(\begin{bmatrix} 12 & 0 \\ 0 & 10 \end{bmatrix} \left(\begin{bmatrix} 12 & 0 \\ 0 & 10 \end{bmatrix} + \begin{bmatrix} 1 & 0 \\ 0 & 1 \end{bmatrix} \right) \begin{bmatrix} \frac{1}{\sqrt{2}} & \frac{1}{\sqrt{2}} \\ \frac{1}{\sqrt{2}} & -\frac{1}{\sqrt{2}} \end{bmatrix} \right)$$

Resultant H_{TDC} signal is

$$H_{TDC} = \begin{bmatrix} 133 & 23 \\ 23 & 133 \end{bmatrix}$$

When applied on the signals and images, TDCE achieved the better results in terms of noise reduction (performance is evaluated by measuring SNR of images) while preserving image details as shown in Figure 2.23 and 2.24 [134].

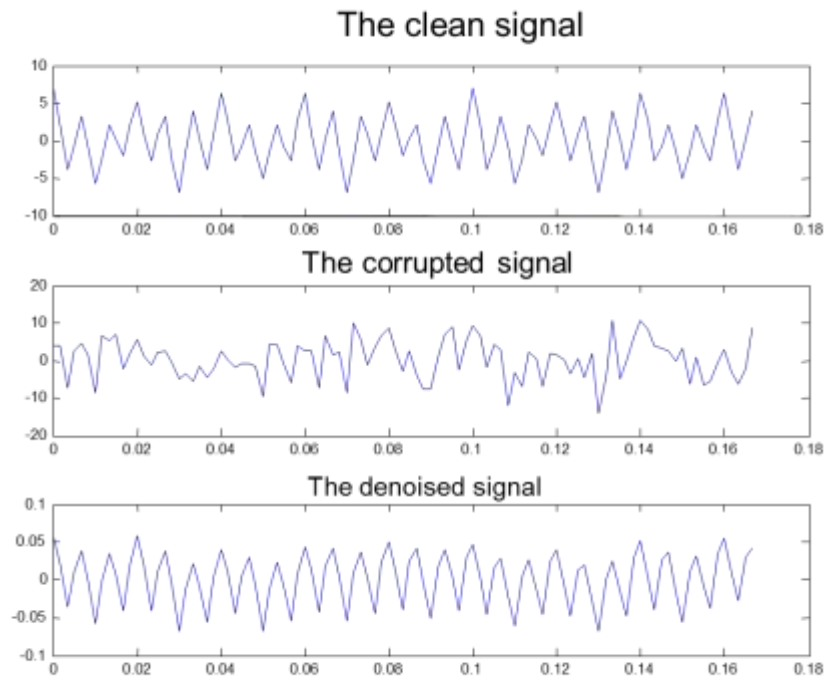


Figure 2.23 TDCE on Signal [6]



Noisy Image



Denoised Image



Noisy Image



Denoised Image

Figure 2.24 TDCE on Standard Test Images

2.8 Summary

Diabetic Retinopathy is the damage of the retinal vasculature that is a common complication of the diabetes mellitus disease. It is estimated that 75% of the people with diabetic retinopathy are living in developing countries. Eye screening is important for the detection of diabetic retinopathy [32]. DR has five stages No-DR to PDR but the progression of DR starts from Mild NPDR to Severe NPDR and ends with PDR, which is the complete vision loss stage. These DR categories are characterised by the presence of pathologies, such as haemorrhages, exudates and changes in the veins.

There are basically two ways to acquire fundus image, i.e., the Fundus fluorescein angiogram image (invasive method) and digital colour fundus image (non-

invasive method). The Fundus fluorescein angiogram is an injection-based method in which fluorescein dye is injected into a patient's blood vessel to increase the contrast level of the retinal vasculature (Retinal vasculature is a network of vessels in the retinal layer) of it. The digital colour fundus is captured by a fundus camera without injecting the contrast agent into the blood vessels.

Pathologies that occur in the retinal fundus image are such as microaneurysms, haemorrhages and exudates. Microaneurysms (MAs) are the first clinical signs of DR in the fundus image. MAs that appear as small dark red lesions in the colour fundus images (in white circles) are clearly seen as small round lesions with sharp edges and an irregularly brighter rim in the FFA images. A haemorrhage appears as round shaped or irregular shaped, sharp or diffusely delineated and deep red (colour of intravenous blood) in fundus images. Exudates are random whitish or yellowish patches found in the retinal fundus image with different sizes and shapes, and at different locations. FAZ is the central region of the fovea that is usually free of capillaries. The enlargement of FAZ is often observed in the eye with diabetic retinopathy and progresses with DR severity as the diabetic condition causes capillary loss in the perifoveal capillary network.

The first automatic detection method for diabetic retinopathy was developed by Baudoin *et al* [51] to detect the microaneurysms from fluorescein angiograms. Further, Xiahui and Chutatape *et al* [59, 60] proposed a method for the detection of haemorrhages by using the principal component analysis and features that were extracted by the support vector machine to classify the image patch. Goldbaum *et al*. [80] proposed a method of exudate detection algorithm based on the template matching and edge detection approach. In medical research, it is reported that an enlargement of the Foveal avascular zone (FAZ) causes vision loss because the small capillaries surrounding the FAZ possibly tend to be blocked due to higher hemodynamic stress. Ahmad Fadzil *et al* [28, 96] and his team worked on the determination of the FAZ area in the colour fundus image to reduce the use of the invasive method, FFA. Ahmad Fadzil and Lila *et al* [96] developed the method for analysis of FAZ in colour fundus images based on the vessel extraction and reconstruction for grading of DR and achieved a 92.2% accuracy. Later, Hanung *et al*

[28] developed an automated determination of FAZ for DR grading and named it RETINO and it gave the accuracy of 95%.

Retinal fundus images suffer from low and varied contrast. Contrast enhancement techniques have played a vital part to enhance the tiny low contrast objects. All of the techniques have been proposed for a solution to the most common problems of varied and low contrast images. The medical image normalisation technique for varied contrast has been categorised into two types, i.e., the Prospective and Retrospective contrast normalisation techniques. Image enhancement techniques for low contrast images are divided into two categories, namely, spatial domain and frequency domain for low contrast images. The spatial domain techniques involve a process of the contrast enhancement by adjusting the luminous intensity histogram of the processed image and subsequently, they perform the enhancement process in the frequency domain of the image. Ahmad Fadzil *et al* [17] developed a non-invasive image enhancement technique which is the combination of two techniques, Retinex and Independent Component Analysis (ICA) and is known as RETICA. The technique was created to overcome the problem of varied and low contrast. The Retinex algorithm is used for varied contrast problems and ICA is used for low contrast problems.

In image processing, noise reduction and the restoration of an image is expected to improve the qualitative inspection of an image and the performance criteria of the quantitative image analysis techniques. Especially, medical images are captured through imaging modalities which give noise. Due to the noise, the image details cannot be analysed clearly. There are three basic image noise models namely, additive, multiplicative and additive plus multiplicative noise models. Retinal fundus images are captured by using a fundus camera and they contain noise. Due to the noise, it is very difficult to analyse the tiny capillaries.

Image denoising problem is still a challenge for the researchers because removal of noise causes the artefacts and image blurring. Image denoising is classified into two types i.e., spatial domain and Transform domain denoising methods. These methods are mainly used for noise reduction but there are some disadvantages of using these methods i.e., mean filter, median filter and wiener filter

and these methods are mostly used by researcher to denoised different types of images. Mainly these filters make the image blur and smooth. Image details are lost due to blurring and smoothness affect. In transform domain, many researchers used the wavelet transform. Wavelet transform contained the higher frequency components and higher frequency components produce artefacts. Low frequency component of wavelet transform is based on wiener filter and wiener filter make the image smooth that affects the details of image. Linear sub-space estimator is based on different linear estimator to control the noise and signal distortion. The least squares and the minimum variance do achieve significant improvement in image denoising but at the expense of signal distortion. Recently, a novel subspace technique has been proposed that addresses signal distortion and noise reduction named Time Domain Constraint Estimator and in this research work TDC is used to improve the SNR of retinal colour fundus image. TDC estimator can control signal distortion and reduce the noise also. TDC estimator is based on the singular value decomposition. The Singular value decomposition (SVD) is used to determine the signal sub-space; the SVD is defined in below sub-section. The underlying principle of subspace denoising is to null the noise subspace and control the noise contribution in the signal subspace.

From the literature review, five main problems have been observed in the retinal colour fundus image and these problems need to be solved.

1. Varied contrast is one of the problems in the medical images due to the geometrical surface and configuration of image modalities.
2. Low contrast is also one of the key problems in the medical images. The low contrast of tiny objects of interest needs to be extracted and enhanced selectively for analysis.
3. Non-invasive enhancement method is required to normalise the varied contrast of images and enhance the low contrast of images.
4. Before normalising and enhancing the retinal colour fundus image, it is very important to handle the noise level and identification of the noise. The performance of the image enhancement technique (for low and varied contrast image) can be affected by the noise.

5. Performance evaluation parameters of a non-invasive digital system must be equal or higher than the invasive system and the quality of the non-invasive digital image must be better than the invasive image. This is because invasive systems, such as FFA, are based on contrast injecting agents that give higher contrast of the image as compared to colour fundus images but have other physiological problems.

CHAPTER 3

METHODOLOGY

3.1 Analysis of Fundus Images

Digital colour fundus images have been observed to suffer from noise and varying low contrast problems. The resultant noise observed in fundus images may be due to improper acquisition process and system noise. The varied contrast is due to the uneven illumination of the uneven curved retina surface. The biological nature of the retina results in the different amounts of light being reflected and hence the low and varied contrast.

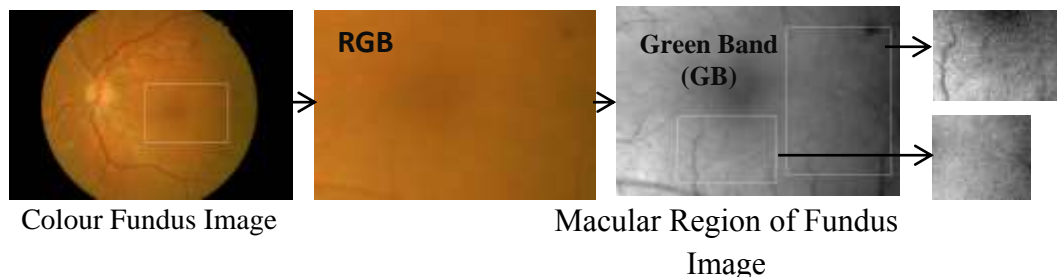


Figure 3.1 Illustration of noise in Fundus Images

Referring to Figure 3.1, colour fundus image contain noise due to which the blood vessels against their background cannot be observed clearly but the green band (GB) image of colour fundus image also contained noise due to which the details of the image are lost.

In Figure 3.2, macular regions of the fundus images are shown and different regions are marked with white circles within the macula of the fundus image. It can be seen that the contrast is low and varied in different regions of selected macular region of the colour fundus images. This is due to varying illumination of the macular region as a result of improper and uneven illumination acquisition.

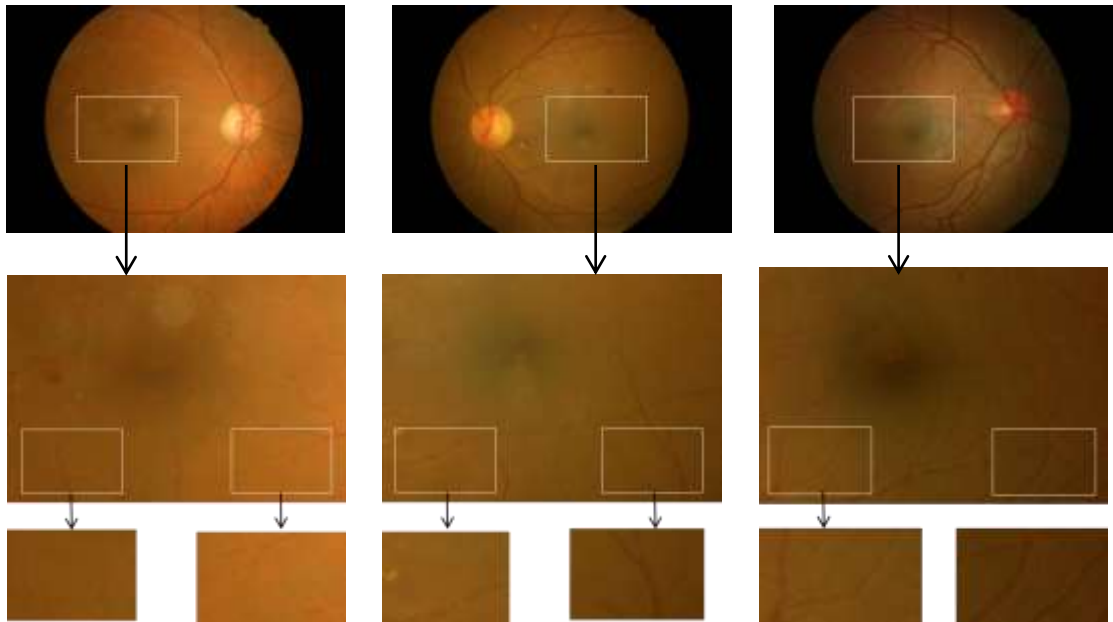


Figure 3.2 Illustration of noise varying contrast in Fundus Images

The RETICA method applies the Retinex algorithm [29] for contrast normalisation to overcome the varied contrast followed by the Independent Component Analysis [30] for contrast enhancement to overcome the low contrast of blood vessels against background. RETICA was tested on the developed model fundus images to investigate the effectiveness of the technique.

Results show that RETICA successfully normalises the varied contrast in colour model fundus images with contrast normalisation of $R_{sdc} = 0.756$ better than other a non-invasive enhancement methods [17]. RETICA outperforms other enhancement methods in producing better contrast of retinal blood vessels $C_{av} = 76.83$ followed by Contrast Stretching (CS), Histogram Equalisation (HE) and Contrast Limited Adaptive Histogram Equalisation (CLAHE) with 69.11,68.81 and 42.81 respectively [17]. Using the green band image as reference, RETICA achieves the highest contrast improvement of 5.389 comparable to that of invasive FFA with CIF of 5.796 [17]. However, Hanung A.Nugroho *et al* [17] did not investigate nor validate the performance of RETICA on real fundus images in FINDeRS database and more importantly the effects of noise in fundus images on RETICA.

3.2 Problem Formulation

To address the issues related with the analysis of fundus images, it is important to understand the nature of the noise in fundus images and to develop a suitable noise reduction technique to address noise prior to any contrast enhancement. Noise that arises from the image acquisition by fundus camera will have to be investigated thoroughly in order to identify the type(s) of noise. Available noise reduction schemes should be investigated to obtain the most effective noise reduction for the type(s) of noise in fundus images.

In improving the contrast of the fundus images, it is clear that the RETICA method has the potential to address varied and low contrast effectively as described from Hanung.A.Nugroho *et al* [17]. However, there is a need to ascertain its performance with real fundus images.

RETICA is based on the two hypotheses as follows:-

1. First, the digital colour fundus images are taken with a fundus camera and these images suffer from a varied contrast problem. The colour fundus image has a problem of uneven illumination. According to the image formulation model, the image intensity is the product of illumination and reflectance. Due to uneven illumination, the image has a varied contrast which affects its quality. Therefore, in order to achieve a uniform contrast image, it is necessary to normalise the image contrast and separate the illumination from the reflectance. Retinex makes this possible by separating the illumination from the reflectance part of the image to give a contrast normalised image.
2. Secondly, the objects of interest (macular region of the fundus image) suffer from low contrast because it is related to the reflectance. The independent component analysis is used to enhance the objects without introducing noise or any artefacts.

In Hanung.A.Nugroho *et al* [17], the above two problems of varied and low contrast were formulated and addressed on statistical models of fundus image. The performance of RETICA is evaluated in terms of the contrast improvement factor and

it successfully achieved an average of 5.38 contrast improvement factor on the model fundus images. However, RETICA was not validated on the real fundus image.

In this research, it is hypothesised that noise affects the performance of RETICA and that the RETICA performance can be improved with fundus images of better SNR. The noise in fundus images is therefore studied and its effect on the performance of RETICA with real colour fundus image is investigated.

3.3 Design of Experimental Work

The experimental work is described in the following sub-sections.

3.3.1 Implementation of RETICA on a Real Fundus Image

Referring to Figure 3.3, the Red, Green, and Blue colour channels of the macular region of the fundus image are processed by the Retinex algorithm (refer to section 2.6.3.1 in Chapter 2 on Retinex algorithm) to normalise the varied contrast of the image. Next, ICA (refer to Sect 2.6.3.2 in Chapter 2 on ICA algorithm) is performed to obtain the independent components – macular (Red Channel), haemoglobin (Green Channel), and melanin pigments (Blue Channel), - from the colour channels of the retinal colour fundus image.

The haemoglobin image (Green Band) is selected from the three independent components because it has higher contrast as compared to other two independent components. This enhanced image of the macular region of the fundus image is called the RETICA image. The two databases are analysed through the RETICA method. The first database contained 35- Fundus images with corresponding FFA images in which there are 11 No_DR, 6 Mild NPDR, 6 Moderate NPDR, 4 Severe NPDR and 8 PDR images. This database is known as the 35-Fundus database (refer to Appendix 1). The second database contains 175 fundus images in which there are 50 No_DR, 40 Mild NPDR, 30 Moderate NPDR, 18 Severe NPDR and 37 PDR images. This database is known as FINDeR's database (refer to Appendix 2).

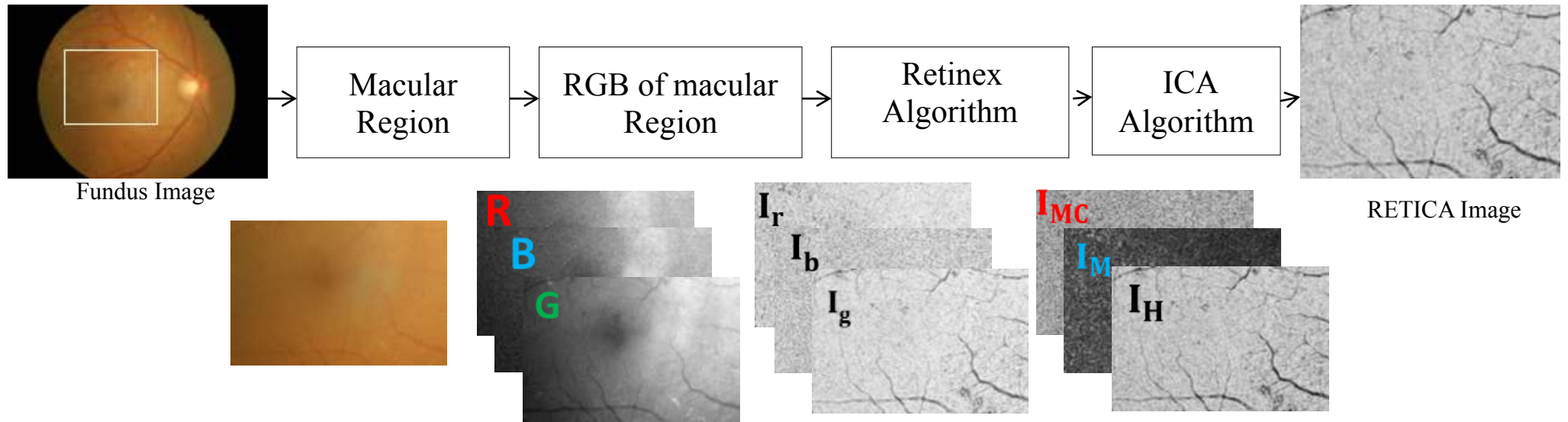


Figure 3.3 RETICA Method

3.3.2 Measurement of the Contrast and the Contrast Improvement Factor of Fundus Images

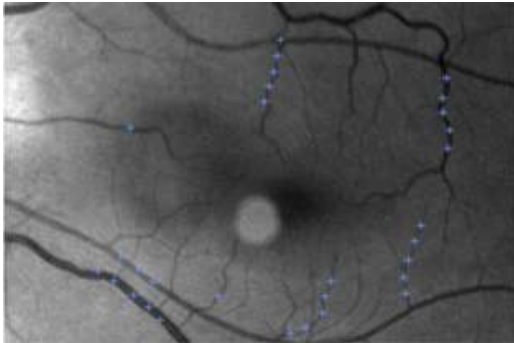
Two parameters are used to evaluate the RETICA performance. The first is the measurement of the contrast between the blood vessels against the background of the macular region of the green band image, FFA image, Haemoglobin (Green Component) or RETICA image. The second is the contrast improvement factor of the RETICA image versus the green band image and the FFA image versus the green band image.

To measure the contrast of the image, the 50 intensity points or pixels of the blood vessels and the background within the macular region are selected randomly as depicted by the blue dots in Figure 3.4. Similarly, intensities of the retinal blood vessels against the surrounding background of the macular region of green band image, FFA image and haemoglobin image due to RETICA are selected randomly. The image contrast is analysed between the blood vessels against the surrounding background of the macular regions of the green band image, the FFA image and the RETICA image.

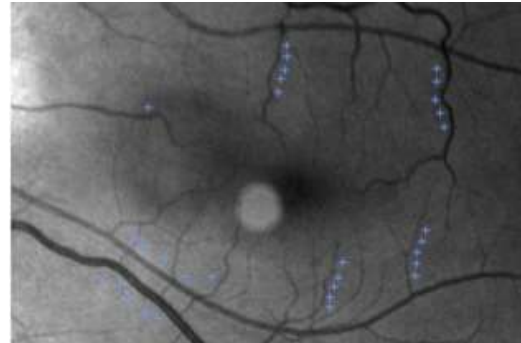
The contrast of the retinal blood vessels against the surrounding background region is the absolute mean intensity difference between the retinal blood vessels and the background of the retinal image. It was determined according to Equation 3.1.

$$C_{|bv-bg|} = \left| \frac{1}{n} (\sum_{i=1}^n I_{bvi} - \sum_{i=1}^n I_{bgi}) \right| \quad (3-1)$$

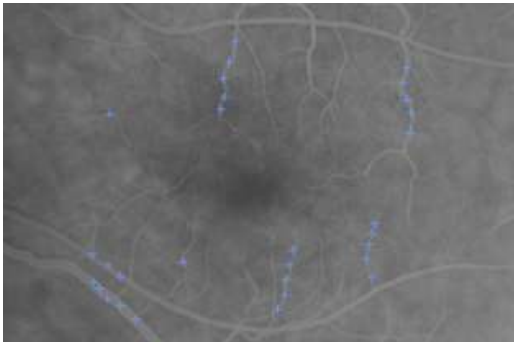
Here, $C_{|bv-bg|}$ is the contrast measured of the retinal blood vessels against the surrounding background. The terms I_{bvi} and I_{bgi} refer to the intensities of the retinal blood vessels and the background, respectively. The n variable indicates the random number of the data points (pixels) for the retinal blood vessels against the surrounding background in the fundus image. In this study, n= 50 and the data points (pixel locations) are randomly selected.



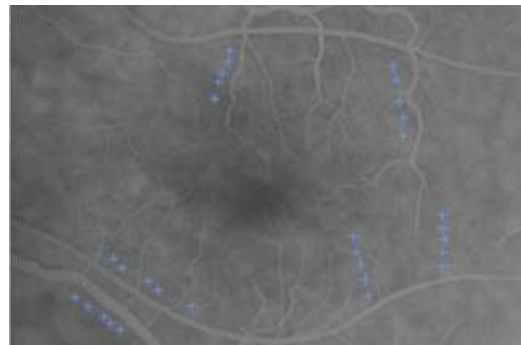
Green Band Blood vessels intensity selection



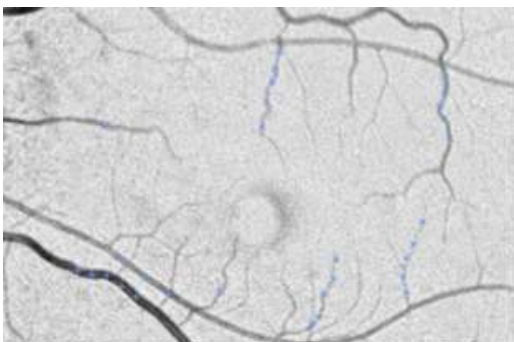
Green Band Background Intensity Selection



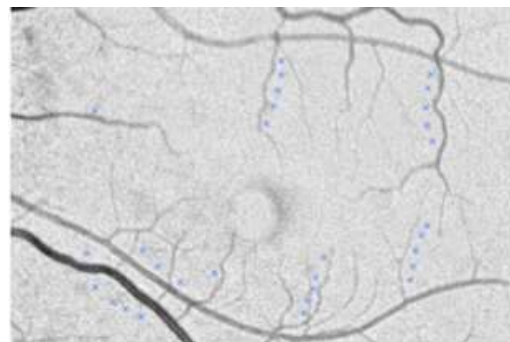
FFA Blood vessels intensity selection



FFA Background Intensity Selection



Haemoglobin Blood vessel intensity Selection



Haemoglobin Background Intensity selection

Figure 3.4 Selection of intensity data points (blood vessel and background) for Green band, FFA and RETICA images

The contrast improvement factor (CIF) for the FFA image is calculated as the ratio of the contrast between the grey scale values of the FFA image and the reference green band image. The contrast improvement factor (CIF) for the haemoglobin image or RETICA image is defined as the ratio of the contrast between the haemoglobin image and the reference green band image as formulated in Table 3.1.

Table 3.1 Formula of Contrast Improvement Factor

RETICA	FFA
$CIF_{RETICA} = \frac{C_{RETICA}}{C_{REF}}$	$CIF_{FFA} = \frac{C_{FFA}}{C_{REF}}$

CIF_{RETICA} represents the contrast improvement factor of RETICA and CIF_{FFA} represents the contrast improvement factor of FFA. Here, C_{RETICA} is the contrast blood vessel against the surrounding background of the RETICA image and C_{FFA} is the contrast of the blood vessels against the surrounding background of the FFA image. C_{REF} is the contrast of the blood vessels against the surrounding background of the green band image.

3.3.3 Measurement of the Signal to Noise Ratio of the Fundus Images

The evaluation of noise types in the digital retinal fundus image is based on the Peak Signal to Noise Ratio values of the images. It is an engineering term for the ratio between the maximum possible power of a signal or image and the power of the corrupting noise in the image that affects the quality of a digital image [135]. Mathematically, it is shown in Equation 3.2.

$$PSNR = 20 \log_{10}\left(\frac{255}{\sigma}\right) \quad (3-2)$$

In the Equation 3-2, the σ is the standard deviation of the image intensities and 255 is considered as peak intensity of a digital image.

3.3.4 Measurement of the Signal Energy of the Fundus Image

Signal Energy is main term in the signal and image processing to determine the strength of signal. In signal processing, signal as a function of varying amplitude through time, it seems to reason that a good measurement of the strength of a signal would be the area under the curve. In image processing, the image contains the distribution of pixels. Signal energy of image shows how the grey levels are distributed in image or any particular channels. There are many methods to calculate the signal energy of image. The Signal energy is represented by Equation 3-3.

$$\text{Signal Energy} = \sum_{i,j} |I(i,j)|^2 \quad (3-3)$$

Let assumed $I(i,j)$ is image with intensities values.

3.3.5 Noise Identification in the Fundus Image

The noise identification technique in the retinal fundus image has been proposed. It has been based on three filters according to a noise model (additive, multiplicative and additive plus multiplicative). The performance of the noise identification technique has been evaluated in terms of PSNR. The highest improvement of the specified filters (additive, multiplicative and additive plus multiplicative) indicates the noise types in the retinal fundus image. The noise identification technique for the retinal fundus is tested on both the model and the real retinal fundus images and effect of noise on Retinex algorithm is also observed.

Three wiener filters are developed for the removal of the various types of noise. The first adaptive wiener filter is basically designed to remove the additive noise. The second adaptive wiener filter, named the multiplicative wiener filter, is

designed as a multiplicative filter to remove multiplicative noise and the third adaptive wiener filter, named the additive and multiplicative wiener filter, is designed to deal with both the multiplicative plus additive noise. In Figure 3.5, the three adaptive wiener filters (additive, multiplicative, and additive plus multiplicative filters) are designed according to the noise models defined in the equations below.

Assumption #01: Noise is Additive and uncorrelated with signal

$$I'(x, y) = I(x, y) + n(x, y) \quad (3-4)$$

Assumption #02: Noise is multiplicative and correlated with signal

$$I'(x, y) = I(x, y) * n(x, y) \quad (3-5)$$

Assumption #03: Noise is both Additive and Multiplicative

$$I'(x, y) = I(x, y) * n(x, y) + n(x, y) \quad (3-6)$$

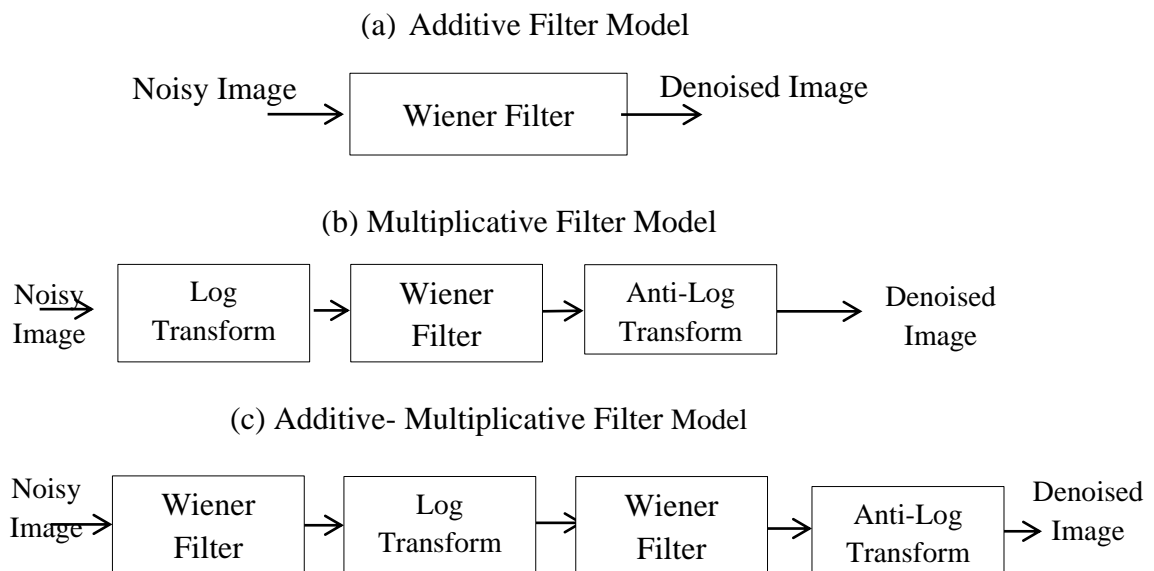


Figure 3.5 Modelling of Adaptive Wiener Filter

3.3.5.1 Study 1

Study 1 is based on an adaptive wiener filters (additive, multiplicative, and additive plus multiplicative filters). Adaptive wiener filters are applied on the green band of the fundus model image and the real fundus image in study 1 and the main purpose of study 1 is to determine the noise type in the green band fundus image.

Referring Figure 3.6 of study 1, the first the PSNR of green is calculated. In the second step the green band image is processed through the additive wiener filter and its PSNR is calculated similarly in third and fourth steps the green band image is processed to multiplicative wiener filter and additive plus multiplicative wiener filter and its PSNR of filtered image is calculated. The performance evaluation is based on the highest PSNR improvement between the PSNR of filtered green band image and PSNR of green band image. The filter which resulted in the highest PSNR improvement indicates the type of noise in green band fundus image.

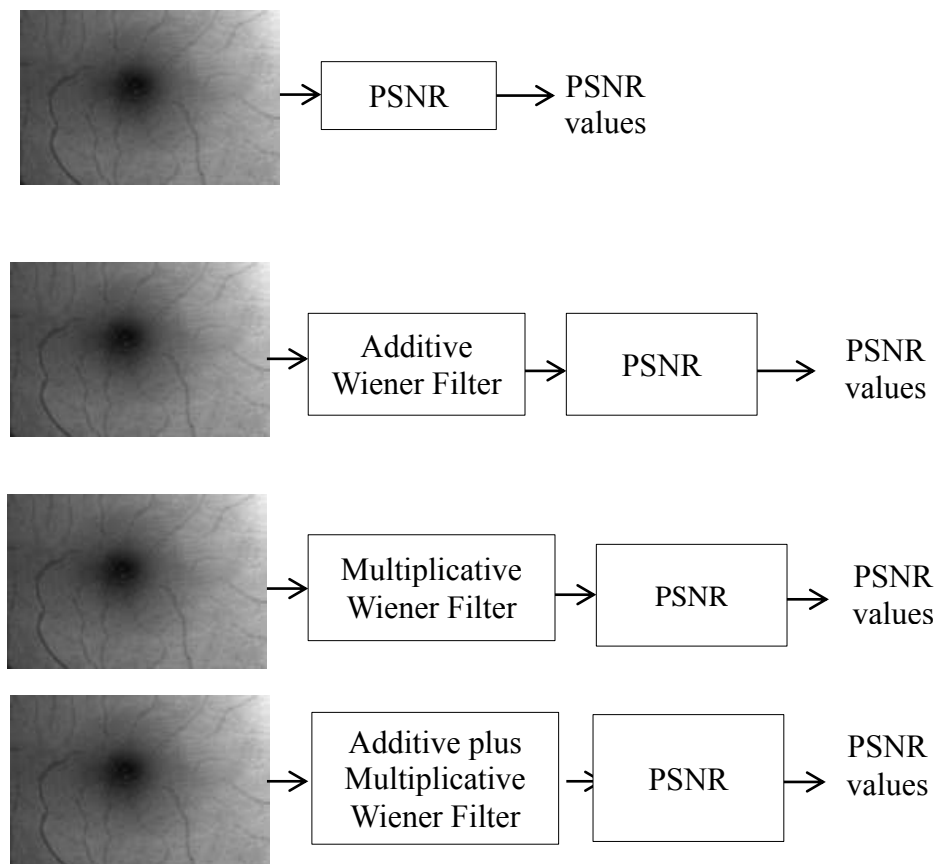


Figure 3.6 Study 1

3.3.5.2 Study 2

Study 2 is based on applying adaptive wiener filters (additive, multiplicative, and additive plus multiplicative filters) followed by the Retinex process as shown in Figure 3.6. Referring Figure 3.7 of study 2 the PSNR of the unfiltered Retinex image has also been determined. Then after the green band image is processed through the additive wiener filter then into Retinex and its PSNR of Retinex is calculated. Similarly the green band image is processed to multiplicative wiener filter and additive plus multiplicative wiener filter then after, it is process through Retinex algorithm and finally, PSNR of filtered Retinex image is calculated. The PSNR improvement is observed between the PSNR of the unfiltered Retinex image and the PSNR of the filtered Retinex image to determine the effect of Retinex and adaptive wiener filtering on the noise in fundus images.

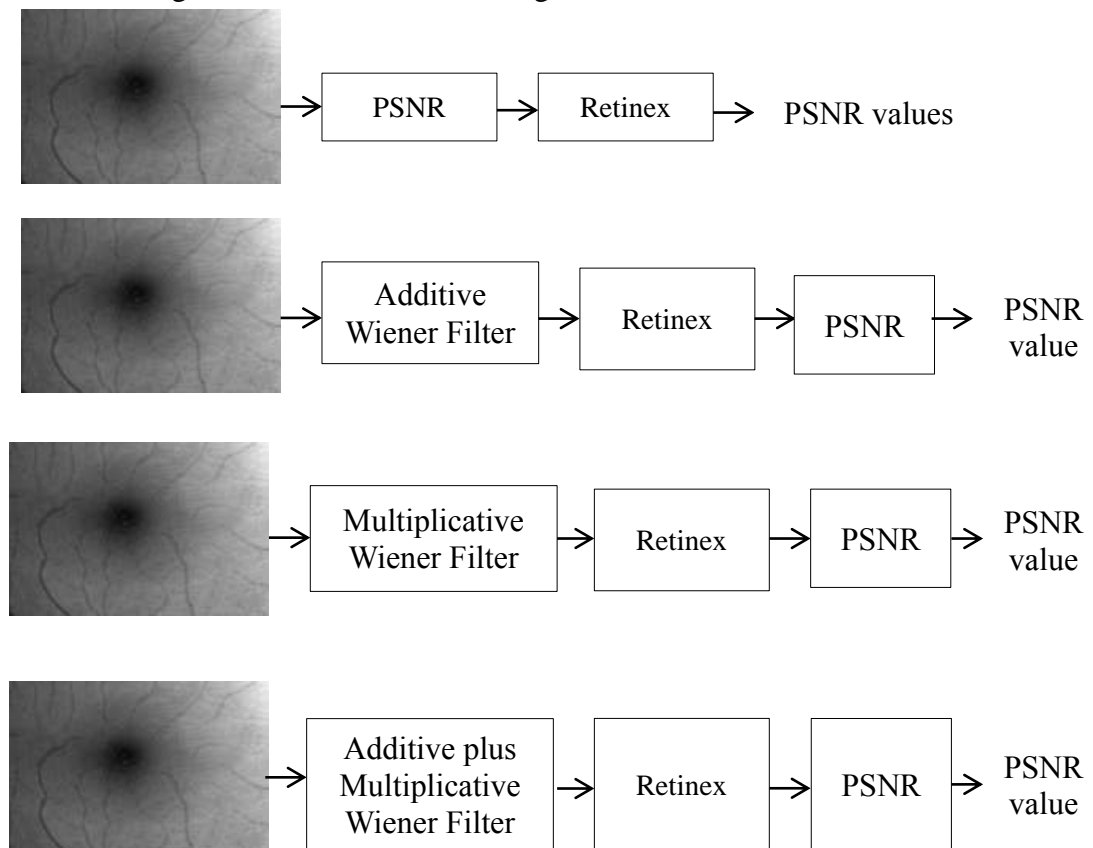


Figure 3.7 Study 2

3.3.5.3 Study 3

Study 3 is based on Retinex process followed by adaptive wiener filters (additive, multiplicative, and additive plus multiplicative filters) to study the noise types in Retinex images. In Study 3, the filters are applied after the Retinex algorithm and the PSNR at each stage has been calculated as shown in Figure 3.8. Referring Figure 3.8 of study 3 the PSNR of the unfiltered Retinex image has also been determined. In the second step the green band image is processed through Retinex then after it is process to additive wiener filter and PSNR of filtered Retinex image is calculated. Similarly, the green band image is processed through Retinex the processed to multiplicative wiener filter and additive plus multiplicative wiener filter and finally PSNR of filtered Retinex image is calculated. The PSNR improvement is observed between the PSNR of the unfiltered Retinex image and the PSNR of the filtered Retinex image to determine the the noise types in Retinex images. The filter which resulted in the highest PSNR improvement indicates the type of noise in the Retinex.

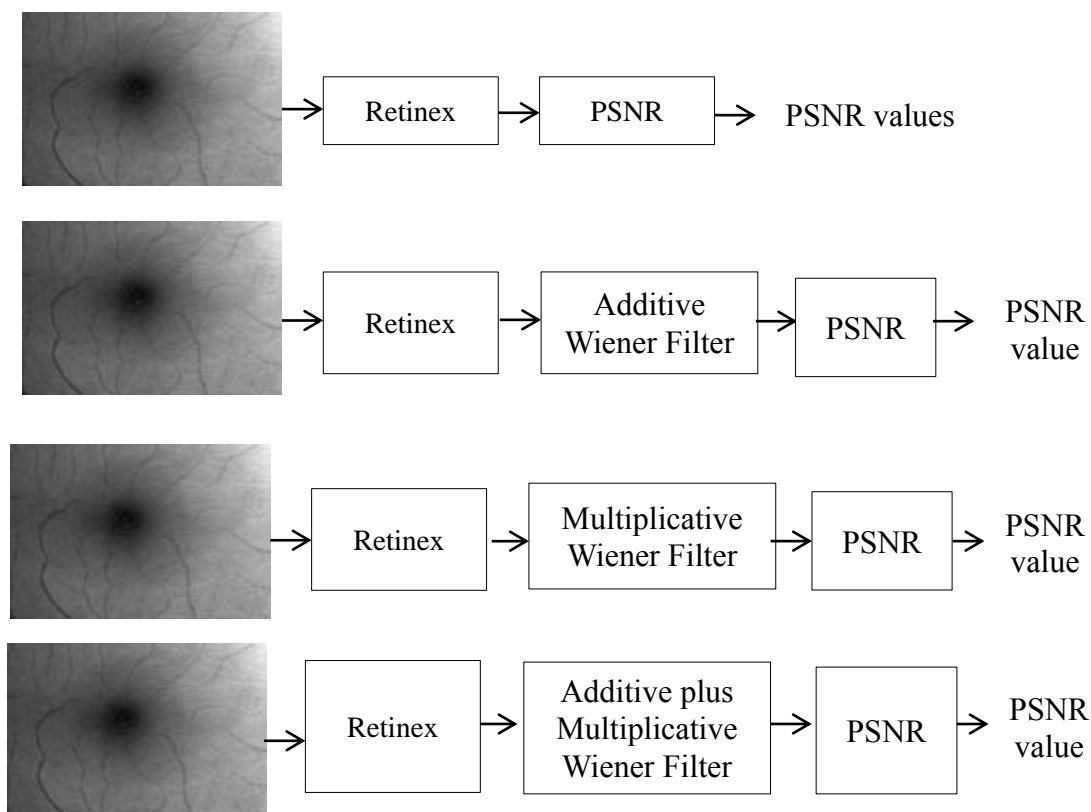


Figure 3.8 Study 3

The main three studies is to identify the noise types in the fundus model green band image, real green band fundus images, and the Retinex images. Secondly, observed the effect of noise on RETICA algorithm. Study 1 is based on identification of the noise types in green band image (Model or real fundus image). Study 2 is based on the effect on noise reductions using filters and Retinex. Study 3 is based on identification of noise type of Retinex image. The results are explained in chapter 4.

3.4 Denoising Methods for Retinal Fundus Images

In retinal fundus images, the macular region is analysed and evaluated based on the PSNR improvement between the green band image and its denoised image as shown in Figure 3.8.

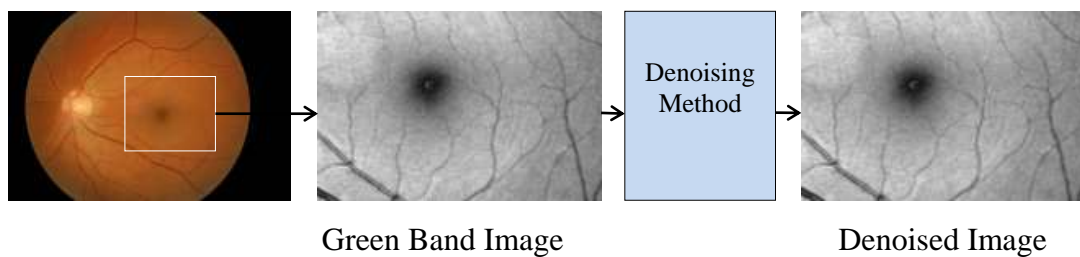


Figure 3.9 Noise reduction

The PSNR improvement ($\text{PSNR of denoised Image} - \text{PSNR of Green band Image}$) is determined for each method to select suitable noise reduction schemes and results are elaborated in chapter 4.

3.5 Improving the SNR of the Fundus Image

In this thesis, TDCE (refer to section 2.7.3.3 in Chapter 2 on TDCE) has been applied on the real colour fundus image. Referring Figure 3.9 of implementation of TDCE in the MATLAB, there are three steps to get estimated TDC image.

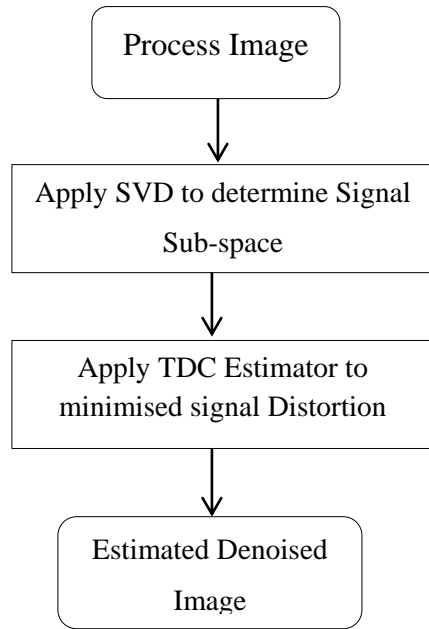


Figure 3.10 Implementation of TDCE in MATLAB

Steps of implementation of TDCE in MATLAB are explained as follow.

1. Process the image.
2. Apply the Singular value decomposition to determine the signal space. Because the noise removal is achieved by nulling the noise subspace and controlling the noise distribution in the signal (signal + residual noise) subspace. In the signal (signal + residual noise) sub-space contained required information and residual noise affects the details of image because linear estimation of the clean image is performed using TDC estimator to keep residual noise energy below the threshold while minimizing the signal distortion.
3. Apply TDCE to minimised the signal distortion and determine the estimated TDC denoised image.

The performance of TDCE is evaluated by measuring PSNR. Illustration of TDCE on retinal fundus images are shown in Figure 3.10.

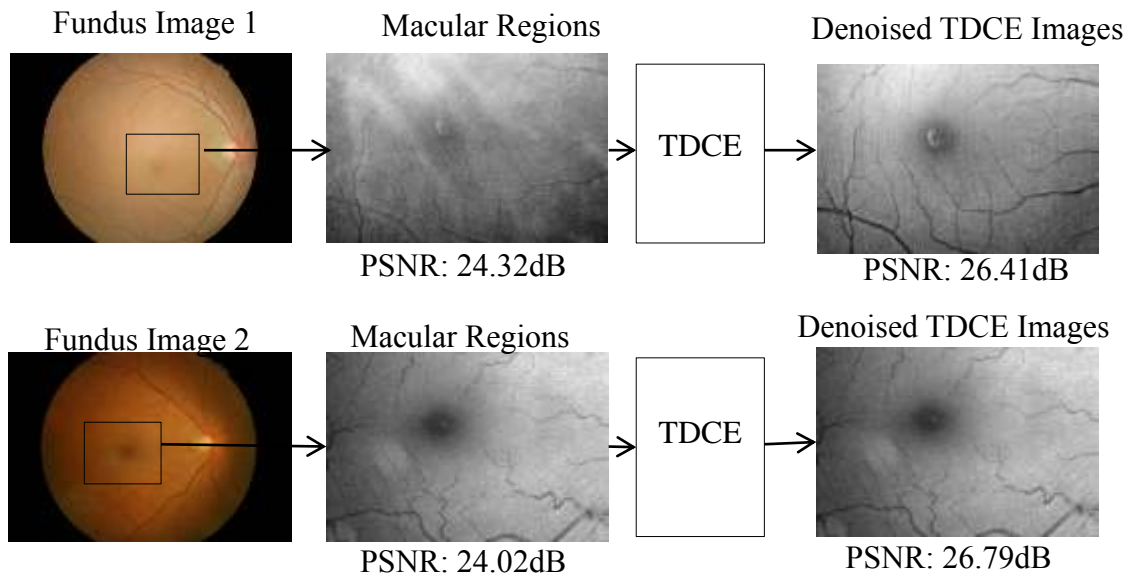


Figure 3.11 Illustration of TDCE on Retinal Fundus Image

Linear Sub-Space TDCE successfully denoised the image gave PSNR improvement (image1:2.09dB and image2: 2.77dB). Tiny blood vessels against the surrounding background of macular regions of retinal fundus image is more enhanced and clearly observed in TDCE denoised image. Consider Image 2 in the Figure 3.10, the tiny blood vessels surrounding its background cannot be observed clearly but they will be observed in TDCE denoised and it is very important to analyze these tiny capillaries for early analysis of eye-related diseases. Instead of this, TDCE images maintain the contrast of the image. There are three many reasons of applying TDCE on retinal fundus image because it maintains the contrast of the image and detail of the image also with reduced noise.

It is hypothesized that noise affects the performance of RETICA and that RETICA can be improved with better SNR of fundus images. Referring to Figure 3.11, the Red, Green, and Blue color channels of the macular region of the fundus image are processed by TDCE to improve the SNR. Next, the output of the TDCE

images is processed with RETICA for measuring contrast improvement factor for RETICA performance on improved SNR images.

The novelty of this proposed method is that TDCE is used to reduce the noise level in the colour fundus image whilst RETICA addresses the varied and low contrast problems.

Three main issues in the real retinal colour fundus images are being addressed in this method. These problems are the noise that occurred due to the improper acquisition process and the noise observed in the image which (1) degraded the image quality and (2) affected the performance of RETICA. The linear sub-space time domain constraint estimator (TDCE) is used to improve the quality of the image by reducing noise, maintaining contrast and preserving the image details. The problems of varied and low contrast are addressed by the Retinex and ICA in RETICA. So, a fully computerised-based non-invasive image enhancement technique that contained TDCE and RETICA is developed and investigated in this research. The results of experiment work are elaborated in the chapter 4.

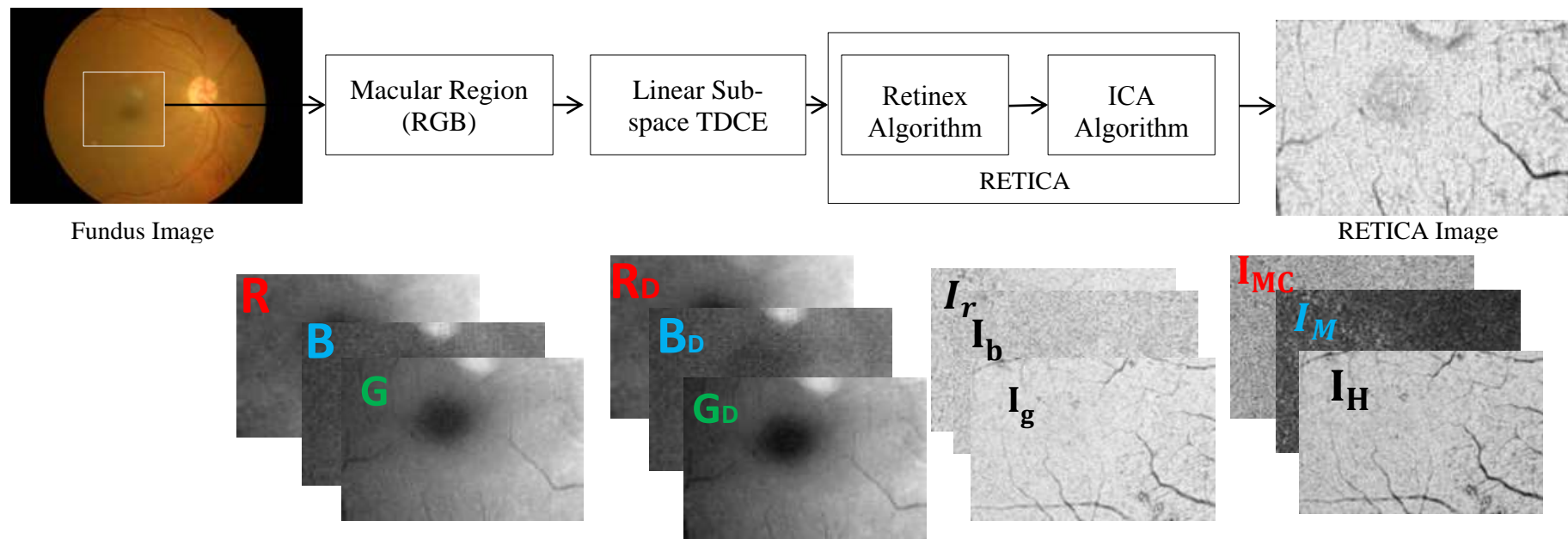


Figure 3.12 Proposed Non-Invasive Image Enhancement Techniques (TDCE+ RETICA)

3.6 Summary

The problem of varied and low contrast and noise often occurs in medical images. Colour digital fundus images are obtained by the fundus camera and through analysis of these images some eye related diseases such as Diabetic Retinopathy can be determined. Analysis of the tiny retinal vasculatures in the retinal fundus becomes difficult because the retinal fundus images suffer from noise, and very low and varied contrast between the retinal vasculature and the background in the image. As a result, a digital image enhancement technique is required to give the best visualisation of the retinal blood vessels.

In this chapter, RETICA is validated on real digital colour fundus images instead of model fundus images. Two databases are used; the first dataset is known as the 35-fundus image database and the second dataset is the FINDeR's database. The performance of RETICA is evaluated by measuring the contrast and the contrast improvement factor. The method of the contrast improvement has been defined. RETICA is able to handle the problem of varied and low contrast but the fundus image also contained noise. The noise affected the performance of RETICA because it is observed that RETICA gave two different performances on two different databases as the result elaborated in chapter 4. It is observed that noise affected the performance of RETICA and in order to achieve better performance of RETICA as with FFA then the SNR of the fundus image has to be improved before being processed by RETICA. But, it is very important to identify the nature of noise in the fundus before applying any denoising method.

In this chapter, the automated image filtering technique based on an identifying noise is developed for fundus images. It is based on the three studies. Study 1 is based on an adaptive wiener filters (additive, multiplicative, and additive plus multiplicative filters). Adaptive wiener filters are applied on the green band of the fundus model image and the real fundus image in study 1 and main purpose of study 1

is to determine the noise type in green band image. Study 2 is based on applying adaptive wiener filters (additive, multiplicative, and additive plus multiplicative filters) followed by the Retinex process and the main purpose of study 2 the PSNR of the unfiltered Retinex image has also been determined. Study 3 is based on Retinex process followed by adaptive wiener filters (additive, multiplicative, and additive plus multiplicative filters) to study the noise types in Retinex images. The main purpose of the three studies is to identify the noise types in the fundus model green band image, real green band fundus images, and the Retinex images. Secondly, observed the effect of noise on RETICA algorithm. The results of three studies are elaborated in the chapter 4.

The second objective is to reduce the noise as it has been hypothesised that if the contrast improvement factor is dropped due to noise then the contrast improvement factor of the FINDeRS database will be increased by improving the PSNR of the FINDeRS image database. The results are elaborated in chapter 4. The non-invasive image enhancement technique along with TDCE and RETICA has a fair potential to reduce the need for the invasive fundus fluorescein angiogram method and other such methods as they pose other physiological problems.

CHAPTER 4

RESULTS AND DISCUSSION

4.1 Performance Analysis of RETICA Method on Real Fundus Images

The performance of RETICA is evaluated on real fundus images obtained from two databases. The first database comprises 35 colour fundus images of various DR severities with their corresponding FFA images; 11 No_DR, 6 Mild NPDR, 6 Moderate NPDR, 4 Severe NPDR and 8 PDR images. This database is known as the 35-Fundus database. The second database has 175 colour fundus images of various DR severities in which there are 50 No_DR, 40 Mild NPDR, 30 Moderate NPDR, 18 Severe NPDR and 37 PDR images. This database is known as the FINDeRS (Fundus Image for Non-invasive Diabetic Retinopathy System) database.

The contrast improvement factor achieved by the RETICA method for the 35 colour fundus images compared to their corresponding FFA images in the 35-Fundus database is shown in Table 4.1. Referring to Table 4.1, the RETICA method resulted in higher contrast improvement factors as compared to the FFA method for all DR stages with an average CIF of 5.12 (FFA) and 5.46 (RETICA).

Note: The contrast improvement factor of FFA image is the contrast ratio of the FFA image and its green band image, which is used as the reference.

Table 4.1 shows the contrast values of green band (**CGB**), FFA (**CFFA**), and RETICA or haemoglobin (**CHI**) images, and the CIF achieved for FFA (**CIFFFA**) and haemoglobin (**CIFHI**) of the 35-Fundus database. As shown in Table 4.1, it is observed that RETICA achieved higher average contrast 43.1 as compared to FFA method 40.4. RETICA achieved average CIF of 5.46 as compared to 5.12 of FFA. It is also observed that some images have very high contrast values (contrast is above 50

for RETICA and FFA and above 10 for green band images) as highlighted in the table.

Table 4.1 Contrast and CIF of 35–Fundus database

No	Image	CGB	CFFA	CHI	CIFFFA	CIFHI
1	No DR_1	6	33.8	34.4	5.63	5.73
2	No DR_2	6.9	38.3	39.4	5.55	5.71
3	No DR_3	5.6	28.4	31.1	5.07	5.55
4	No DR_4	6.3	31.6	35.8	5.01	5.68
5	No DR_5	6.2	33.2	35.5	5.35	5.72
6	No DR_6	11.7	53.3	60.1	4.55	5.13
7	No DR_7	6.4	34.9	35.3	5.45	5.51
8	No DR_8	9.1	47.7	48.2	5.24	5.29
9	No DR_9	8.5	34.3	47.5	4.03	5.58
10	No DR_10	7.1	40.9	36.9	5.76	5.19
11	No DR_11	8.7	35	45.5	4.02	5.22
12	Mild_1	5.2	28.7	29.9	5.51	5.75
13	Mild_2	5.3	29.2	26.9	5.50	5.07
14	Mild_3	12.9	73	68.5	5.65	5.31
15	Mild_4	12.9	50.2	67.1	3.89	5.20
16	Mild_5	5.1	26.1	29.3	5.11	5.74
17	Mild_6	10.7	54.9	58.9	5.13	5.50
18	Moderate_1	5.6	28.3	30	5.05	5.35
19	Moderate_2	5.1	27.6	26.5	5.41	5.19
20	Moderate_3	7.8	44.4	39.2	5.69	5.02
21	Moderate_4	9.3	49.5	52.8	5.32	5.67
22	Moderate_5	14.2	75.5	82.2	5.31	5.78
23	Moderate_6	9.9	42.1	53.8	4.25	5.43
24	Severe_1	6.5	34.9	36.1	5.36	5.55
25	Severe_2	5.1	29.2	31.2	5.72	6.11
26	Severe_3	10.9	54.2	54.9	4.97	5.03
27	Severe_4	11.2	59.8	59.9	5.33	5.34
28	PDR_1	5.2	26.5	29.8	5.09	5.73
29	PDR_2	5.2	27.1	29.6	5.20	5.69
30	PDR_3	3.9	14.9	21.1	3.82	5.4
31	PDR_4	6.3	32	31.8	5.07	5.04
32	PDR_5	9.5	42.8	48.7	4.50	5.12
33	PDR_6	4.6	27.2	25.6	5.91	5.56
34	PDR_7	15.8	87.3	82.2	5.52	5.20
35	PDR_8	7.4	38.5	43.4	5.20	5.86
Average		7.9	40.4	43.1	5.12	5.46


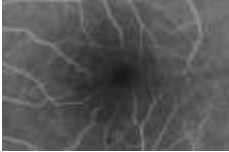
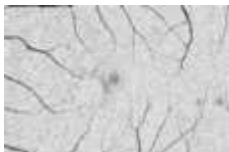

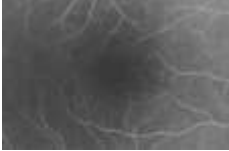


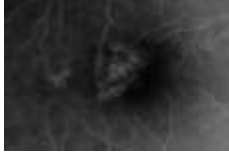
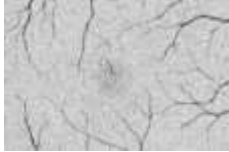
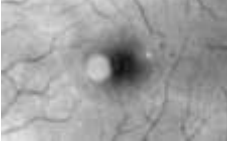









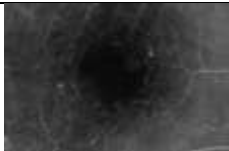

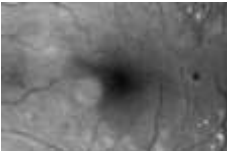
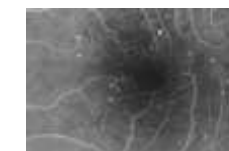

Image	Green Band	FFA Image	Haemoglobin Image
No_DR_6	 Contrast: 11.17	 Contrast: 53.3	 Contrast:60.1
Mild_3	 Contrast: 12.9	 Contrast:73	 Contrast: 68.5
Mild_4	 Contrast: 12.9	 Contrast: 50.9	 Contrast: 58.9
Mild_6	 Contrast: 10.7	 Contrast: 54.9	 Contrast: 58.9
Moderate_5	 Contrast: 14.2	 Contrast: 75.5	 Contrast: 82.2
Severe_3	 Contrast: 10.9	 Contrast: 54.2	 Contrast: 54.9
Severe_4	 Contrast: 11.2	 Contrast: 59.8	 Contrast: 59.9
PDR_7	 Contrast: 15.8	 Contrast: 87.3	 Contrast: 82.2

Figure 4.1 Comparison of selected FFA and RETICA images

Referring to Figure 4.1, the green band of No_DR_6 image clearly shows blood vessels with contrast of 11.17. The RETICA (haemoglobin) image is also more enhanced with smaller retinal blood vessels more observable as compared to FFA image; RETICA image have the contrast of 60.1 as compared to FFA 53.3. Similarly, RETICA images of Mild_4, Mild_6, Moderate_5, Severe_3 and Severe_4 clearly show tiny capillaries as compared to their corresponding FFA images. For Mild_3 and PDR_7, the FFA gave better contrast compared to RETICA. It can be seen that the retinal blood vessels are brighter due contrasting agent. Nonetheless, blood vessels can also be observed from the corresponding RETICA (haemoglobin) image.

Referring Figure 4.2, the contrast improvement factor of 35 images pairs is shown for various DR severity stages. RETICA outperformed the FFA in improving the contrast of the green band images. RETICA method resulted in higher contrast improvement factors as compared to the FFA method for all DR stages with an average CIF of 5.12 (FFA) and 5.46 (RETICA).

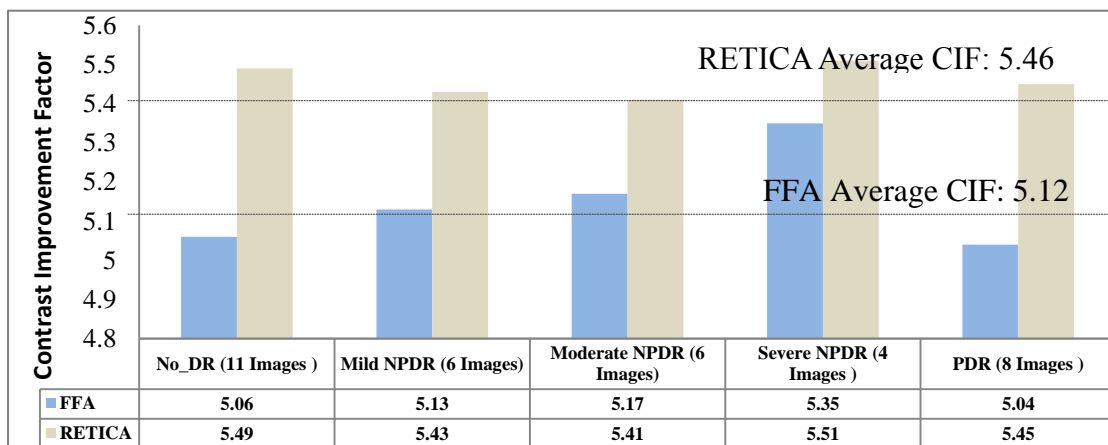


Figure 4.2 Contrast Improvement Factor of RETICA and FFA

The contrast improvement factors achieved by the RETICA method for the various DR stages in the FINDeRS database are shown in Figure 4.3 with an average CIF of 5.02.

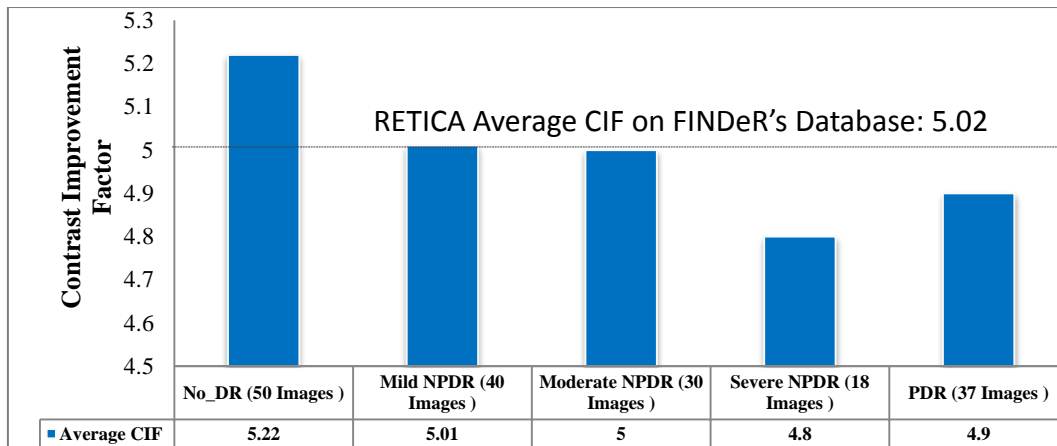


Figure 4.3 Contrast Improvement Factor of FINDeRS Database

It is observed that the contrast improvement factor (5.02) achieved by RETICA with the colour fundus images of FINDeRS database is lower compared to contrast improvement factor (5.46) for the colour fundus images of the 35-Fundus. Figure 4.4 shows the comparison of the CIF between images of FINDeRS and 35-Fundus databases for all DR stages.

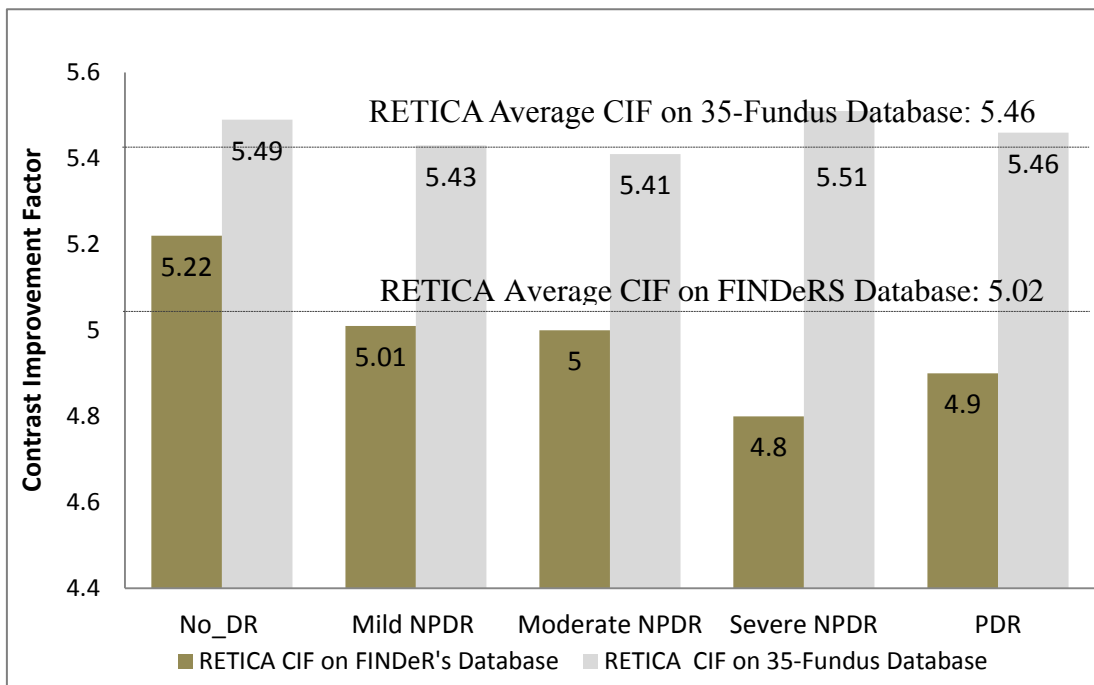


Figure 4.4 Contrast Improvement Factor Comparison between Images from FINDeRS and 35-Fundus Databases

The difference in RETICA performance for the two databases in particular, the causes for the lower CIF performance for the FINDeRS database is investigated by measuring the peak signal-to-noise (PSNR) levels for the database images. Referring to Figure 4.5, the FINDeRS database gave a lower PSNR of 24.34dB in comparison to the PSNR of 27.59dB of the 35-Fundus database.

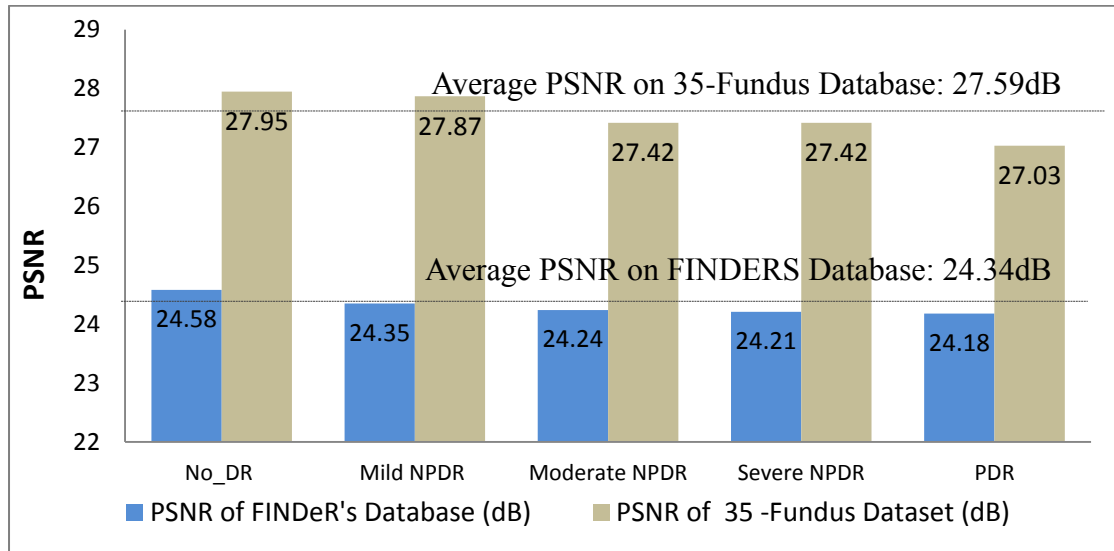


Figure 4.5 PSNR Comparisons between FINDeRS Database and 35 Fundus Image Database

From the signal-to-noise ratio analysis of the two databases (refer to Figure 4.4), the images in FINDeRS database generally have PSNR values that are 3dB lower compared to the images in the 35-Fundus database for all DR stages. The lower CIF for FINDeRS database in RETICA corresponds to lower PSNR of the images. The 3dB difference indicates either the signal levels of the fundus images in FINDeRS is about half of the signal levels in the 35-Fundus database or the noise levels in FINDeRS are higher as shown in Figure 4.5. Referring to Figure 4.6, the FINDeRS database has a lower average signal energy of $1.42E+09$ in comparison to average signal energy of $2.30E+09$ of the 35-Fundus database. This corresponds to the 3dB difference in PSNR values between the two databases.

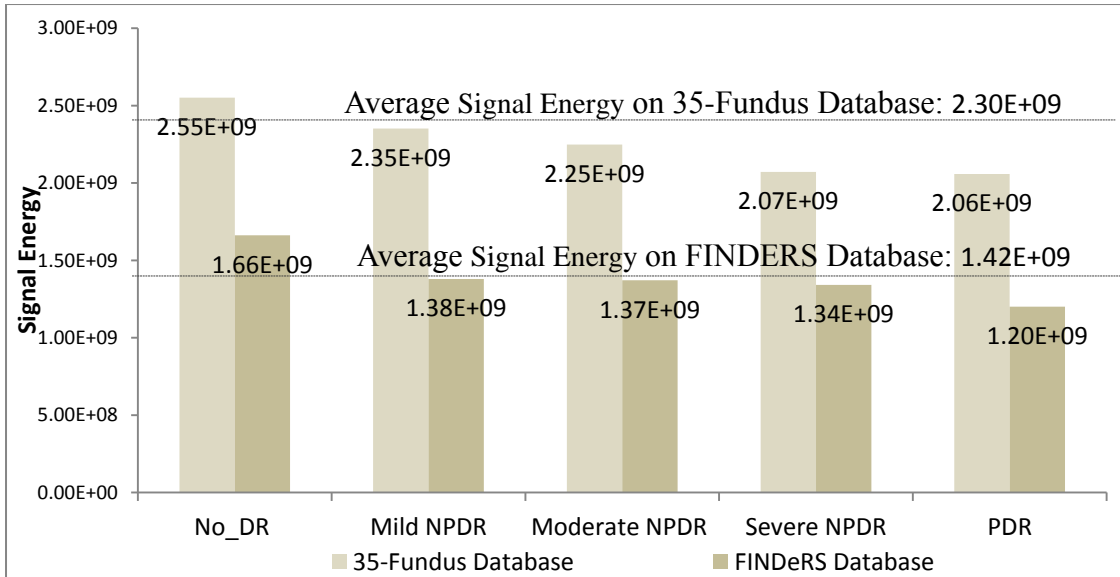


Figure 4.6 Average signal energy of fundus images for the two databases (35-Fundus and FINDeRS Database) for various DR stages

In addition, the RETICA algorithm produced no artefacts. The normalised and enhanced contrast image resulted in a higher contrast in the retinal blood vessels and this is advantageous for the diagnosis of retina-related eye diseases such as Diabetic Retinopathy (DR). The improvement of the contrast achieved by the RETICA is significantly important to reduce the use of invasive procedures such as the FFA.

Figure 4.7 shows samples of No_DR, Mild NPDR, Moderate NPDR, Severe NPDR and PDR images. All fundus images shown are clearly of varied and low contrast. For No_DR image shown, the green band image contains a bright spot artefact (shown in red circle). However, the RETICA process resulted in a normalised image with no bright spot and blood vessels can be seen clearly as compared to green band image. The RETICA achieved the contrast improvement factor of 5.52 for the No_DR image. For the Mild NPDR image shown, the green band also contains a bright spot artefact and retinal blood vessels are difficult to visualise. The RETICA normalises the varied contrast and enhanced contrast of background giving a clearer image of retinal capillaries with uniform contrast of background and blood vessels. The Moderate NPDR, Severe NPDR and PDR

images shown contain several artefacts within its macula region (as shown in red circles) and Retinex image of these images contained noise.

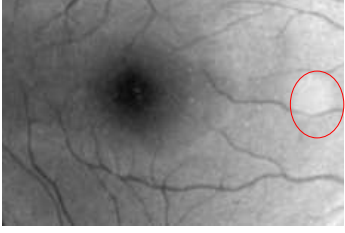
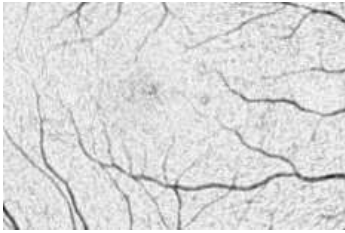

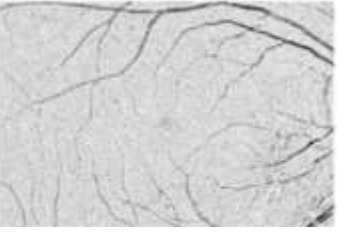
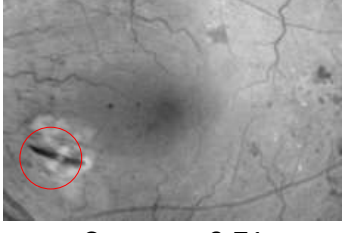
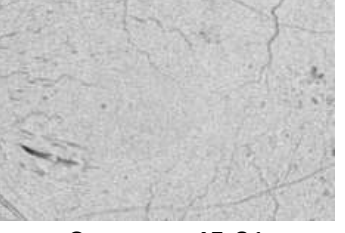
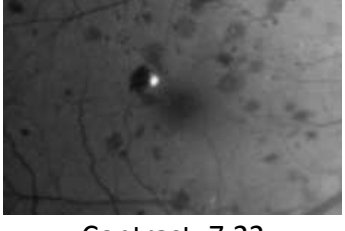

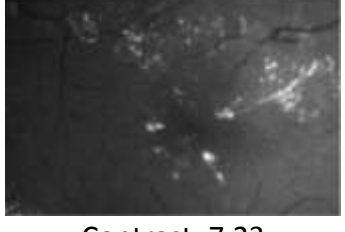

DR-Stages	Green Band	RETICA
No_DR	 Contrast : 15.01	 Contrast:82.75
	Contrast Improvement Factor: 5.52	
Mild NPDR	 Contrast:11.98	 Contrast:60.59
	Contrast Improvement Factor:5.05	
Moderate NPDR	 Contrast: 9.71	 Contrast: 45.81
	Contrast Improvement Factor:4.72	
Severe NPDR	 Contrast: 7.22	 Contrast: 30.13
	Contrast Improvement Factor: 4.17	
PDR	 Contrast: 7.23	 Contrast: 29.81
	Contrast Improvement Factor: 4.12	

Figure 4.7 Analysis of Green Band Image and RETICA Image of FINDeRS Database

The noise affect RETICA process and thus tiny blood vessels with macula region are not observable. Lower contrast improvement factors below 5 are obtained.

It is therefore hypothesised that noise affects the contrast of the image and consequently affects RETICA performance in contrast improvement factor. This can be validated by the improving the PSNR of the images in FINDeRS database. However, before attempting to improve PSNR by reducing noise in retinal fundus images, it is necessary to identify the nature of noise in the fundus images.

4.2 Results and Analysis of Identification of Noise Approach

The following two subsections discusses the identification of noise types in the fundus images and proposes appropriate noise reduction schemes to improve the PSNR of fundus images.

4.2.1 Study 1

Study 1 (Refer to Sect 3.4.4 in Chapter 3) is based on an adaptive wiener filters (additive, multiplicative, and additive plus multiplicative filters). Adaptive wiener filters are applied on the green band of the fundus model image and the real fundus image in study 1 as shown in Figure 4.8. Referring Figure 4.8 of study 1, the first the PSNR of green band image is calculated. In the second step the green band image is processed through the additive wiener filter and its PSNR is calculated. Similarly the green band image is processed to multiplicative wiener filter and additive plus multiplicative wiener filter and PSNR of filtered image is calculated. The performance evaluation is based on the highest PSNR improvement between the PSNR of filtered green band image and PSNR of green band image. The filter which resulted in the highest PSNR improvement indicates the type of noise in green band fundus image

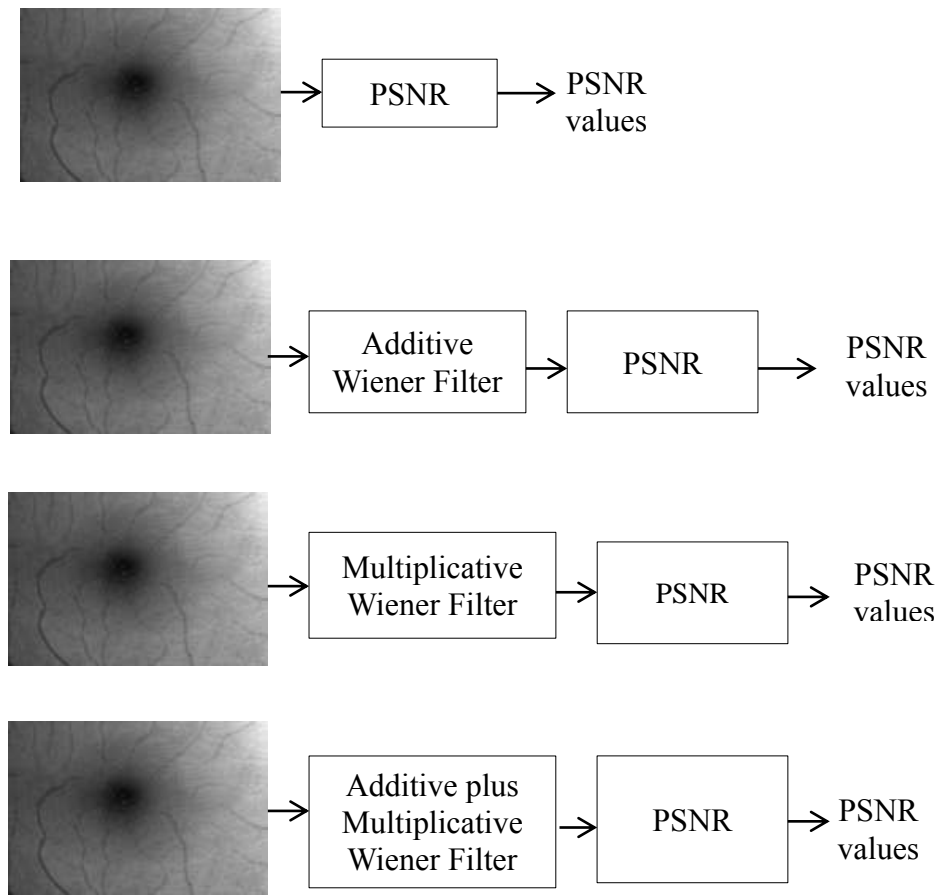


Figure 4.8 Study 1

Figure 4.9 shows the PSNR values for the green band fundus model image and the results after filtering by the three wiener filters.

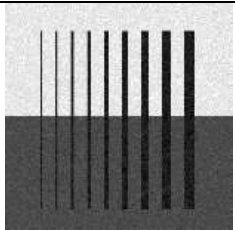
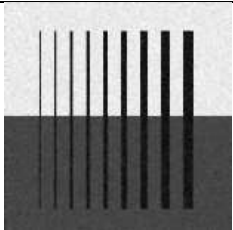
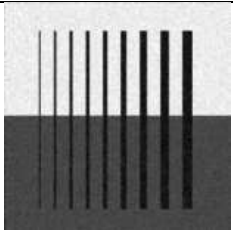
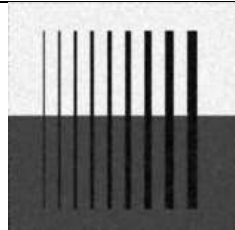
Green Band Model Fundus Image	An Additive Wiener Filtered Green Band Image	A Multiplicative Wiener Filtered Green Band Image	An Additive-Multiplicative Wiener Filter Green Band Image
			
PSNR: 24.69dB	PSNR: 24.89dB	PSNR:25.01dB	PSNR:26.98dB

Figure 4.9 Results of Study 1of Model Fundus Images

Referring Figure 4.9, based on the comparison of the PSNR improvements achieved by the different filters, it is seen that the additive and multiplicative wiener filter gives the best PSNR improvement of 2.29dB. This clearly implies that the fundus model image has both additive and multiplicative noise.

Similarly, the macular region of the colour fundus image is processed through the three adaptive wiener filters and the PSNR values are shown in Figure 4.10. The highest PSNR improvement (1.1dB) is achieved with the additive and multiplicative wiener filter. Thus, the macular region of the green band image contains both additive and multiplicative noise.





Green Band Image	An Additive Wiener Filtered Green Band Image	A Multiplicative Wiener Filtered Green Band Image	An Additive-Multiplicative Wiener Filter Green Band Image
			
PSNR:26.03dB	PSNR:26.96dB	PSNR:27.05dB	PSNR:27.13dB

Figure 4.10 Results of Study 1 on Green Band Fundus Image

FINDeRS database is used in Study 1. The PSNR improvement between the additive and multiplicative wiener filtered macular green band image of the FINDeRS database and the unfiltered green band image is observed.

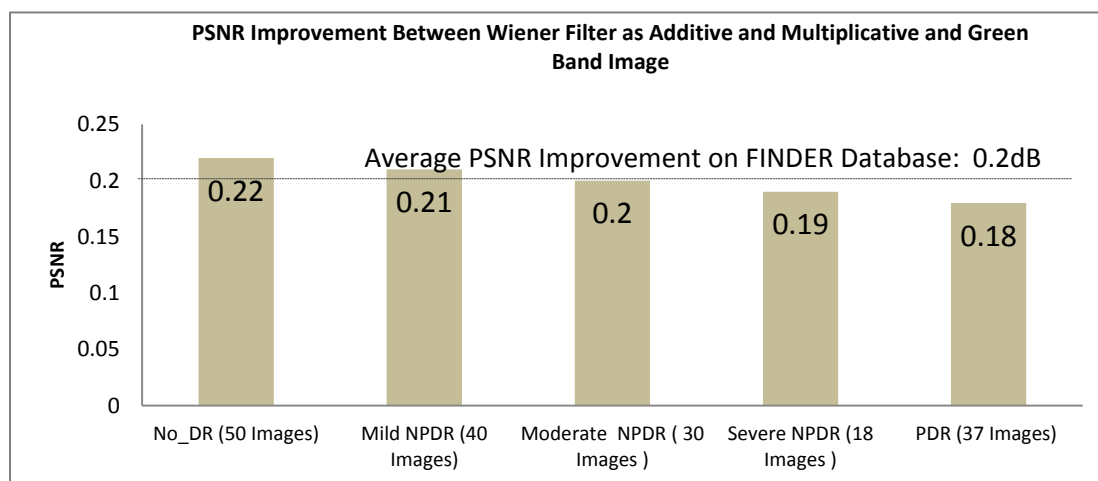


Figure 4.11 PSNR Improvement of Proposed Study 1 on FINDeRS Database

As shown in Figure 4.11, the average PSNR improvement at No_DR is 0.22dB, at Mild NPDR-0.21dB, at Moderate NPDR-0.2dB, at Severe NPDR-0.19dB, and at PDR-0.18dB. Average PSNR improvement of proposed study 1 is 0.2dB on FINDeRS database

4.2.2 Study 2

Study 2 (Refer to Sect 3.4.4 in Chapter 3) is based on applying adaptive wiener filters (additive, multiplicative, and additive plus multiplicative filters) followed by the Retinex process as shown in Figure 4.12.

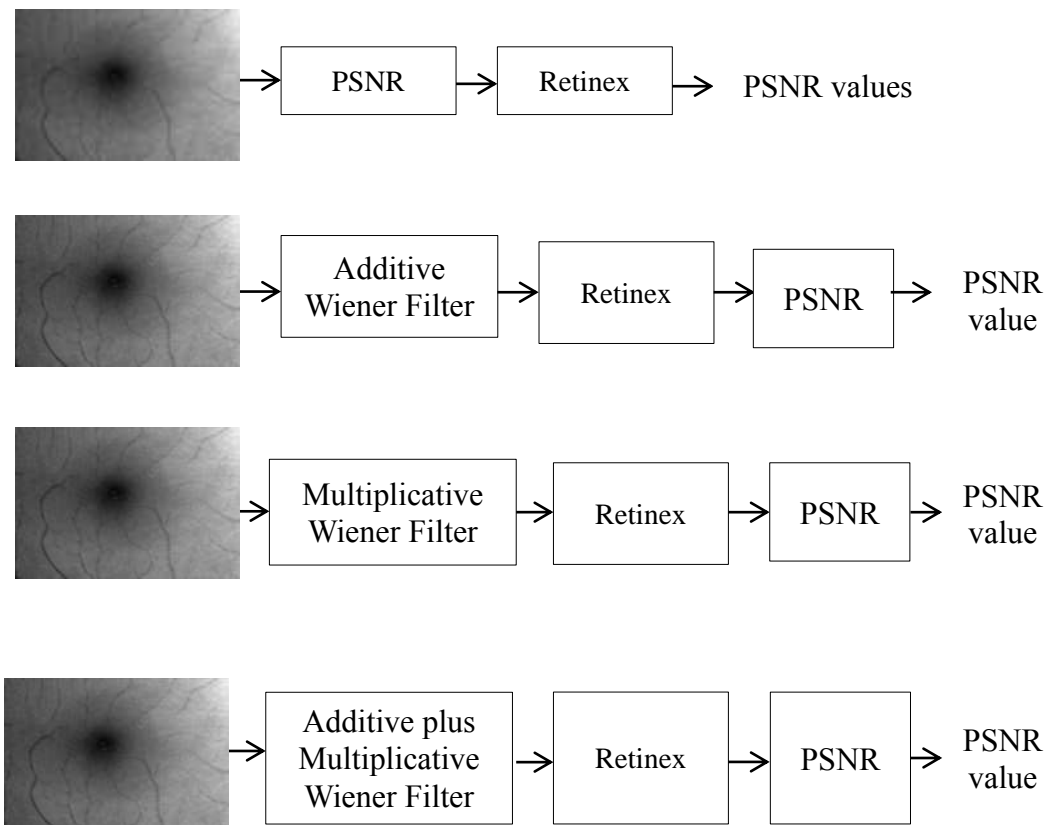


Figure 4.12 Study 2

Referring Figure 4.12 of study 2 the PSNR of the unfiltered Retinex image has also been determined. Then after the green band image is processed through the

additive wiener filter then into Retinex and finally, the PSNR of Retinex image is calculated. Similarly the green band image is processed to multiplicative wiener filter and additive plus multiplicative wiener filter then after, it is process through Retinex algorithm and finally, PSNR of filtered Retinex image is calculated. The PSNR improvement is observed between the PSNR of the unfiltered Retinex image and the PSNR of the filtered Retinex image to determine the effect of Retinex and adaptive wiener filtering on the noise in fundus images.

The results are tabulated in Figure 4.13, as expected, the additive and multiplicative wiener filter with Retinex give the highest PSNR improvement (1.92dB). Comparing results in this study with Study 1 on model fundus images, it is also seen that the Retinex process provides further noise reduction; an additional 1dB.

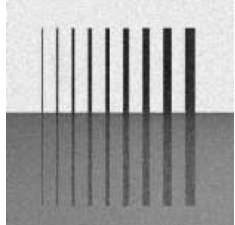
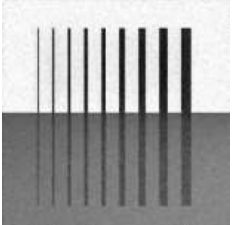
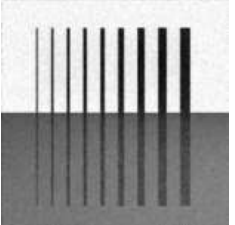
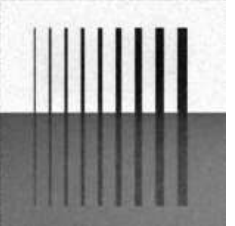
Retinex (Without Filtering)	An Additive Wiener Filtered with Retinex	A Multiplicative Wiener Filter with Retinex	An Additive- Multiplicative Wiener Filter with Retinex
			
PSNR: 26.68dB	PSNR:27.01dB	PSNR:27.58dB	PSNR:27.93dB

Figure 4.13 Results of proposed Method 2 on Model Fundus Image

Similarly, Study 2 is applied on the macular region of the real fundus images as shown in Figure 4.14. Referring Figure 4.14, it is clearly seen that the additive and multiplicative wiener filter gives the highest PSNR improvement of 2.35dB. Note that the PSNR values are higher for Retinex images because the Retinex process changes the pixel values altogether with the background having high grey level values compared to the blood vessels which have low grey level values.



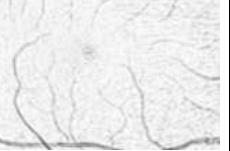

Retinex Image (Without Filtering)	An Additive Wiener Filtered Retinex Image	A Multiplicative Wiener Filter Retinex Image	An Additive- Multiplicative Wiener Filter Retinex Image
			
PSNR: 39.56dB	PSNR:40.57dB	PSNR:41.03dB	PSNR:41.91dB

Figure 4.14 Results of Study 2 on Retinex Fundus Image

The FINDeRS database is used for the validation of the proposed Study 2. The PSNR improvement between an additive and multiplicative wiener filtered macular region of the Retinex image and the unfiltered Retinex image is calculated. Referred Figure 4.15, the No_DR images give an average PSNR improvement of 4.03dB, Mild NPDR is 3.99 dB, Moderate NPDR is 2.96 dB, Severe NPDR is 2.56 dB and PDR is 1.96dB. Average PSNR improvement of proposed study 2 is 3.24dB on FINDeRS database.

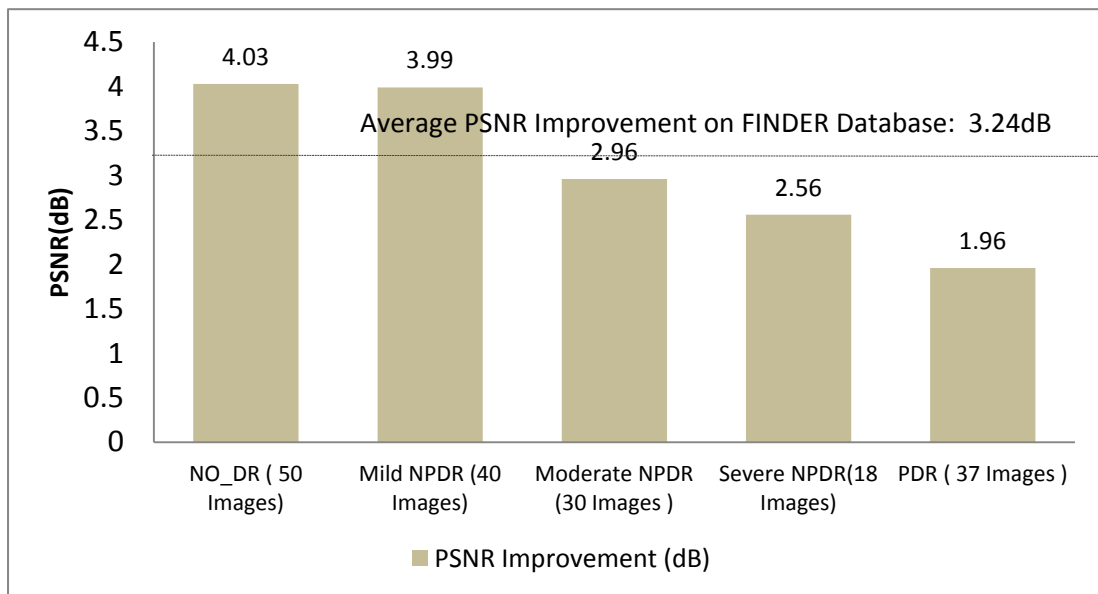


Figure 4.15 PSNR Improvement of Proposed study 2 on FINDeRS Database

4.2.3 Study 3

Study 3 (Refer to Sect 3.4.4 in Chapter 3) is based on Retinex process followed by adaptive wiener filters (additive, multiplicative, and additive plus multiplicative filters) to study the noise types in Retinex images. In Study 3, the filters are applied after the Retinex algorithm and the PSNR at each stage has been calculated as shown in Figure 4.16.

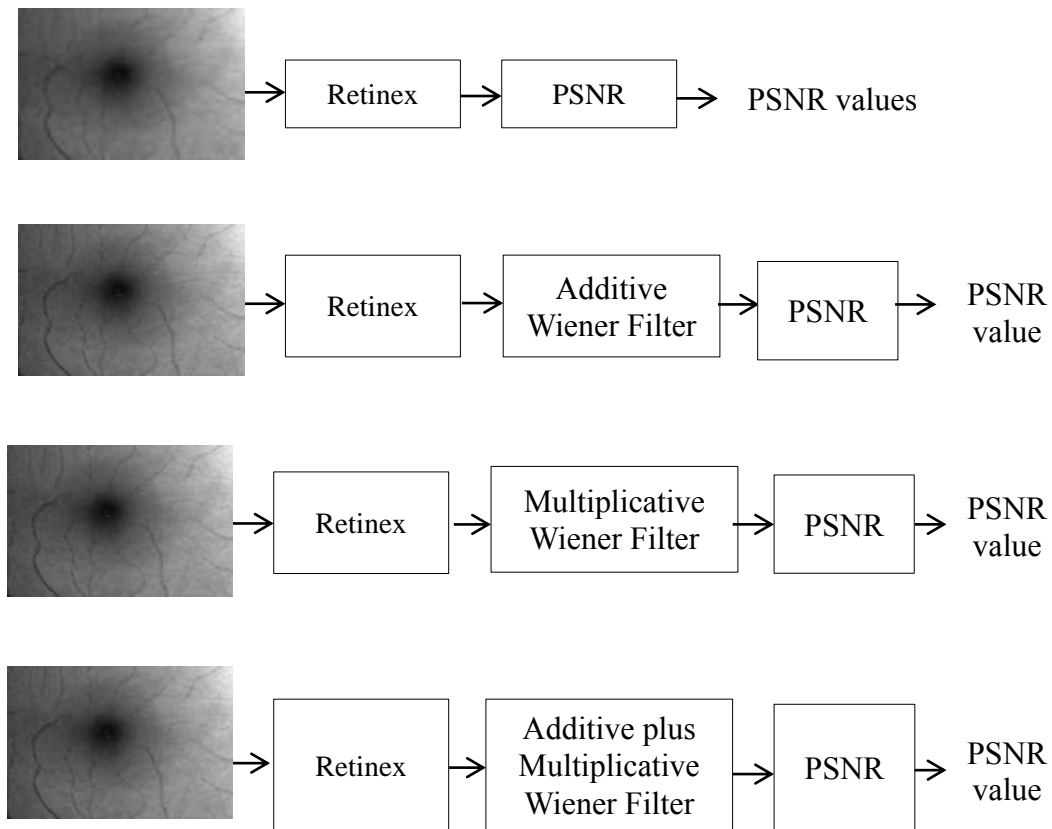


Figure 4.16 Study 3

Referring Figure 4.16 of study 3 the PSNR of the unfiltered Retinex image has also been determined. In the second step the green band image is processed through Retinex then after it is process to additive wiener filter and PSNR of filtered Retinex image is calculated. Similarly, the green band image is processed through Retinex the processed to multiplicative wiener filter and additive plus multiplicative wiener filter and finally PSNR of filtered Retinex image is calculated. The PSNR improvement is observed between the PSNR of the unfiltered Retinex image and the PSNR of the filtered Retinex image to determine the noise types in Retinex images. The filter which resulted in the highest PSNR improvement indicates the type of noise in the Retinex.

The results are tabulated in Figure 4.17. Again, the additive and multiplicative wiener filter give the highest PSNR improvement (2.23dB), which implies the Retinex image contains both additive and multiplicative noise.

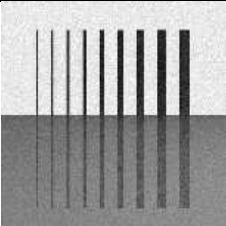
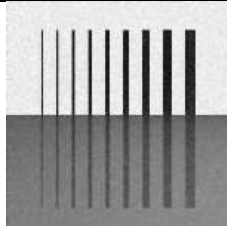
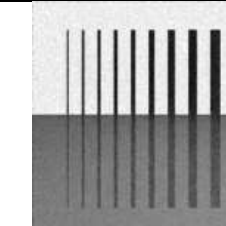
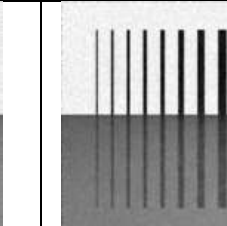
Retinex Image (Without Filtering)	An Additive Wiener Filtered Retinex Image	A Multiplicative Wiener Filter Retinex Image	An Additive- Multiplicative Wiener Filter Retinex Image
			
PSNR:26.68dB	PSNR:27.09dB	PSNR:27.82dB	PSNR:28.91dB

Figure 4.17 Results of proposed study 3 on Model Fundus Image

Similarly, Study 3 is applied on the macular region of the real fundus images as shown in Figure 4.18. It is clearly seen that the additive and multiplicative wiener filter gives the highest PSNR improvement of 3.26dB, which indicates that the Retinex fundus image contains both additive and multiplicative noise.



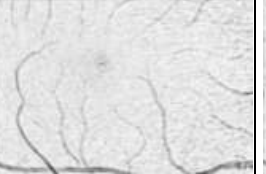
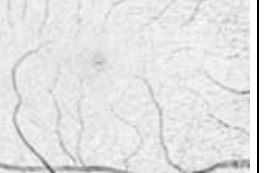
Retinex Image (Without Filtering)	An Additive Wiener Filtered Retinex Image	A Multiplicative Wiener Filter Retinex Image	An Additive- Multiplicative Wiener Filter Retinex Image
			
PSNR:39.56dB	PSNR:41.05dB	PSNR:41.93dB	PSNR:42.82dB

Figure 4.18 Results of study 3 on Retinex Fundus Image

The FINDeRS database is used for the validation of the proposed method 3. The PSNR improvement between an additive and multiplicative wiener filtered macular region of the Retinex image and the unfiltered Retinex image is calculated. Referred Figure 4.19, the No_DR images give an average PSNR improvement of 4.87dB, Mild NPDR is 4.51dB, Moderate NPDR is 3.99dB, Severe NPDR is 3.18dB and PDR was 2.14dB. Average PSNR improvement of Study 3 is 3.88dB on FINDeRS database.

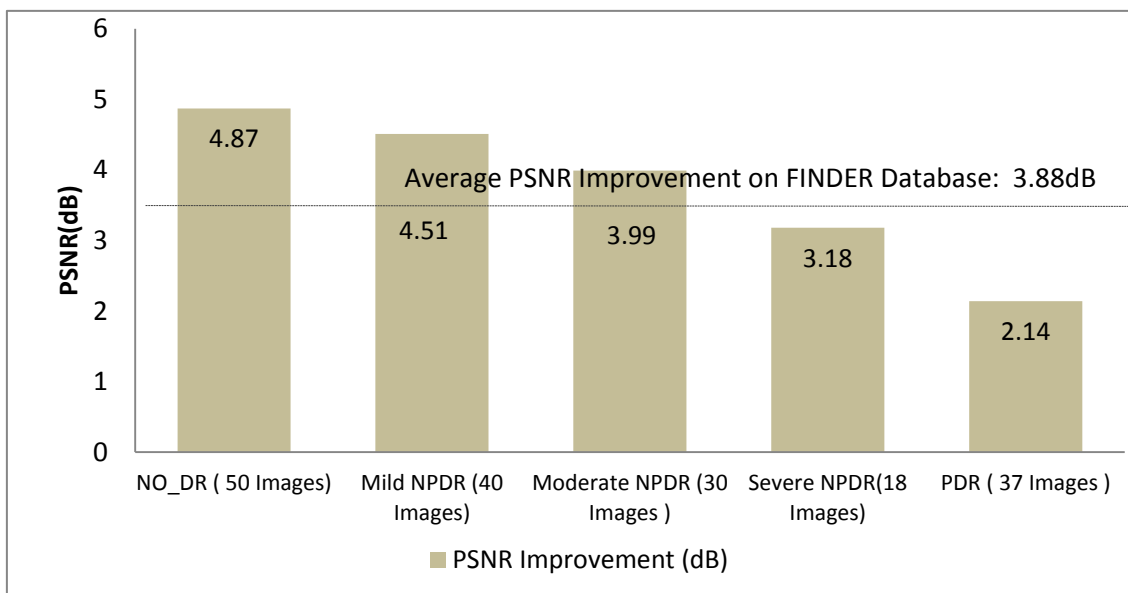


Figure 4.19 PSNR Improvement of Proposed Method 3 on FINDeRS Database

The PSNR improvements based on the analysis of the three studies prove that the model fundus image, green band fundus images, and the Retinex images contain additive and multiplicative noise. Secondly, noise affects the performance of the RETICA algorithm. It has been observed that the Retinex algorithm also improved the SNR of the image but its performance is affected due to the noise coming from the image modality. In addition, the performance of RETICA (Retinex and ICA) can be improved by improving the SNR of the green band fundus image. The additive and multiplicative noise occurring in the retinal fundus image is due to the fundus camera. Multiplicative noise occurred due to the flash of the fundus camera and the additive noise is due to the camera electronics. Denoising techniques are thus required to improve the SNR green band fundus image for improving the performance of RETICA to achieve higher contrast image.

4.3 Results and Analysis of Denoising Methods for Fundus Image

Referring to Figure 4.20, TDCE is applied as the technique for denoising. In this particular example, a 24.56dB is the calculated value of the PSNR of the green band image. Upon the application of TDCE, there is an improvement of PSNR of 2.75dB.

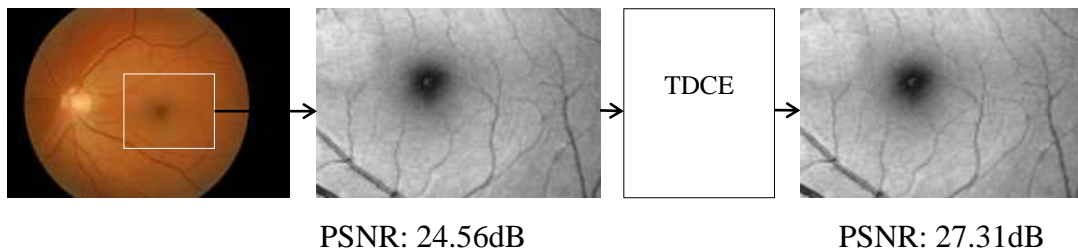


Figure 4.20 Green bands is denoised by using TDCE

Processing of the fundus images from the FINDeRS database is performed and Figure 4.21 presents the overall results. It can be seen that the average PSNR of the green band images of the FINDeRS database is 24.31dB and the average PSNR of the TDCE denoised images is 27.19dB giving an average PSNR improvement of 2.88dB.

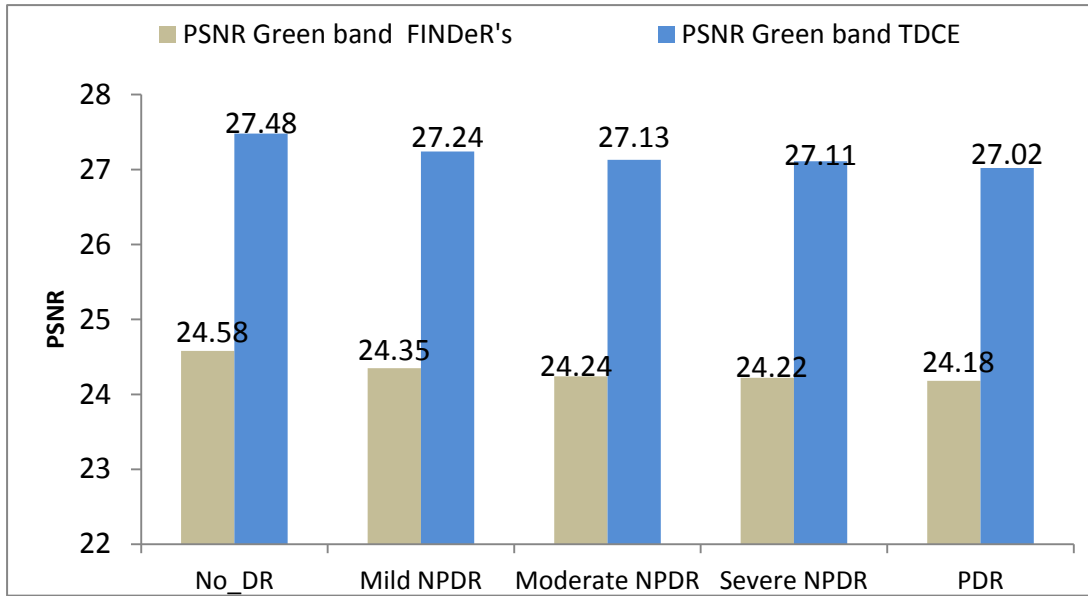


Figure 4.21 Analysis based on TDCE

Figure 4.22 shows the results obtained before and after using Wiener filter for denoising. An average PSNR of 25.14dB for the Wiener Filtered denoised images is obtained resulting in an average PSNR improvement of 0.83db.

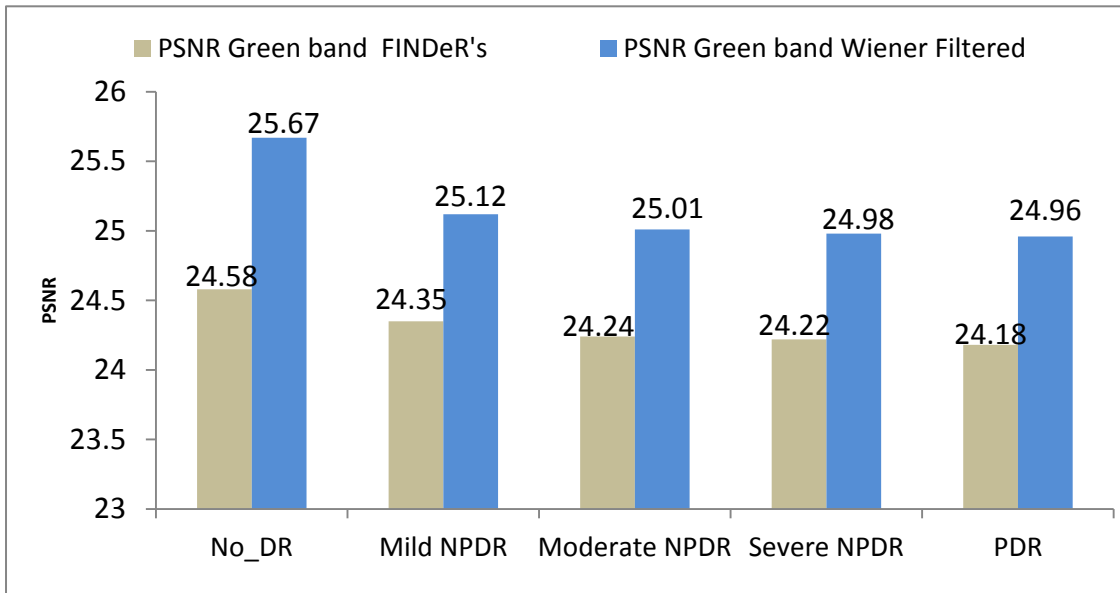


Figure 4.22 Analysis based on Wiener Filter

Using the SWT approach, the average PSNR of 26.13dB is obtained for the SWT denoised images. A PSNR improvement of 1.82dB for the fundus images is achieved. Figure 4.23 shows the average PSNR for each DR category before and after denoising.

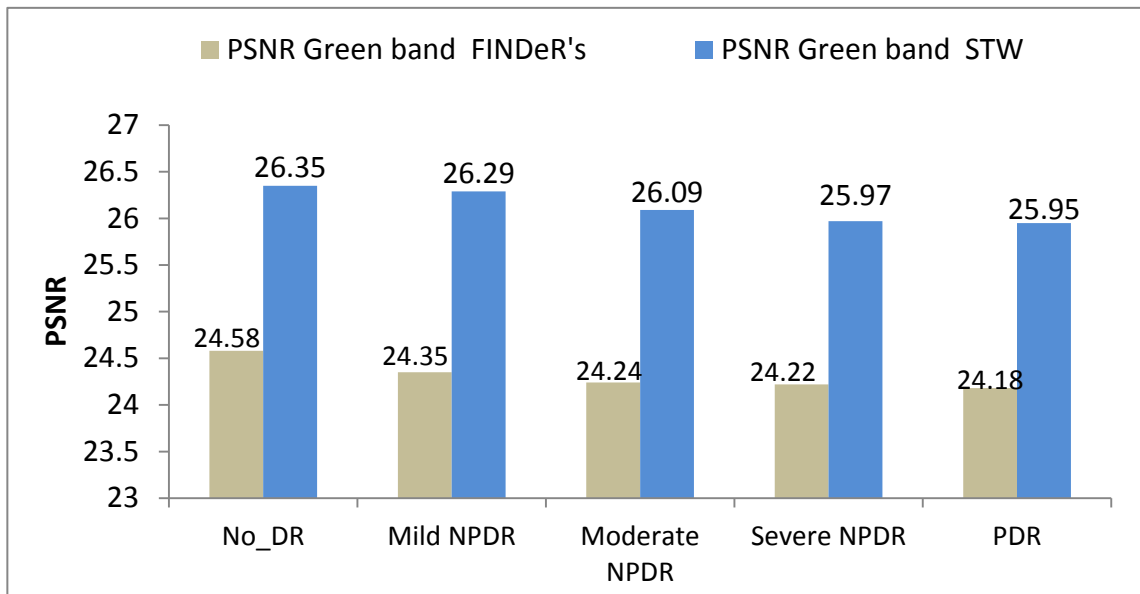


Figure 4.23 Analysis based on SWT

Referring to the results in Figure 4.24, an average PSNR of 26.13dB is obtained for the LSE denoised image, i.e. an average improvement of PSNR of 1.86dB.

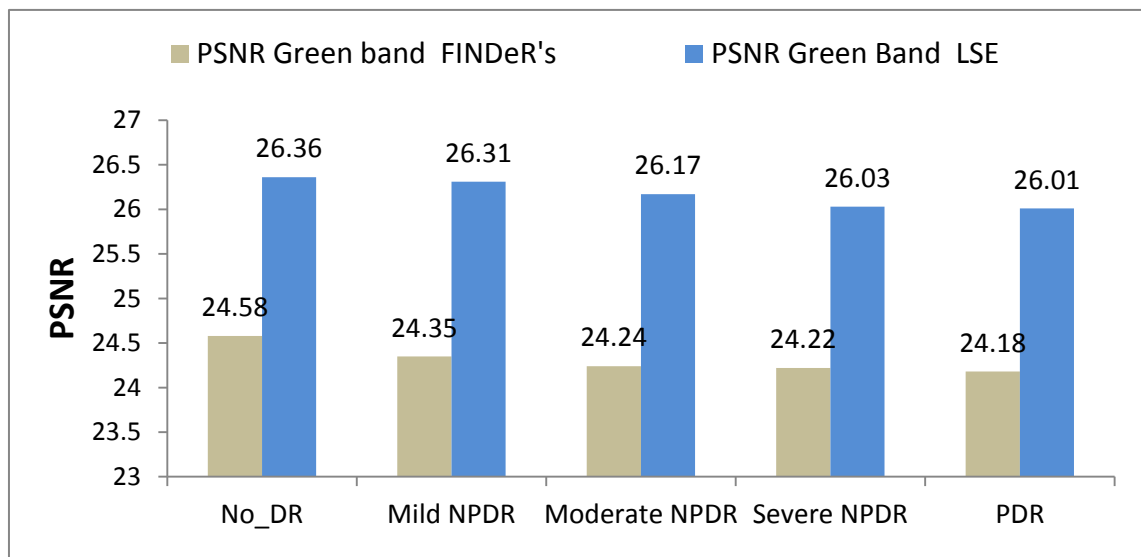


Figure 4.24 PSNR Analysis based on LSE

Referring to results in Figure 4.25, the Minimum Variance Estimator (MVE) used to denoised the fundus image resulted in average PSNR of 26.02dB. There is an overall average improvement of PSNR of 1.71dB.

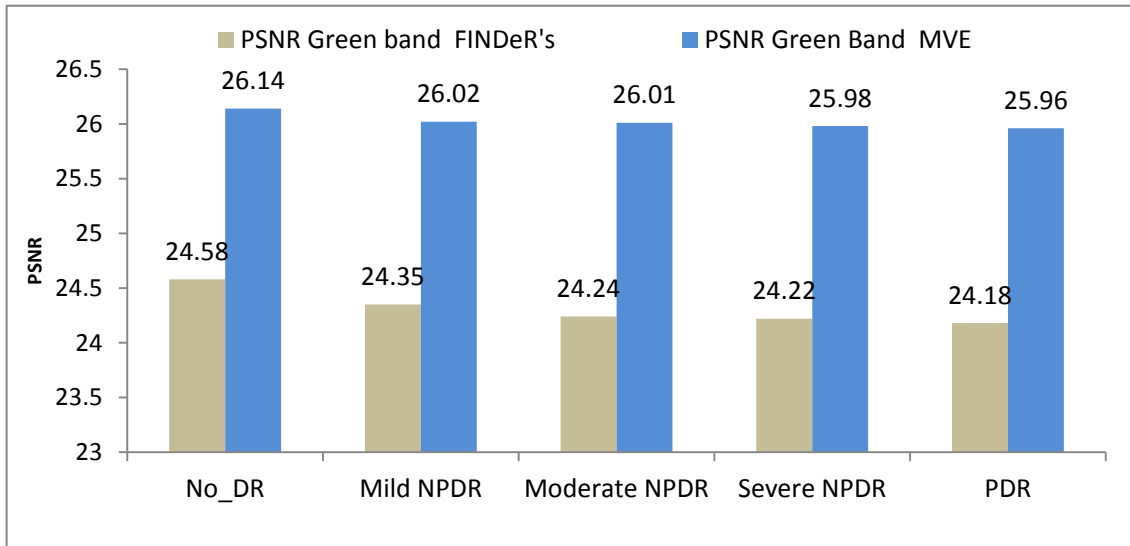


Figure 4.25 Analysis based on MVE

Based on the analysis of PSNR improvement of various methods used for denoising images in the FINDeRS database as shown in Figure 4.26, it is found that the TDCE provided the best performance, improving PSNR by 2.88dB.

Figure 4.27 presents a two sample retinal fundus images (green band) with their corresponding denoised images for various denoising methods. There is less PSNR improvement achieved with MVE (Image 1:1.74dB and Image 2:1.65dB) as compared to the LSE improvement of PSNR (Image 1:1.79dB and Image 2:1.73dB). TDCE provided an even greater improvement of PSNR (Image1:2.68db and Image 2:2.72dB) as compared to the improvement of PSNR achieved by LSE and MVE. Amongst all of the denoising techniques, the best performance on the retinal images is obtained with TDCE. This is because it is able deal with the noise level and caused no loss of the details of the image.

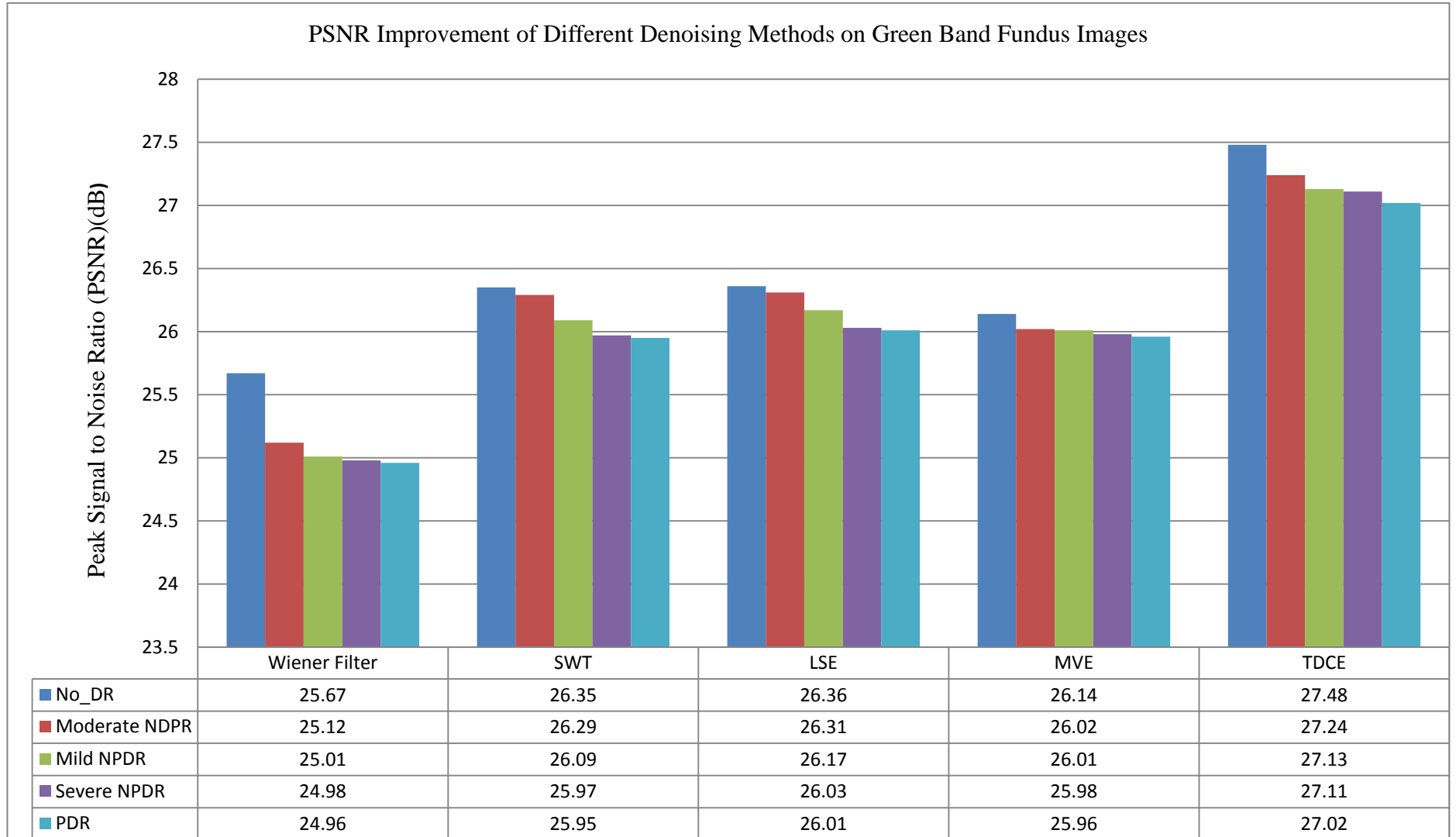


Figure 4.26 PSNR Improvement of Different Denoising Methods on Green band Fundus Images


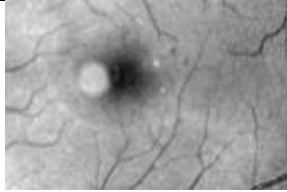



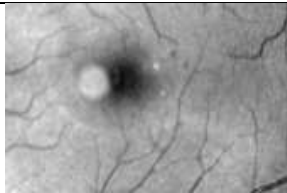






DR-Stages	Image 1	Image 2
Green Band	 PSNR : 24.35db	 PSNR : 24.46db
Wiener Filter	 PSNR : 25.01db	 PSNR : 25.09db
LSE	 PSNR: 26.14db	 PSNR : 26.19db
MVE	 PSNR:26.09db	 PSNR : 26.11db
TDCE	 PSNR:27.03db	 PSNR : 27.18db
SWT	 PSNR:26.06db	 PSNR : 26.12db

Figure 4.27 Analysis of Selected Images

4.4 Results and Analysis of Improving the SNR of the Fundus Image

According to the analysis of the two databases (Refer section 4.2) it is observed that FINDeRS database gives a 3dB lower PSNR as compared to the 35-Fundus database. It is hypothesised that noise may reduce the contrast of the image because the 35-fundus database has a higher PSNR and contrast improvement factor as compared to the PSNR and contrast improvement factor of FINDeRS database. This is validated by the improved the PSNR of the FINDeRS database around the 3dB by using TDCE as the denoised methods and then processing with RETICA to observe their contrast improvement factor (Refer section 3.4.5 of Chapter 3 on improving the SNR of the Fundus Image).

The PSNR of the FINDeRS database has been improved by applying the linear sub-space time domain constraint estimator (TDCE) (described in section 2.7)

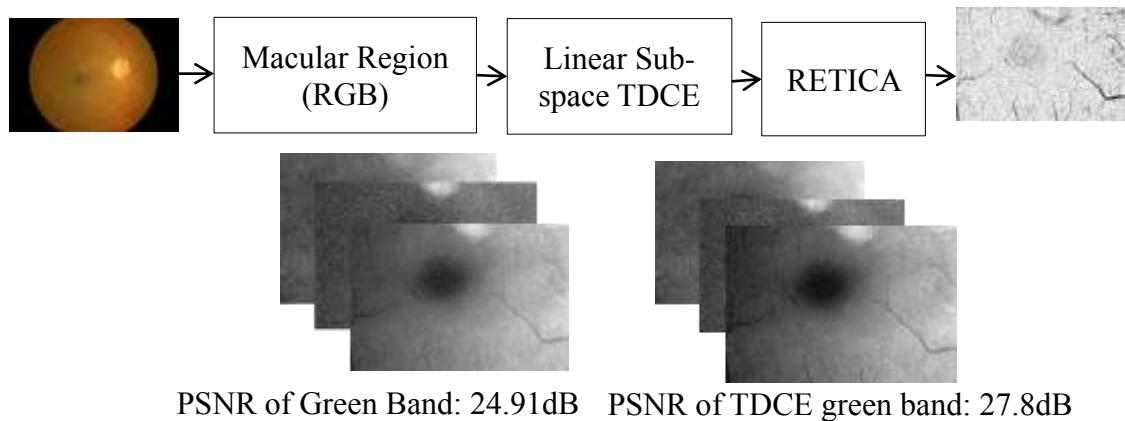


Figure 4.28 Modified RETICA

Considering Figure 4.28, the macular region of the colour fundus image was selected and converted into three colour channels. Each channel is processed in the linear sub-space time domain constraint estimator (TDCE). The output image of the sub-space TDCE is processed through RETICA to achieve the contrast improvement

factor of the final enhanced image. The PSNR of the green band image of the FINDeRS database is 24.91dB and TDCE is applied on the green band image; it gives the improved PSNR of 27.8dB. It gives the PSNR improvement of 2.89dB. It is expected that with improved PSNR of the FINDeRS database, the contrast improvement factor can be increased.

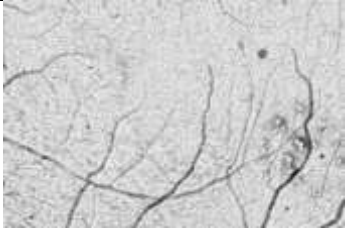
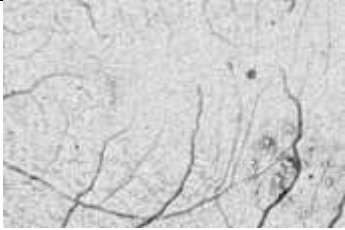
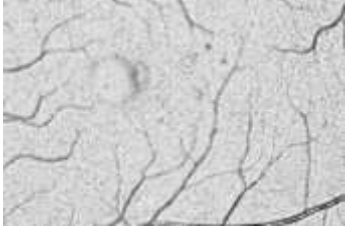
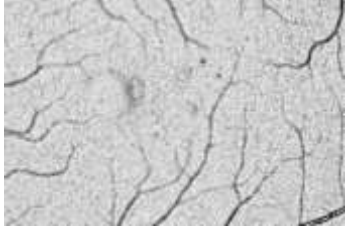
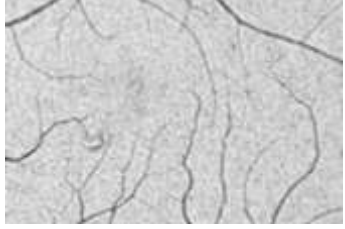
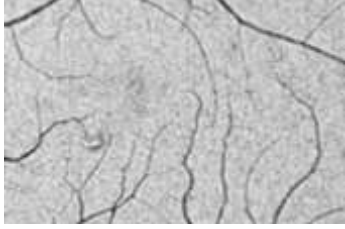
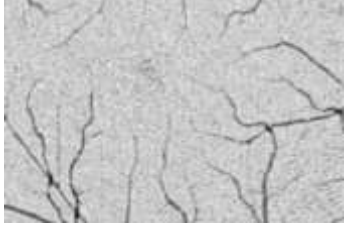
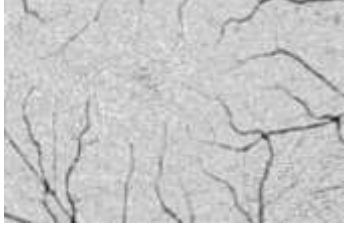
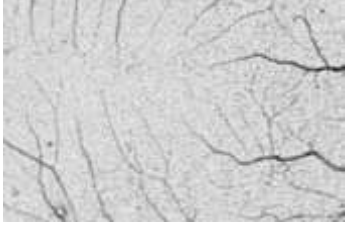
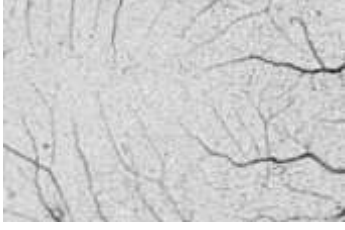
DR-Stages	RETICA Method	TDCE + RETICA Method
No_DR		
Mild NPDR		
Moderate NPDR		
Severe NPDR		
PDR		

Figure 4.29 Comparison of RETICA Image and Modified RETICA

After improving the PSNR of the fundus images in FINDeRS database using TDCE, the images are processed by RETICA. The performance is evaluated by measuring the achieved contrast improvement factor. Figure 4.29 shows sample green band images of the enhanced image due to RETICA only and enhanced image of RETICA image with improved SNR using TDCE. With TDCE, RETICA resulted in better visualisation of tiny capillaries as seen from Figure 4.29.

Referring to Figure 4.30, the PSNR of the FINDeRS database at every stage of DR has been improved up to 2.88dB by applying the sub-space TDCE on the green band image and it is almost equal to the PSNR of the 35-Fundus database.

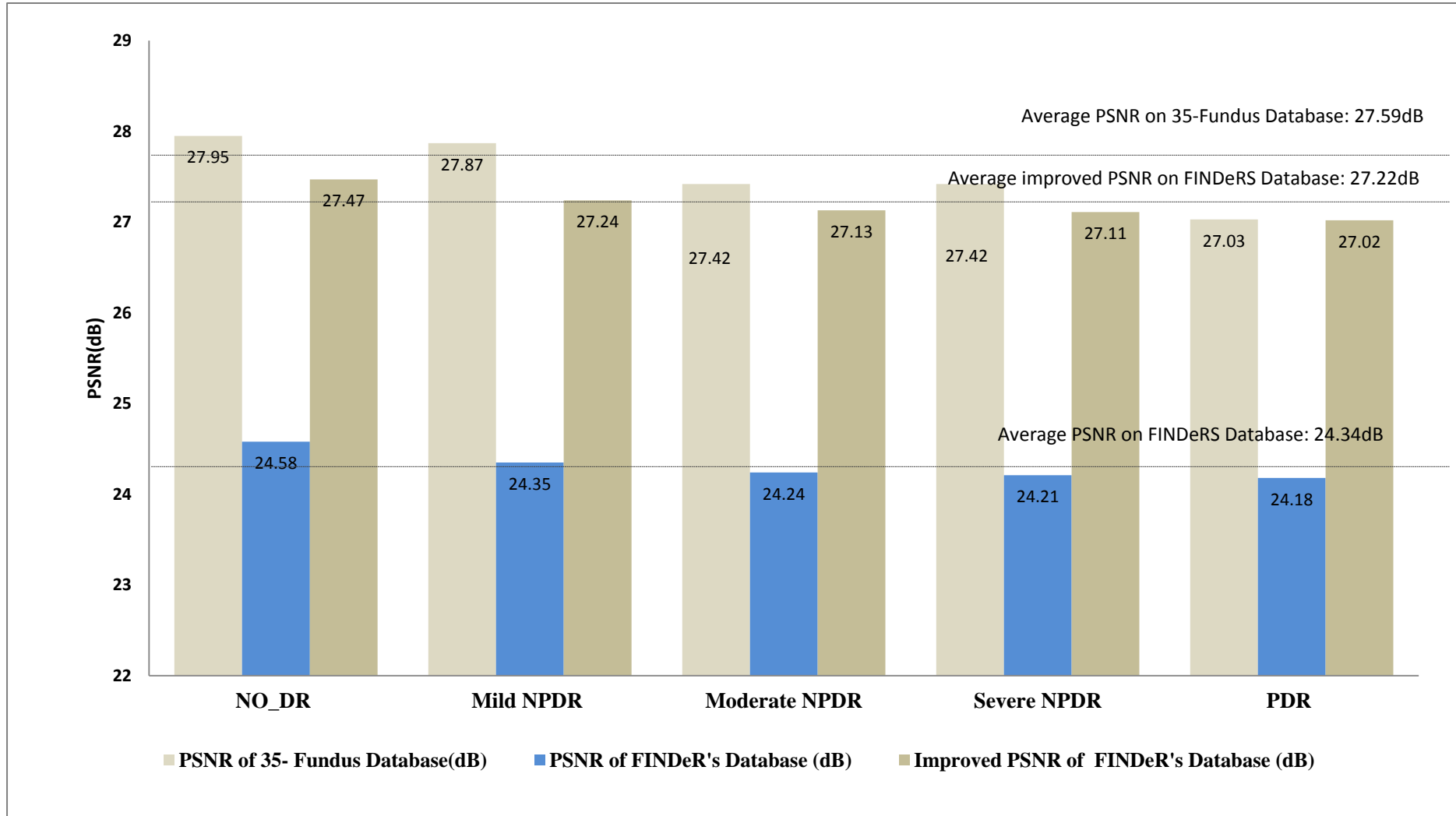


Figure 4.30 Comparisons between PSNR of Improved FINDER's Database and PSNR of 35-Fundus Database

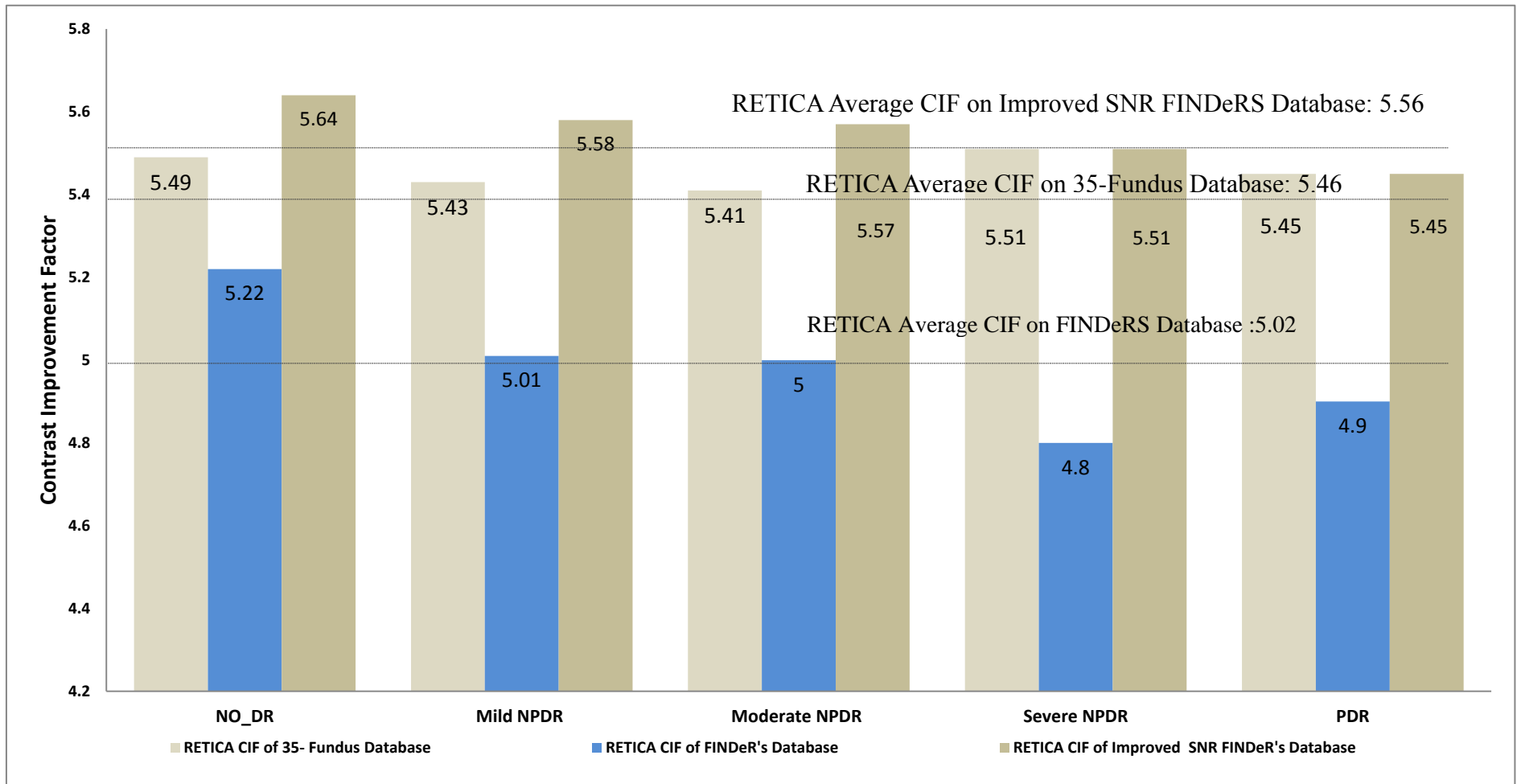


Figure 4.31 Comparison between CIF of Improved FINDER's Database and CIF Of 35- Fundus Database

As seen from Figure 4.31, the contrast improvement factor of the FINDeRS database has been increased to almost equal to the 35-Fundus dataset. The average contrast improvement factor of the FINDeRS database increased from 5.02 to 5.56 and is slightly higher than average contrast improvement factor of 5.46 of the 35-Fundus dataset as shown in Figure 4.31.

This analysis clearly shows that by improving the PSNR of the FINDeRS database by around 3db, the contrast improvement factor of 0.54 can be achieved. In the modified image enhancement technique shown in Figure 4.28, the three main problems of retinal fundus images (noise, and varied and low contrast) have been addressed. The noise level has been effectively reduced by TDCE, with RETICA addressing the varied and low contrast problem of the retinal fundus image.

4.4.1 Comparison of the Improved RETICA with other Algorithms

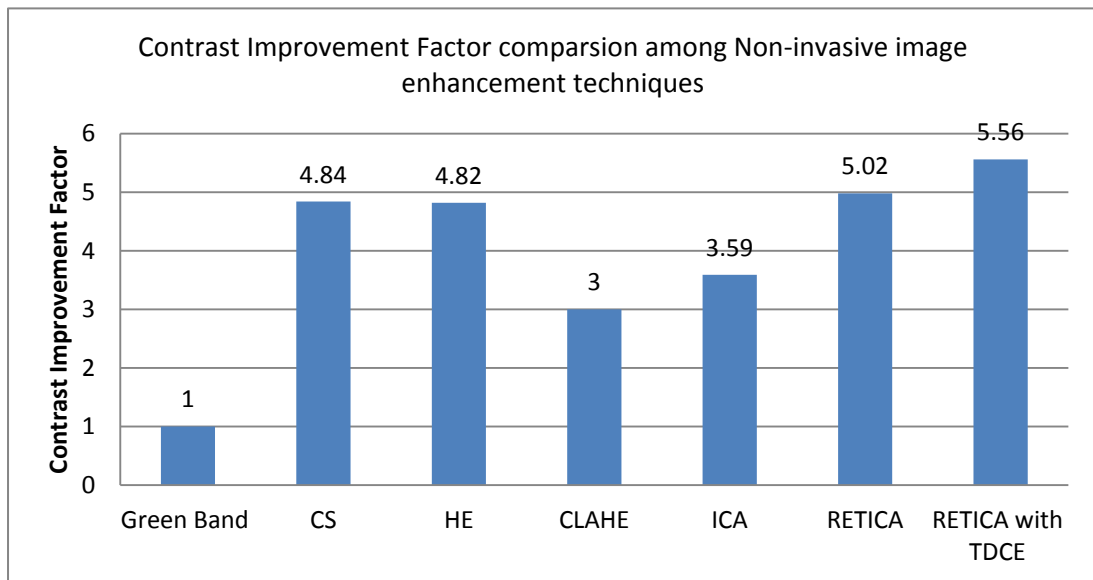


Figure 4.32 Comparison of Contrast Improvement factor among different methods

Referring to Figure 4.32, the comparison amongst different non-invasive digital image enhancement techniques and FFA are shown in terms of the contrast improvement factor. The green band image gave a contrast improvement of 1. The remaining non-invasive digital image enhancement techniques were developed to reduce the problem of varied and low contrast in fundus images. The common enhancement methods, such as Contrast Stretching (CS) and Histogram Equalisation (HE), gave contrast improvement above normal but Contrast Stretching (CS) and Histogram Equalisation (HE) failed to produce a better enhanced image because of the noise that was present in the fundus image. Contrast Limited Adaptive Histogram Equalization (CLAHE) and Independent Component Analysis (ICA) was applied to get better enhanced images. Contrast limited adaptive histogram equalisation (CLAHE) and Independent component Analysis (ICA) gave CIF of above 3, however, they produced artifacts and noise [28].

Analysis of the results of the commonly used non-invasive image enhancement techniques, such as Contrast Stretching (CS), Histogram Equalisation (HE), Contrast Limited Adaptive Histogram Equalization (CLAHE) and Independent Component Analysis (ICA), showed that there should be a requirement for the non-

invasive digital image enhancement technique to handle problems of noise and varying low contrast. Earlier, RETICA is developed by Ahmad Fadzil *et al* [114]. RETICA is played an important role to reduce the use of invasive methods by improving the contrast of the colour fundus image. RETICA achieved a contrast improvement factor of 5.46 in the 35-Fundus database and a contrast improvement factor of 5.02 on the FINDeRS database. After analysis of the results of RETICA, it is observed that the retinal fundus image contained noise and that noise affected the contrast of the image. After improving the SNR of the FINDeRS database through applying the linear sub-space time domain constraint estimator (TDCE), the higher contrast improvement factor of 5.56 is achieved. In summary, image enhancement technique contained RETICA and TDCE is capable to overcome the problem of noise and varying low contrast in the fundus image. Novelty of this proposed technique based on TDCE and RETICA for retinal fundus image is handled noise level (TDCE handles the noise level of the fundus images) and overcome the problem of varying low contrast (RETICA has the potential to overcome the problem of the varied and low contrast of the retinal fundus images). It has a fair potential to reduce the need for invasive fundus fluorescein angiogram (FFA) methods in DR assessment as well as other such methods that pose other physiological problems.

4.5 Summary

The results of applying RETICA method using fundus images from two databases namely FINDeRS and 35-Fundus, are analysed. The contrast improvement factor of the 35-Fundus database is 5.46, is much better than the contrast improvement factor of the FINDeRS database of 5.02. From the signal-to-noise ratio analysis of the two databases (refer to Figure 4.4), the images in FINDeRS database generally have PSNR values that are 3dB lower compared to the images in the 35-Fundus database for all DR stages. The lower CIF for FINDeRS database in RETICA corresponds to lower PSNR of the images. The 3dB difference indicates either the signal levels of the fundus images in FINDeRS is about half of the signal levels in the 35-Fundus database or the noise levels in FINDeRS are higher as shown in Figure 4.5. Referring to Figure 4.5, the FINDeRS database gave average Signal Energy of

1.42E+09 in comparison to average Signal Energy of 2.30E+09 of the 35-Fundus database. Noise seems to be affecting the performance of RETICA. It is therefore hypothesised that noise affects the contrast of the image and consequently affects RETICA performance in contrast improvement factor. This can be validated by the improving the PSNR of the images in FINDeRS database. However, before attempting to improve PSNR by reducing noise in retinal fundus images, it is necessary to identify first the nature of noise in the images.

The noise identification approach proposed is based on the adaptive wiener filters (additive, multiplicative, and additive plus multiplicative filters). The performance using various filters is evaluated by measuring the PSNR improvement. To identify noise in the fundus image or the Retinex fundus image, three studies has been performed. The PSNR improvements based on the analysis of the three studies prove that the model fundus image, green band fundus images, and the Retinex images contain additive and multiplicative noise. Secondly, noise affects the performance of the RETICA algorithm has been proved from study2 else study 1and 3 related to prove the nature of noise in green band image (Model or real) and Retinex image. It has been observed that the Retinex algorithm also improved the SNR of the image but its performance is affected due to the noise coming from the image modality. In addition, the performance of RETICA (Retinex and ICA) can be improved by improving the SNR of the green band fundus image. The additive and multiplicative noise occurring in the retinal fundus image is due to the fundus camera. Multiplicative noise occurred due to the flash of the fundus camera and the additive noise is due to the camera electronics. Denoising techniques are thus required to improve the SNR green band fundus image for improving the performance of RETICA to achieve higher contrast image.

In the third section, the SNR of the FINDeRS database is improved by around 3dB by applying the time domain constraint estimator (TDCE). Due to improving the SNR of the FINDeRS database (Average PSNR of the FINDeRS database is improved from 24.34dB to 27.22dB), then it process through RETICA. RETICA gives significant performance after improving SNR of FINDeRS database, the contrast improvement factor of the FINDeRS database is increased from 5.02 to 5.56.

The hypothesis is proved successfully that due to noise, the performance of RETICA is affected. The source of noise is the image modality (Fundus camera). The performance of RETICA is improved by improving the SNR of the green band image through TDCE. The Non-invasive image enhancement technique has a fair potential to reduce the need for the invasive fundus fluorescein angiogram method and other such methods which pose other physiological problems.

CHAPTER 5

CONCLUSION AND FUTURE WORK

5.1 Conclusion

It is important to analyse the digital colour fundus image to analyse the eye related disease such as diabetic retinopathy. Colour digital fundus images are obtained by the fundus camera. The analysis of retinal vasculature in digital fundus images is significant for diagnosing eye related diseases. However the digital colour fundus images are suffering from low and varied contrast. With the added presence of noise it becomes difficult to analyse retinal vasculature digitally requiring the use of fundus angiogram modality. The fundus fluorescein angiogram (FFA) modality gives 5 to 6 time's higher contrast for the retinal vasculature but it is an invasive method that can lead other physiological problems. In order to avoid using FFA, digital image enhancement techniques are developed to overcome the problem of the varied contrast and low contrast of retinal fundus images, and to obtain the best visualisation of the retinal blood vessels. Hanung *et al* [28] developed an image enhancement technique to overcome the problems of varied and low contrast of fundus images. The developed technique named RETICA has been successfully tested on model retinal fundus images achieving a contrast improvement factor of 5.38. Hanung however did not validate the RETICA technique with real fundus images nor consider the effects of noise levels in fundus images.

RETICA has been validated on real digital colour fundus images in this research work using two databases namely 35-Fundus and FINDeRS databases. The 35-Fundus database contains 35 colour fundus images with corresponding FFA images. For this database, RETICA gives a better average contrast improvement factor of 5.46 as compared to a contrast improvement factor 5.12 of FFA images. The

FINDeRS database contains 175 colour fundus images of various DR severities in which there are 50 No_DR, 40 Mild NPDR, 30 Moderate NPDR, 18 Severe NPDR and 37 PDR images. For this database, RETICA gives a contrast improvement factor of 5.02. The lower CIF performance of RETICA for the FINDeRS database is found to be due to noise inherent in colour fundus images as well as the images generally having lower signal energies. Signal-to-noise ratio consequently affects RETICA performance and thus, it is necessary to identify the nature of noise in the images and to reduce the noise.

The second objective is related to the noise identification approach. The noise identification approach proposed is based on the adaptive wiener filters (additive, multiplicative, and additive plus multiplicative filters). The performance using various filters is evaluated by measuring the PSNR improvement. To identify noise in the fundus image or the Retinex fundus image, three studies has been performed. The PSNR improvements based on the analysis of the three studies showed that the model fundus image, green band images from real fundus images, and Retinex images contain additive and multiplicative noise. Secondly, noise affects the performance of the RETICA algorithm. It has been observed that the Retinex algorithm also improved the SNR of the image but its performance is affected due to the noise coming from the image acquisition modality. The additive and multiplicative noise occurring in the retinal fundus image is due to the fundus camera. Multiplicative noise occurred due to the flash of the fundus camera and the additive noise is due to the camera electronics. In addition, the performance of RETICA (Retinex and ICA) can be improved by raising the SNR of the green band fundus image. Denoising techniques are thus required to improve the SNR green band fundus image.

The third objective is related to the performance of RETICA when noise has been addressed. The SNR of the FINDeRS database is improved by around 3dB by applying the time domain constraint estimator (TDCE). Due to the better SNRs of the FINDeRS database images (average PSNR of the FINDeRS database is improved from 24.34dB to 27.22dB), RETICA achieved a significant performance improvement; the contrast improvement factor of the FINDeRS database is increased from 5.02 to 5.56. The hypothesis that the performance of RETICA is affected by noise levels has been proven true. The proposed technique based on

TDCE and RETICA overcomes the problem of noise (TDCE), varying and low contrast (RETICA) of the retinal fundus images. The proposed technique achieves comparable and better CIF and is thus a better alternative to the invasive fundus fluorescein angiogram (FFA) method in eye and DR assessment. Five major contributions have been achieved from this research work.

1. The validation of the earlier developed non-invasive image enhancement technique RETICA on real fundus images.
2. Comparative study of colour Fundus images (RETICA Images) and FFA images. In the comparative study, the RETICA image gives an average contrast improvement factor of 5.46 as compared to a 5.12 contrast improvement factor of FFA. The RETICA (haemoglobin) image has better contrast.
3. RETICA has been improved by adding the denoising technique linear sub-space time domain constraint estimator (TDCE) before the Retinex Algorithm
4. Proposition of the noise identification techniques based on the image filter with noise estimation models. So far, no researchers have contributed or discussed the noise problems in the colour fundus image. It is a very appreciative achievement in the field of image processing to identify the nature of noise in the fundus image as additive and multiplicative because multiplicative noise occurs due to image modality (Fundus camera).
5. TDCE along with RETICA has overcome the need for the invasive fundus fluorescein angiogram (FFA) method in DR assessment.

5.2 Suggestion for Future Works

For future work, RETICA with linear sub-space TDCE is one of the more proficient techniques for the analysis of the macular region of the retinal fundus image. Research can also be conducted for the implementation of algorithm of the automated segmentation of retinal blood vessels by applying this non-invasive enhancement technique before extraction technique of blood vessels and it may give

more improved accurate detection of retinal vessels end points as compared to previous algorithms. Research can also be conducted using this image enhancement technique before applying pathologies detection techniques because TDCE along with RETICA overcomes three main problems (noise, varied and low contrast) and thus reduce false detection of pathologies. The research can be carried out to incorporate this image enhancement technique in different fundus cameras to reduce the use of the FFA method.

REFERENCES

- [1] T. Etgen, H. Gräfin von Einsiedel, M. Röttinger, K. Winbeck, B. Conrad, and D. Sander, "Detection of Acute Brainstem Infarction by Using DWI/MRI," *European Neurology*, vol. 52, pp. 145-150, 2004.
- [2] A. Agarwal, "fundus fluorescein and indocyanine green angiography " *Thorofare, NJ: SLACK 2008*.
- [3] R. E. Gonzalez, "Digital Image Processing " *Upper Saddle River NJ: Prentice Hall 2008*, 3rd ed.
- [4] <http://www.oculist.net/downat0502/prof/ebook/duanes/pages/v1/v1c063.html>. [Last Accessed 22-06-14, 12:10pm]
- [5] P. Goh, "Status of Diabetic Retinopathy Among Diabetics Registered to the Diabetic Eye Registry, National Eye Database," *The Med Journal of Malaysia*, vol. 63, pp. 24-28, 2007.
- [6] C. Sinthanayothin, V. Kongbunkiat, S. Phoojaruenchanachai, and A. Singalavanija, "Automated screening system for diabetic retinopathy," in *Image and Signal Processing and Analysis, 2003. ISPA 2003. Proceedings of the 3rd International Symposium on*, 2003, Vol.2 pp. 915-920.
- [7] M. Niemeijer, B. van Ginneken, M. J. Cree "Retinopathy Online Challenge: Automatic Detection of Microaneurysms in Digital Color Fundus Photographs," *Medical Imaging, IEEE Transactions on*, vol. 29, pp. 185-195, 2010.
- [8] Peritoneal Dialysis Malaysia, "Clinical Practice Guidelines (CPG) Management of Type 2 Diabetes Mellitus," *Ministry of Health Malaysia, Malaysian Endocrine and Metabolic Society, Academy of Medicine Malaysia*, 2009.
- [9] O. Faust, R. Acharya "Algorithms for the Automated Detection of Diabetic Retinopathy Using Digital Fundus Images: A Review," *Journal of Medical Systems*, pp. 1-13, 2010.
- [10] M. H. Ahmad Fadzil, L. I. Izhar, and H. A. Nugroho, "Determination of foveal avascular zone in diabetic retinopathy digital fundus images," *Computers in Biology and Medicine*, vol. 40, pp. 657-664, 2010.
- [11] M. H. A. Fadzil, H. A. Nugroho, P. A. Venkatachalam, H. Nugroho, and L. I. Izhar, "Determination of Retinal Pigments from Fundus Images using Independent Component Analysis 4th Kuala Lumpur International Conference on Biomedical Engineering 2008.", N. A. Abu Osman, F. Ibrahim, W. A. B. Wan Abas, H. S. Abdul Rahman, H.-N. Ting, and R. Magjarevic, Eds., ed: Springer Berlin Heidelberg, 2008, vol. 21, pp. 555-558.
- [12] M. K. Nair "Digital and Advanced Imaging in Endodontics: A Review," *Journal of Endodontics*, vol. 33, pp. 1-6, 2007.
- [13] U. Vovk, F. Pernus, and B. Likar, "A Review of Methods for Correction of Intensity Inhomogeneity in MRI," *Medical Imaging, IEEE Transactions on*, vol. 26, pp. 405-421, 2007.
- [14] M. Foracchia, E. Grisan, and A. Ruggeri, "Luminosity and contrast normalization in retinal images," *Medical Image Analysis*, vol. 9, pp. 179-190, 2005.
- [15] Ephraim and Van Trees "A comparison between objective and subjective image quality measurements for a full field digital mammography system," *Phys. Med. Biol.*, vol. 51, p. 2441, 2006.

- [16] S. W. Smith, H. Lopez, and W. J. Bodine Jr, "Frequency independent ultrasound contrast-detail analysis," *Ultrasound in Medicine & Biology*, vol. 11, pp. 467-477, 1985.
- [17] H. A. Nugroho, "Non-Invasive Image Enhancement of Colour Retinal Fundus Image for Computerised Diabetic Retinopathy Monitoring and Grading System," *Phd Thesis Electrical and Electronics Engineering Programme*, Universiti Teknologi PETRONAS, 2012.
- [18] Michelson E. Peli, "Contrast in complex images," *Journal of the Optical Society of America A*, vol. 7, pp. 2032-2040, 1990/10/01 1990.
- [19] N. M. Salem and A. K. Nandi, "Novel and adaptive contribution of the red channel in pre-processing of colour fundus images," *Journal of the Franklin Institute*, vol. 344, pp. 243-256, 2007.
- [20] S.Kuo and J. D. Johnston, "Spatial noise shaping based on human visual sensitivity and its application to image coding," *Image Processing, IEEE Transactions on*, vol. 11, pp. 509-517, 2002.
- [21] Ahmad Fadzil M Hani, Toufique Ahmed Soomro, Ibrahima Faye, Nidal Kamel, Norashikin Yahya, "Identification of Noise in the Fundus Images," *IEEE International Conference on Control System, Computing and Engineering*, 2013.
- [22] S. Aja-Fernandez, R. Estepar, C. Alberola-Lopez, and C. F. Westin, "Image Quality Assessment based on Local Variance," in *Engineering in Medicine and Biology Society, 2006. EMBS '06. 28th Annual International Conference of the IEEE*, 2006, pp. 4815-4818.
- [23] P. A. Van den Elsen and M. A. Viergever, "Medical image matching-a review with classification," *Engineering in Medicine and Biology Magazine, IEEE*, vol. 12, pp. 26-39, 1993.
- [24] L. A. Yannuzzi, K. T. Rohrer, "Fluorescein angiography complication survey," *Ophthalmology*, vol. 93, pp. 611-617, 1986.
- [25] A. Long, A. Lepoutre, E. Corbillon, and A. Branchereau, "Critical review of non- or minimally invasive methods (duplex ultrasonography, MR- and CT-angiography) for evaluating stenosis of the proximal internal carotid artery," *European journal of vascular and endovascular surgery : the official journal of the European Society for Vascular Surgery*, vol. 24, pp. 43-52, 2002.
- [26] M. Folke, L. Cernerud, M. Ekström, and B. Hök, "Critical review of non-invasive respiratory monitoring in medical care," *Medical and Biological Engineering and Computing*, vol. 41, pp. 377-383, 2003/07/01 2003.
- [27] Christos M. Michail, "Non-invasive and quantitative near-infrared haemoglobin spectrometry in the piglet brain during hypoxic stress, using a frequency-domain multidistance instrument," *Phys. Med. Biol.*, vol. 46, p. 41, 2001.
- [28] H. A. Nugroho, "Non-Invasive Image Enhancement of Colour Retinal Fundus Image for Computerised Diabetic Retinopathy Monitoring and Grading System," *Phd Thesis Electrical and Electronics Engineering Programme*, Universiti Teknologi PETRONAS, 2012.
- [29] B. Funt, F. Ciurea, and J. McCann, "Retinex in MATLAB™," *Journal of Electronic Imaging*, vol. 13, pp. 48-57, 2004.
- [30] A. Hyvarinen, E., , "Independent Component analysis: algorithms and applications,," *Neural Networks*, vol. 13, 2000.

- [31] A. K. khurana "Ophthalmology " *New Age Publishers,ISBN:8122414710*, 2003.
- [32] O. Faust, R. Acharya and J. Suri, "Algorithms for the Automated Detection of Diabetic Retinopathy Using Digital Fundus Images: A Review," *Journal of Medical Systems*, vol. 36, pp. 145-157, 2012/02/01 2012.
- [33] M. Ahmad Fadzil, L. Izhar, H. Nugroho, and H. Nugroho, "Analysis of retinal fundus images for grading of diabetic retinopathy severity," *Medical and Biological Engineering and Computing*, vol. 49, pp. 693-700, 2011.
- [34] A.Marrugo and M. S. Millán, "Retinal image analysis: preprocessing and feature extraction," *Journal of Physics: Conference Series*, vol. 274, p. 012039, 2011.
- [35] G. Zahlmann, B. Kochner, D. Schuhmann, B. Liesenfeld, A. Wegner "Hybrid fuzzy image processing for situation assessment [diabetic retinopathy]," *Engineering in Medicine and Biology Magazine, IEEE*, vol. 19, pp. 76-83, 2000.
- [36] C. Sinthanayothin, J. F. Boyce, T. H. Williamson, H. L. Cook, E. Mensah, S. Lal., "Automated detection of diabetic retinopathy on digital fundus images," *Diabetic Medicine*, vol. 19, pp. 105-112, 2002.
- [37] M. Niemeijer, B. van Ginneken, J. Staal, M. S. A. Suttorp-Schulten, and M. D. Abramoff, "Automatic detection of red lesions in digital color fundus photographs," *Medical Imaging, IEEE Transactions on*, vol. 24, pp. 584-592, 2005.
- [38] G. K. Matsopoulos, N. A. Mouravliansky, K. K. Delibasis, and K. S. Nikita, "Automatic retinal image registration scheme using global optimization techniques," *Information Technology in Biomedicine, IEEE Transactions on*, vol. 3, pp. 47-60, 1999.
- [39] J. T. Wu, "Review of diabetes: Identification of markers for early detection, glycemic control, and monitoring clinical complications," *Journal of Clinical Laboratory Analysis*, vol. 7, pp. 293-300, 1993.
- [40] W. Huan, W. Hsu, G. Kheng Guan, and L. Mong Li, "An effective approach to detect lesions in color retinal images," in *Computer Vision and Pattern Recognition, 2000. Proceedings. IEEE Conference on*, 2000, vol.2, pp. 181-186.
- [41] <http://medweb.bham.ac.uk/easdec/eyetextbook/dminternet.htm>. [Last Accessed 22-06-14, 12:10pm]
- [42] G. Patrick J. Saine and Marshall E. Tyler "fluorescein and Icg Angiography," *Thieme medical publisher* vol.3 ISBN 0865777128, 1998.
- [43] J. Conrath, R. Giorgi, D. Raccah, and B. Ridings, "Foveal avascular zone in diabetic retinopathy: quantitative vs qualitative assessment," *Eye*, vol. 19, pp. 322-326, 07/16/2004.
- [44] N. Collins, "Diabetic Retinopathy preferred practice pattern " *American Academy of ophthalmology*, 2003.
- [45] M. J. C. Herbert F.Jelinek, "Automated Image Detection of Retinal Pathology," *CRC Press Taylor and Francis Group (Book)*. .
- [46] P. Kahai, K. R. Namuduri, and H. Thompson, "Decision support for automated screening of diabetic retinopathy," in *Signals, Systems and Computers, 2004. Conference Record of the Thirty-Eighth Asilomar Conference on*, 2004, Vol.2, pp. 1630-1634.

- [47] C. Sinthanayothin, Boyce, J. F., Williamson, T. H., Cook, H. L., Mensah, E., Lal, S., and Usher, D., "Automated detection of diabetic retinopathy on digital fundus images. *Diabetic Medicine* 19 (2002),," pp. 105 – 112.
- [48] G. Larsen, J., Grunkin, M., Lund-Andersen, H., and Larsen, M. , " "Automated detection of diabetic retinopathy in a fundus photographic screeningpopulation.,"" *Invest Ophthalmol Vis Sci.*, Feb;44(2), vol. 10, pp. 767-71, 2003
- [49] A Hansen, Hartvig, N. V., Jensen, M. S., Borch-Johnsen, K., Lund- Andersen, H., and Larsen, M. , "Diabetic retinopathy screening using digital non-mydriatic fundus photography and automated image analysis. ," *Acta Ophthalmologica Scandinavica* 82 (2004).
- [50] D. Usher, Dumskyj, M., Himaga, M., Williamson, T. H., Nussey, S., and Boyce, J., "Automated detection of diabetic retinopathy in digital retinal images: a tool for diabetic retinopathy screening.," *Diabetic Medicine* 21(2003), 84 –90.
- [51] L.ABaudoin CE, Klein JC., "Automatic detection of microaneurysms in diabetic fluorescein angiography," *Computers And Biomedical Research* vol. 27, pp 254-61. (1995-96).
- [52] T. Spencer, Olson, J. A., Mchardy, K. C., Sharp, P. F., and Forrester, J. V., "An image-processing strategy for the segmentation and quantification of microaneurysms in fluorescein angiograms of the ocular fundus," *Computers And Biomedical Research* vol. 29 pp. 284 – 302., (1996).
- [53] T. Walter, J. C. Klein, P. Massin, and A. Erginay, "A contribution of image processing to the diagnosis of diabetic retinopathy-detection of exudates in color fundus images of the human retina," *Medical Imaging, IEEE Transactions on*, vol. 21, pp. 1236-1243, 2002.
- [54] G. Gardner, Keating, D., Williamson, T. H., and Elliott, A. T., "Automatic detection of diabetic retinopathy using an artificial neural network: a screening tool.," *British Journal of Ophthalmology* 80, (1996),.
- [55] D. Usher, Dumskyj, M., Himaga, M., Williamson, T. H., Nussey, S., and Boyce, J. F., "Automated detection of diabetic retinopathy in digital retinal images: a tool for diabetic retinopathy screening.," *Diabetic Medicine* 21 (2003), 84 –90.
- [56] G. Luo, Chutatape, O., Lei, H., and Krishnan, S. M., "Abnormality detection in automated mass screening system of diabetic retinopathy," *In Proceedings of the IEEE Symposium on Computer-Based Medical Systems (CBMS2001)* (2001), pp. 132 – 137.
- [57] A. Enrico Grisan, "Segmentation of candidate dark lesions in fundus images based on local thresholding and pixel density.," *In Proceedings of the 29th Annual International Conference of the IEEE Engineering in Medicine and Biology Society (EMBS2007)* (2007),, pp. 6735 – 6738.
- [58] M. Garc'ia, S'anchez, C. I., L'opez, M. I., D'iez, A., and Hornero, R., "Automatic detection of red lesions in retinal images using a multilayer perceptron neural network.," *In Proceedings of the Annual International Conference of the IEEE Engineering in Medicine and Biology Society (EMBS2008)* (2008),, pp. 5425 – 5428.
- [59] X. Zhang, and Chutatape, O., "A svm approach for detection of hemorrhages in background diabetic retinopathy.," *In Proceedings of International Joint Conference on Neural Networks* vol. 4, pp. 2435 – 2440., (2005)
- [60] X. Zhang, and Chutatape, O., "Top-down and bottom-up strategies in lesion detection of background diabetic retinopathy," *In Proceedings of the IEEE Computer Society Conference*

on *Computer Vision and Pattern Recognition (CVPR2005)* . , vol. 2, pp. 422 – 428., (June 2005).

- [61] G. Quellec, Lamard, M., Josselin, P. M., Cazuguel, G., Cochener, B., and Roux, C., "Optimal wavelet transform for the detection of microaneurysms in retina photographs.," *IEEE Transactions On Medical Imaging* 27, pp. 1230 – 1241., 9 (September 2008),.
- [62] G. Quellec, Lamard, M., Josselin, P. M., Cazuguel, G., Cochener, B., and Roux, C., "Detection of lesions in retina photographs based on the wavelet transform," *In Proceedings of the 28th Annual International Conference of the IEEE Engineering in Medicine and Biology Society (EMBS 2006)*, pp. 2619 – 2621, (2006), .
- [63] A. Bhalerao, A. Patanaik, S. Anand, and P. Saravanan, "Robust Detection of Microaneurysms for Sight Threatening Retinopathy Screening," presented at the Proceedings of the 2008 Sixth Indian Conference on Computer Vision, Graphics & Image Processing, 2008.
- [64] B. M. Ege, O. K. Hejlesen "Screening for diabetic retinopathy using computer based image analysis and statistical classification," *Comput Methods Programs Biomed*, vol. 62, pp. 165-175, 07/01 2000.
- [65] P. Pallawala, W. Hsu, M. L. Lee, and S. S. Goh, "Automated Microaneurysm Segmentation and Detection using Generalized Eigenvectors," presented at the Proceedings of the Seventh IEEE Workshops on Application of Computer Vision (WACV/MOTION'05) - Volume 01, 2005.
- [66] M. J. Cree, J. A. Olson, K. C. McHardy, J. V. Forrester, and P. F. Sharp, "Automated microaneurysm detection," in *Image Processing, 1996. Proceedings., International Conference on*, 1996, vol.3, pp. 699-702.
- [67] A. J. Frame, P. E. Undrill "A comparison of computer based classification methods applied to the detection of microaneurysms in ophthalmic fluorescein angiograms," *Computers in Biology and Medicine*, vol. 28, pp. 225-238, 5// 1998.
- [68] J. H. Hipwell, F. Strachan, J. A. Olson, K. C. McHardy, P. F. Sharp, and J. V. Forrester, "Automated detection of microaneurysms in digital red-free photographs: a diabetic retinopathy screening tool," *Diabetic Medicine*, vol. 17, pp. 588-594, 2000.
- [69] G. Yang, Gagnon, L., Wang, S., and Bouche, M.-C, "Algorithm for detecting microaneurysms in low-resolution color retinal images.," *In Proceedings of Vision Interfaces (VI2001)*, pp. 265 – 271., (2001).
- [70] T. Walter, and Klein, J.-C., "Automatic detection of microaneurysms in color fundus images of the human retina by means of the bounding box closing.," *In Medical Data Analysis*, pp. 210–220., (2002),.
- [71] T. Walter and J.-C. Klein, "Automatic Detection of Microaneurysms in Color Fundus Images of the Human Retina by Means of the Bounding Box Closing," in *Medical Data Analysis*. vol. 2526, A. Colosimo, P. Sirabella, and A. Giuliani, Eds., ed: Springer Berlin Heidelberg, 2002, pp. 210-220.
- [72] A.Fleming, Philip, S., Goatman, K. A., Olson, J. A., and Sharp, P. F, "Automated microaneurysm detection using local contrast normalization and local vessel detection.," *IEEE Transactions On Medical Imaging* 25, pp. 1223– 1232, 9 (2006),.
- [73] B. Ege, Hejlesen, O. K., Larsen, O. V., Mller, K., Jennings, B., Kerr, D., and Cavan, D. A., "Screening for diabetic retinopathy using computer based image analysis and statistical classification.," *Computer Methods and Programs in Biomedicine* 62, pp., 165 – 175., (2000).

- [74] Y. Hatanaka, Nakagawa, T., Hayashi, Y., Mizukusa, Y., Fujita, A., Kakogawa, M., and Takeshi Hara, K. K., and Fujita, H., "Cad scheme to detect hemorrhages and exudates in ocular fundus images.," *In Proceedings of the SPIE Medical Imaging 2007: vol. 6514, Computer-Aided Diagnosis (2007)*,.
- [75] Y. Hatanaka, Nakagawa, T., Hayashi, Y., Hara, T., and Fujita, H., "Improvement of automated detection method of hemorrhages in fundus images.," *In Proceedings of the 30th Annual International Conference of the IEEE Engineering in Medicine and Biology Society (EMBS 2008)*, pp. 5429 – 5432., (2008).
- [76] M. Niemeijer, van Ginneken, B., Staal, J., Suttorp-Schulten, M. S. A., and Abramoff, M. D., "Automatic detection of red lesions in digital color fundus photographs.," *IEEE Transactions on Medical Imaging 24*, pp. 584 – 592., 5 (May 2005),.
- [77] H. Wang, Hsu, W., Goh, K. G., and Lee, M. L., "An effective approach to detect lesions in color retinal images," *In Proceedings of the IEEE Computer Society Conference on Computer Vision and Pattern Recognition (CVPR2000)*, vol. 2, pp. 181 – 186., (2000),.
- [78] R. Phillips, Forrester, J., and Sharp, P., " Automated detection and quantification of retinal exudates," *Graefe's Archive for Clinical and Experimental Ophthalmology 231*, 2 (1993), 90 – 94.
- [79] L. Zheng, Chutatape, O., and Shankar, M. K., "Automatic image analysis of fundus photograph.," *In Proceedings of the Annual International Conference of the IEEE Engineering in Medicine and Biology Society (EMBS1997) (1997)*, vol. 2, pp. 524 – 525.
- [80] M. H. Goldbaum, Katz, N. P., Nelson, M. R., and Haff, L. R., "The discrimination of similarly colored objects in computer images of the ocular fundus.," *Investigative Ophthalmology & Visual Science 31* (1990).
- [81] C. Sanchez, Garcia, M., Mayo, A., Lopez, M. I., and Hornero, R., "Retinal image analysis based on mixture models to detect hard exudates.," *Medical Image Analysis 13* (2009), 650658.
- [82] B. M. Ege, Hejlesen, O. K., Larsen, O. V., Miller, K., Jennings, B., Kerr, D., and Cavan, D. A., "Screening for diabetic retinopathy using computer based image analysis and statistical classification.," *Computer Methods and Programs in Biomedicine 62* (2000), pp. 165 – 175.
- [83] M. Niemeijer, Van Ginneken, B., Russell, S. R., and Abramoff, M. S. A. S.-S. M. D., "Automated detection and differentiation of drusen, exudates, and cotton-wool spots in digital color fundus photographs for diabetic retinopathy diagnosis.," *Investigative Ophthalmology and Visual Science 48*, pp. 2260–2267, 5 (2007),.
- [84] T. Walter, and Klein, J.-C., "A computational approach to diagnosis of diabetic retinopathy.," *In Proceedings of the 6th Conference on Systemics, Cybernetics and Informatics (SCI2002) (2002)*, pp. 521 – 526.
- [85] T. Walter, Klein, J.-C., Massin, P., and Erginay, A., "A contribution of image processing to the diagnosis of diabetic retinopathy – detection of exudates in color fundus images of the human retina.," *IEEE Transactions On Medical Imaging 21*, pp. 1236 – 1243., 10 (2002),.
- [86] A. Osareh, "Automated Identification of Diabetic Retinal Exudates and the Optic Disc.," *PhD thesis, Department of Computer Science, University of Bristol, 2004*.
- [87] A. Osareh, Shadgar, B., and Markham, R., "A computational-intelligencebased approach for detection of exudates in diabetic retinopathy images," *IEEE Transactions On Information Technology In Biomedicine 13*, pp. 535 – 545., 4 (2009), .

- [88] K. Ram, and Sivaswamy, J., "Multi-space clustering for segmentation of exudates in retinal color photographs" *In Proceedings of the Annual International Conference of the IEEE Engineering in Medicine and Biology Society (EMBS2009) (2009)*, pp. 1437 – 1440.
- [89] S. J. Ravishankar, A., and Mittal, A., "Automated feature extraction for early detection of diabetic retinopathy in fundus images.," *In Proceedings of the IEEE Computer Society Conference on Computer Vision and Pattern Recognition (CVPR2009) (2009)*, pp. 210 – 217.
- [90] G. Gardner, Keating, D., Williamson, T. H., and Elliott, A. T., "Automatic detection of diabetic retinopathy using an artificial neural network: an screening tool.," *British Journal of Ophthalmology 80 (1996)*, 940 – 944.
- [91] L. Xu, and Luo, S., "Support vector machine based method for identifying hard exudates in retinal images.," *In Proceedings of the IEEE Youth Conference on Information, Computing and Telecommunication (YC-ICT2009) (2009)* pp. 138 –141., (2009).
- [92] M. V. Ibañez and A. Simó, "Bayesian detection of the fovea in eye fundus angiographies," *Pattern Recognition Letters*, vol. 20, pp. 229-240, 1999.
- [93] R.G.H.Bresnick, S.Syrjala,M.Palta,A.Groo,K.Korth,A,, "bnormalities of the fovealavascular zone in diabetic retinopathy," *Arch.Ophthalmol*, pp. 1286–1293., 102(9)-(1984)
- [94] G. Richard, *Fluorescein and ICG angiography : textbook and atlas*, 2nd ed., rev. and expanded ed. Georg Thieme Verlag:: Stuttgart :, 1998.
- [95] M. K. Eladawy, S.M.S.; Elbably, M.; Salem, N.M.A., " "Automatic detection and measurement of foveal avascular zone,"" *Radio Science Conference, 2003. NRSC 2003. Proceedings of the Twentieth National , vol., no., pp.K3,1-7, 18-20 March 2003.*
- [96] L. B. Izhar, "Analaysis of Retinal Vasculature and Foveal Avascular Zone For Grading Of Diabetic Retinopathy," *M.Sc Thesis,Electrical and Electronic Engineering Universiti Teknologi PETRONAS Malaysia*, JULY 2006.
- [97] R. Guillemaud and M. Brady, "Estimating the bias field of MR images," *Medical Imaging, IEEE Transactions on*, vol. 16, pp. 238-251, 1997.
- [98] T. O. Ozanian and R. Phillips, "Enhancement of fluoroscopic images with varying contrast," *Computer Methods and Programs in Biomedicine*, vol. 65, pp. 1-16, 2001.
- [99] D. Tomažević, B. Likar, and F. Pernuš, "Comparative evaluation of retrospective shading correction methods," *Journal of Microscopy*, vol. 208, pp. 212-223, 2002.
- [100] A. Salvatelli, G. Bizai, G. Barbosa, B. Drozdowicz, and C. Delrieux, "A comparative analysis of pre-processing techniques in colour retinal images," *Journal of Physics: Conference Series*, vol. 90, p. 012069, 2007.
- [101] B. M. Dawant, A. P. Zijdenbos, and R. A. Margolin, "Correction of intensity variations in MR images for computer-aided tissue classification," *Medical Imaging, IEEE Transactions on*, vol. 12, pp. 770-781, 1993.
- [102] J. P. Oakley and B. L. Satherley, "Improving image quality in poor visibility conditions using a physical model for contrast degradation," *Image Processing, IEEE Transactions on*, vol. 7, pp. 167-179, 1998.
- [103] L. Kubecka, J. Jan, and R. Kolar, "Retrospective Illumination Correction of Retinal Images," *International Journal of Biomedical Imaging*, vol. 2010, 2010.

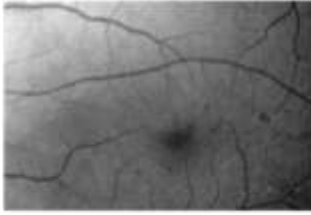
- [104] J. G. Sled, A. P. Zijdenbos, and A. C. Evans, "A nonparametric method for automatic correction of intensity nonuniformity in MRI data," *Medical Imaging, IEEE Transactions on*, vol. 17, pp. 87-97, 1998.
- [105] E. H. Land and J. J. McCann, "Lightness and Retinex Theory," *Journal of The Optical Society of America*, vol. 61, 1971.
- [106] S. M. Pizer, J. D. Austin, R. Cromartie, A. Geselowitz, B. t. H. Romeny, J. B. Zimmerman "Algorithms For Adaptive Histogram Equalization," pp. 132-138, 1986.
- [107] E. Pisano, S. Zong, B. Hemminger "Contrast Limited Adaptive Histogram Equalization image processing to improve the detection of simulated spiculations in dense mammograms," *Journal of Digital Imaging*, vol. 11, pp. 193-200, 1998/11/01 1998.
- [108] Y. Xu, J. B. Weaver, D. M. Healy, Jr., and J. Lu, "Wavelet transform domain filters: a spatially selective noise filtration technique," *Image Processing, IEEE Transactions on*, vol. 3, pp. 747-758, 1994.
- [109] J. Frankle and J. McCann, "*Method and apparatus for lightness imaging*" *Journal of Electronic Imaging*, vol 8 pp 201-12, 1983.
- [110] R. Sobol, "Improving the Retinex algorithm for rendering wide dynamic range photographs," *Journal of Electronic Imaging*, vol. 13, pp. 65-74, 2004.
- [111] Y. Jin, L. M. Fayad, and A. F. Laine, "Contrast enhancement by multiscale adaptive histogram equalization," *Journal of Electronic Imaging*, vol. 06, pp. 206-213, 2001.
- [112] E. H. Land and J. J. McCann, "Lightness and Retinex Theory," *J. Opt. Soc. Am.*, vol. 61, pp. 1-11, 1971.
- [113] P. H. King, K. Hubner, W. Gibbs, and E. Holloway, "Noise Identification and Removal in Positron Imaging Systems," *Nuclear Science, IEEE Transactions on*, vol. 28, pp. 148-151, 1981.
- [114] C. Timothy J, "The Effects of Gain and Noise in Fundus Autofluorescence Imaging," *The Journal of Ophthalmic Photography* vol. 29, 2007.
- [115] X. Zhou, C. Zhou, and B. G. Stewart, "Comparisons of discrete wavelet transform, wavelet packet transform and stationary wavelet transform in denoising PD measurement data," in *Electrical Insulation, 2006. Conference Record of the 2006 IEEE International Symposium on*, 2006, pp. 237-240.
- [116] M. E. Peli, "Contrast in complex images," *J. Opt. Soc. Am. A*, vol. 7, pp. 2032-2040, 10/01 1990.
- [117] C. Yixin and M. Das, "An automated technique for image noise identification using a simple pattern classification approach," in *Circuits and Systems, 2007. MWSCAS 2007. 50th Midwest Symposium on*, 2007, pp. 819-822.
- [118] P. Hansen, "Signal subspace methods for speech enhancement," Ph.D Thesis,, *Technical University of Denmark*, 1997.
- [119] Y. Ephraim and H. L. V. Trees, "'A signal subspace approach for speech enhancement,'" *IEEE Trans. Speech Audio Process.*, , vol. 3,, pp. . 251-266, , 1995.

- [120] Nidal Kamel, N. S. Yahya, Aamir S. Malik, , "Subspace-based technique for speckle noise reduction in SAR images," " *accepted for publication in IEEE Trans. Geosci. Remote Sens.*, 2013.
- [121] D. Brunet, E. Vrscay, and Z. Wang, "The Use of Residuals in Image Denoising," in *Image Analysis and Recognition*. vol. 5627, M. Kamel and A. Campilho, Eds., ed: Springer Berlin Heidelberg, 2009, pp. 1-12.
- [122] D. L. Donoho, "De-noising by soft-thresholding," *Information Theory, IEEE Transactions on*, vol. 41, pp. 613-627, 1995.
- [123] S. Jha and R. D. S. Yadava, "Denoising by Singular Value Decomposition and Its Application to Electronic Nose Data Processing," *Sensors Journal, IEEE*, vol. 11, pp. 35-44, 2011.
- [124] M. Fan and A. L. Tits, "Toward a structure singular value decomposition," in *Decision and Control, 1987. 26th IEEE Conference on*, 1987, pp. 1742-1743.
- [125] M. Moonen, P. v. Dooren, and J. Vandewalle, "A singular value decomposition updating algorithm for subspace tracking," *SIAM J. Matrix Anal. Appl.*, vol. 13, pp. 1015-1038, 1992.
- [126] T. Konda and Y. Nakamura, "A new algorithm for singular value decomposition and its parallelization," *Parallel Comput.*, vol. 35, pp. 331-344, 2009.
- [127] H. Patterson, "Singular value decompositions and digital image processing," *IEEE Trans. on Acoustics, Speech, and Signal Processing*, , vol. ASSP-24, pp. 26–53, 1976.
- [128] Julie L. Kamm, " "SVD-Based Methods For Signal And Image Restoration". *PhD Thesis (1998). Emory University United States.*
- [129] B.Konstantinides and G.S. Yovanof, "Noise Estimation and Filtering Using Block-Based Singular Value Decomposition," *IEEE Trans. Image Processing*, , vol. 6, pp. 479- 483,, March 1997.
- [130] L. Gorodetski, V. Samoilov, and V.A. Skormin, "SVD-Based Approach to Transparent Embedding Data into Digital Images," *Proc. Int. Workshop on Mathematical Methods, models and Architecture for Computer Network Security, Lecture Notes in Computer Science*, vol. 2052, Springer Verlag, 2001.
- [131] K. Baker, "Singular Value Decomposition Tutorial,' *Proc. Int. Workshop on Mathematical Methods, models and Architecture for Computer Network Security, Lecture Notes in Computer Science*, vol. 2052, Springer Verlag, 2001.
- [132] W. C. Mitchell and D. L. McCraith, "Heuristic analysis of numerical variants of the Gram-Schmidt orthonormalization process," Stanford University 1969.
- [133] E. Haykin, " Adaptive Filter Theory. ," *NJ: Prentice-Hall*, 1991.
- [134] N. S. Yahya, N. Kamel, and A. S. Malik, "Subspace-based technique for image denoising," in *National Postgraduate Conference (NPC), 2011*, 2011, pp. 1-5.
- [135] L. Jong-Sen, "Digital Image Enhancement and Noise Filtering by Use of Local Statistics," *Pattern Analysis and Machine Intelligence, IEEE Transactions on*, vol. PAMI-2, pp. 165-168, 1980.

APPENDIX A

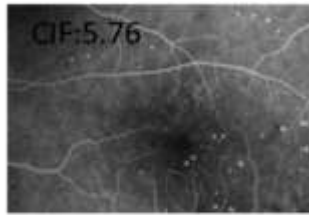
35-FUNDUS DATABASE

Green Band Image



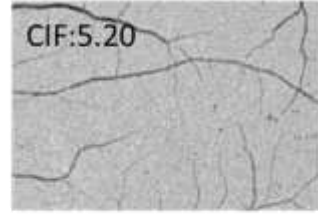
Contrast: 7.1

FFA Image

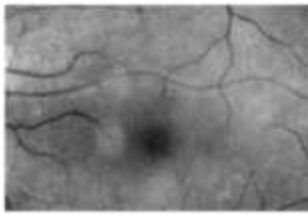


Contrast: 40.9

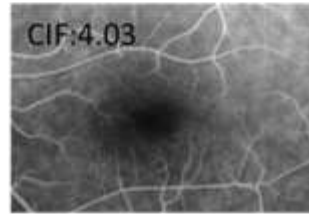
Enhanced Image



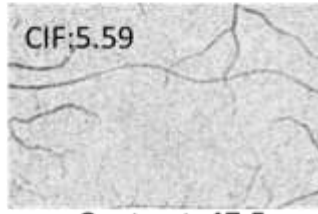
Contrast: 36.9



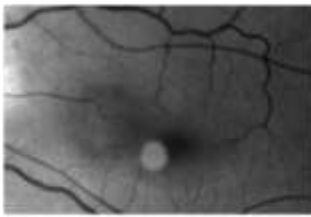
Contrast: 8.5



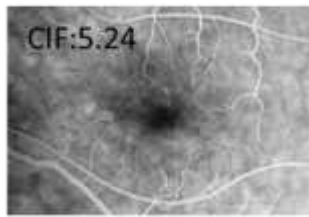
Contrast: 34.3



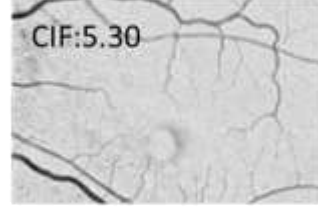
Contrast: 47.5



Contrast:9.1



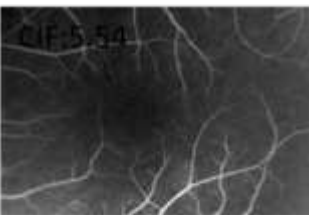
Contrast: 47.7



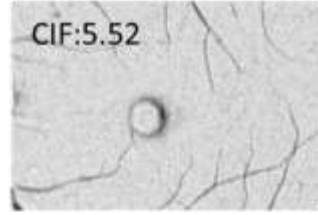
Contrast: 48.2



Contrast: 6.4



Contrast: 34.9



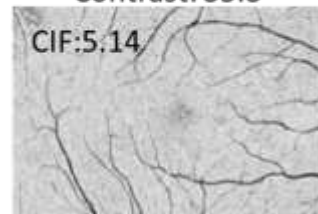
Contrast: 35.3



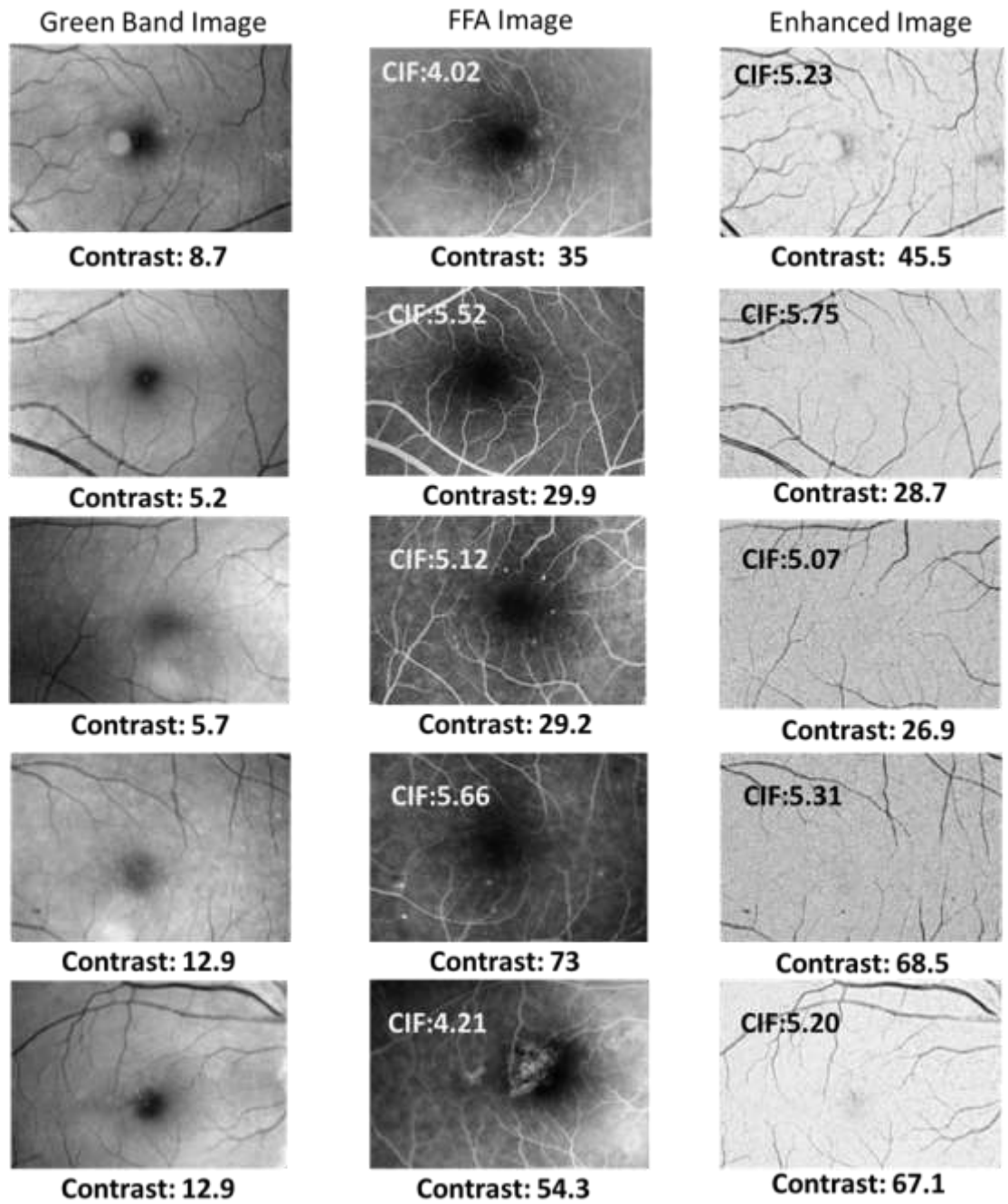
Contrast: 11.7

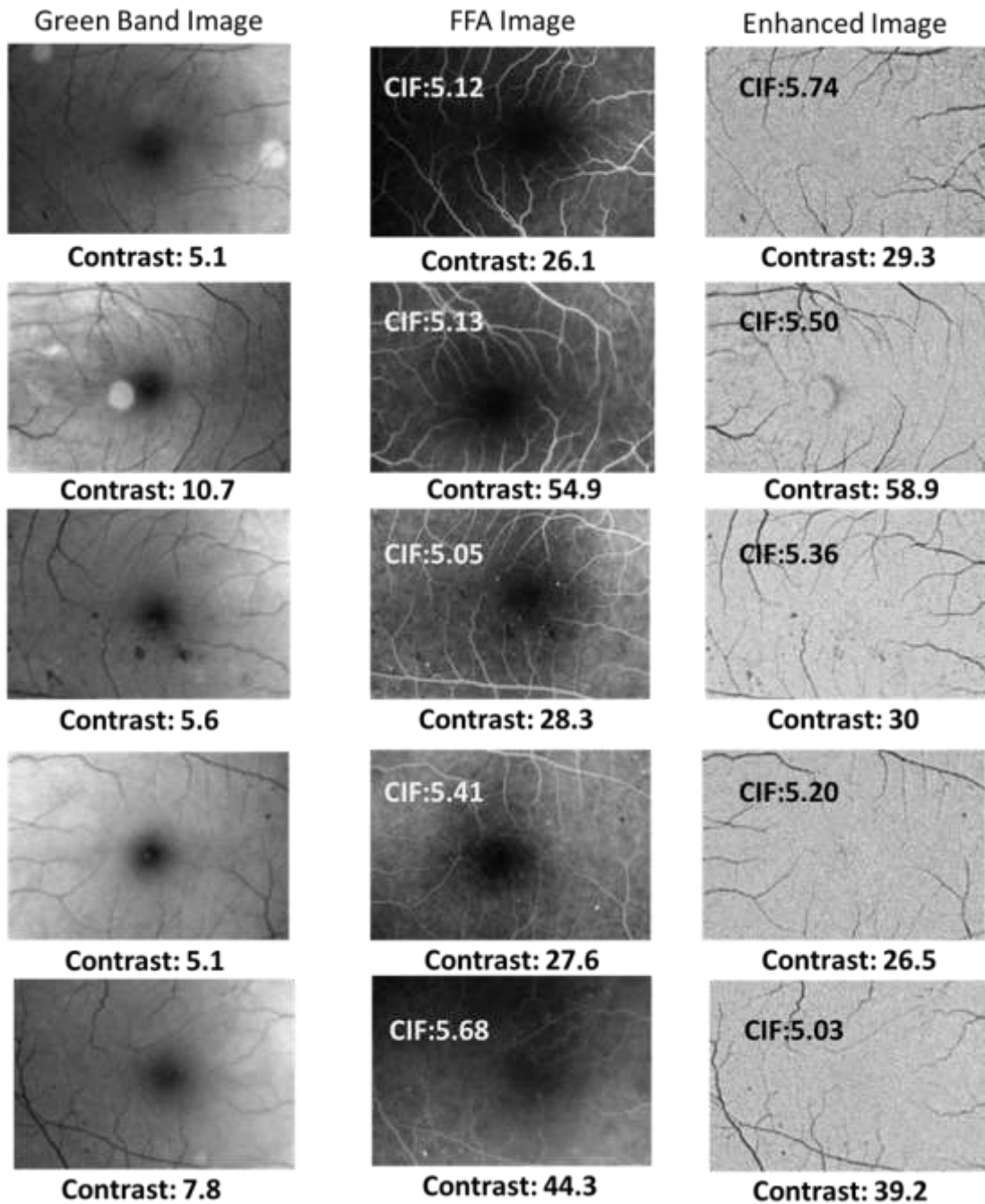


Contrast: 53.3

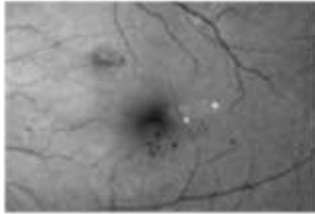


Contrast: 60.1

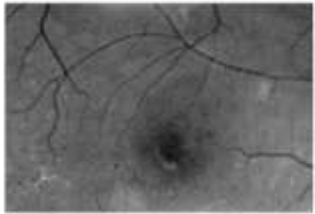




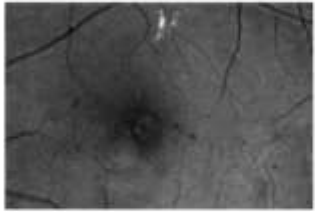
Green Band Image



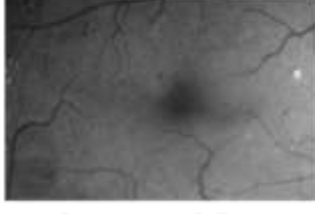
Contrast: 9.3



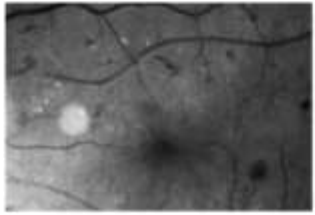
Contrast: 14.2



Contrast: 9.9

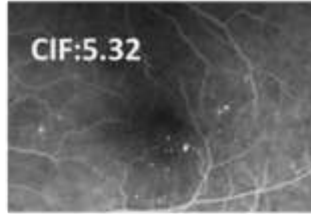


Contrast: 6.5

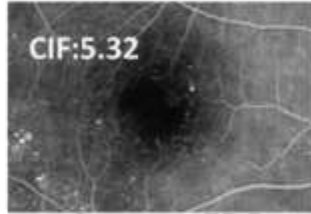


Contrast: 5.1

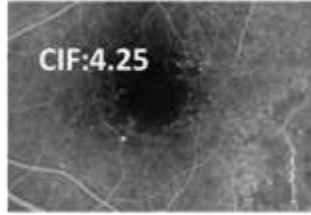
FFA Image



Contrast: 49.5



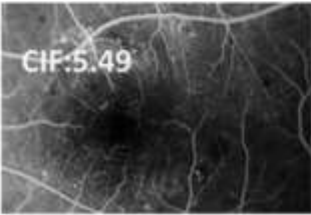
Contrast: 75.5



Contrast: 42.1

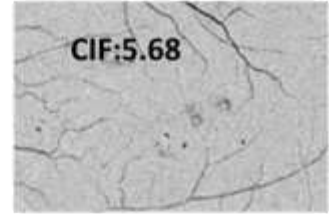


Contrast: 34.9

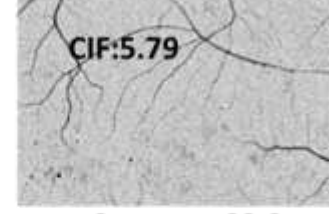


Contrast: 27.9

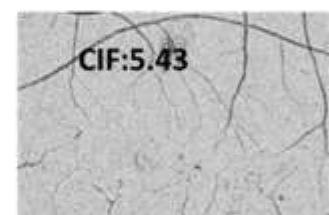
Enhanced Image



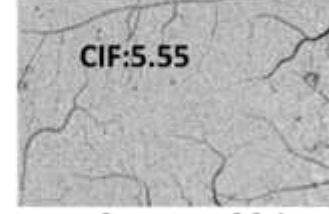
Contrast: 52.8



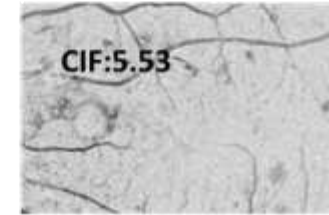
Contrast: 82.2



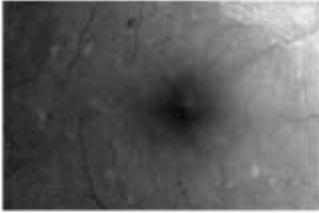

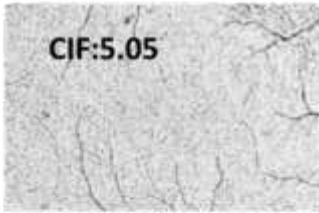
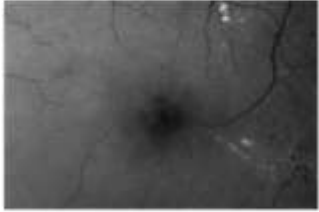
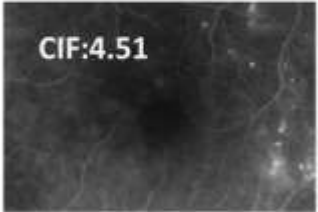
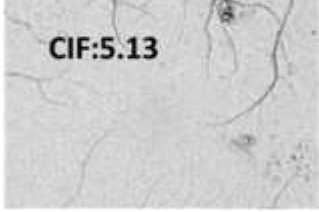
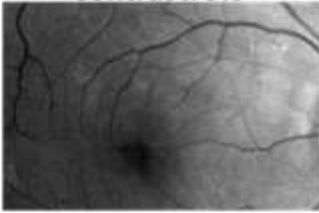
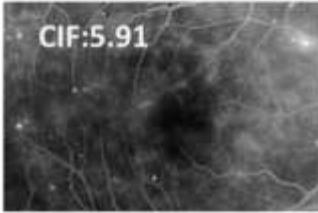

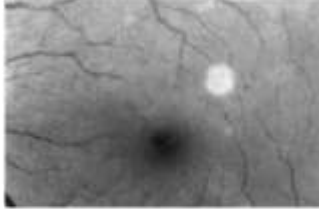


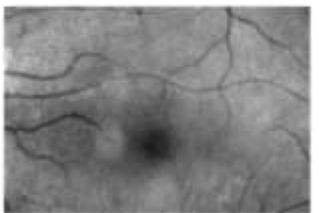
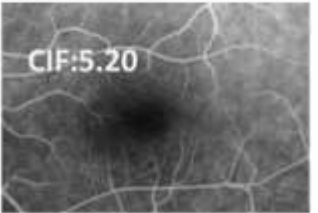
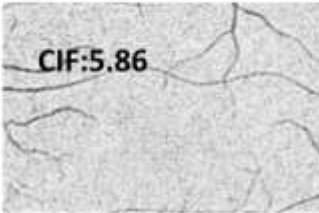
Contrast: 53.8



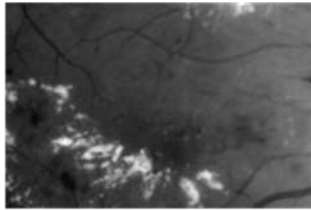
Contrast: 36.1



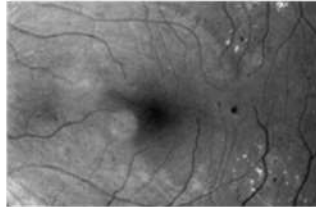
Contrast: 28.2

Green Band Image	FFA Image	Enhanced Image
 Contrast: 6.3	 CIF:5.08 Contrast: 32	 CIF:5.05 Contrast: 31.8
 Contrast: 9.5	 CIF:4.51 Contrast: 42.8	 CIF:5.13 Contrast: 48.7
 Contrast: 4.6	 CIF:5.91 Contrast: 27.2	 CIF:5.57 Contrast: 25.6
 Contrast: 15.8	 CIF:5.53 Contrast: 87.3	 CIF:5.20 Contrast: 82.2
 Contrast: 7.4	 CIF:5.20 Contrast: 38.5	 CIF:5.86 Contrast: 43.4

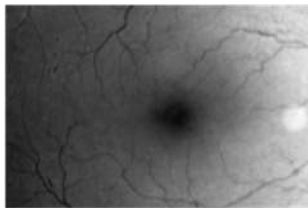
Green Band Image



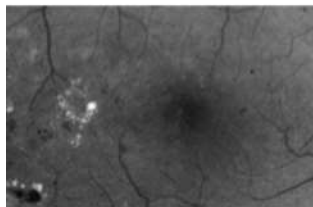
Contrast: 9.6



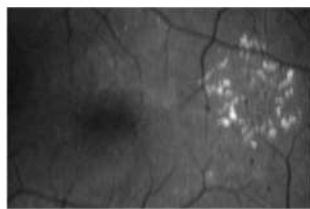
Contrast: 10.8



Contrast: 5.2

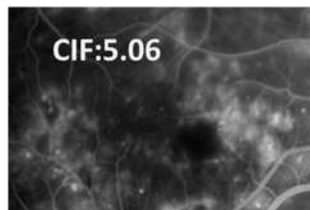


Contrast: 5.2

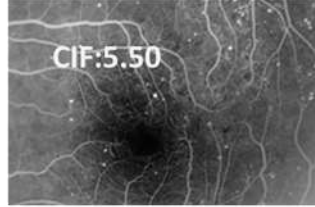


Contrast: 3.9

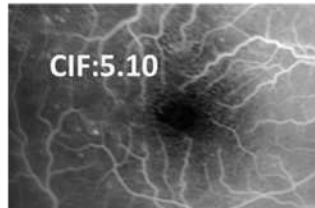
FFA Image



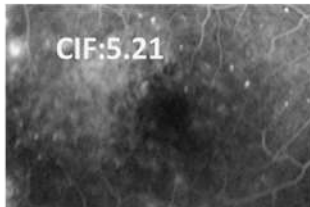
Contrast: 48.6



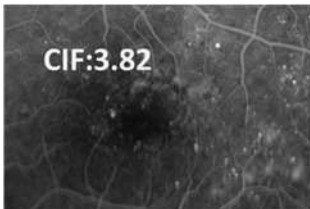
Contrast: 59.4



Contrast: 26.5

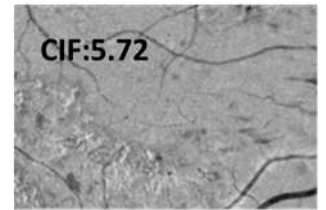


Contrast: 27.1

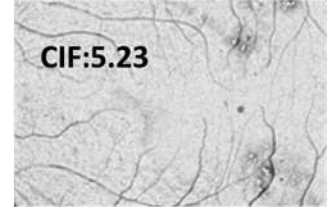


Contrast: 14.9

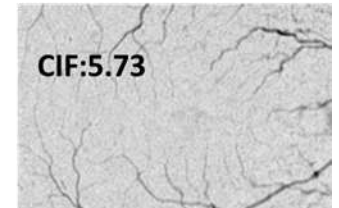
Enhanced Image



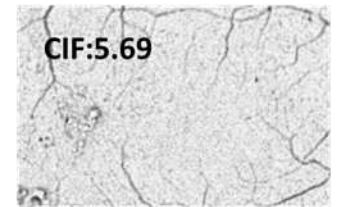
Contrast: 54.9



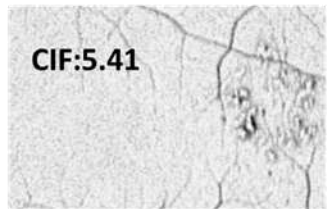
Contrast: 56.5



Contrast: 29.8



Contrast: 29.6

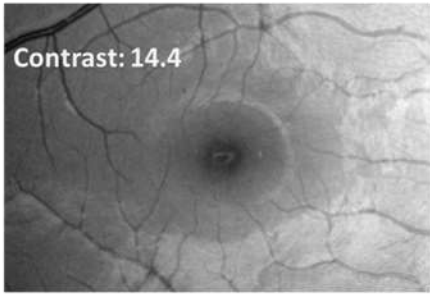
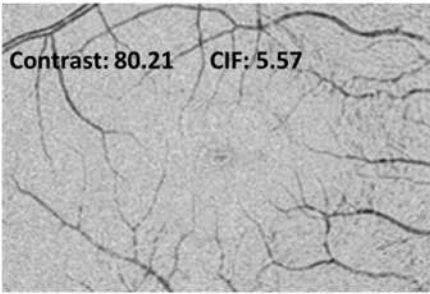
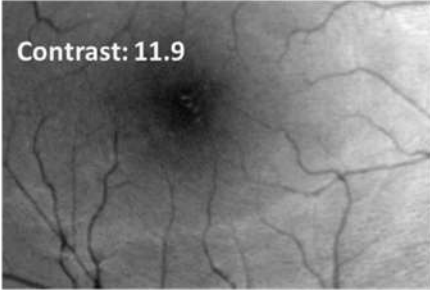
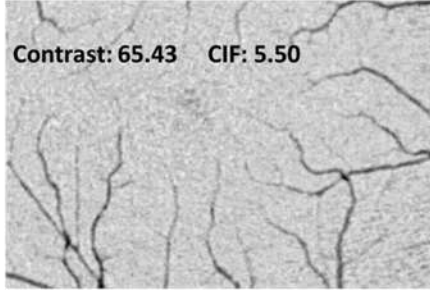
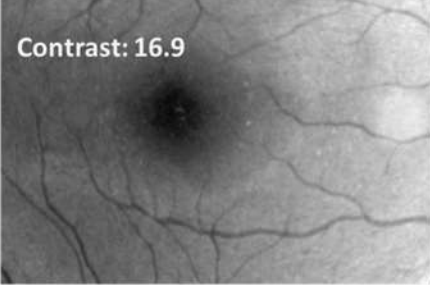
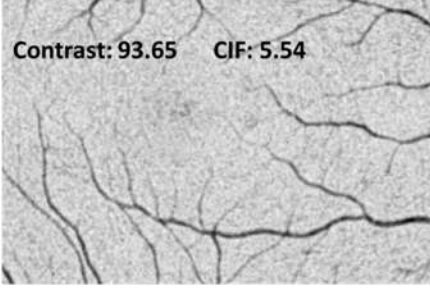
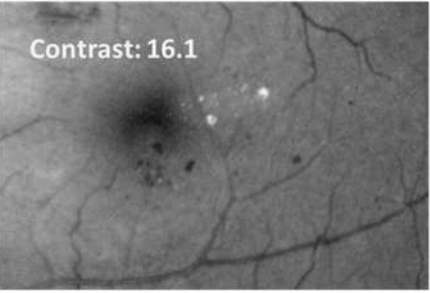
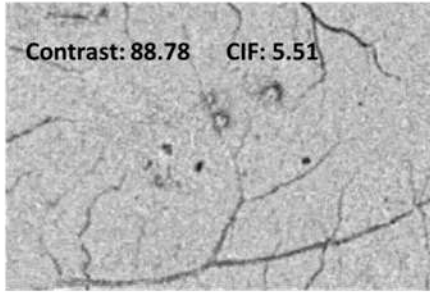

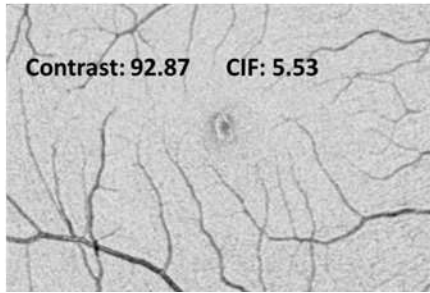


Contrast: 21.1

APPENDIX B

ANALYSIS OF FINDERS DATABASE

APPENDIX B: Analysis of some selected images of FINDeR's database through Non-Invasive Image Enhancement Technique (TDCE along with RETICA).

Green Band Image	Enhanced Image
 <p>Contrast: 14.4</p>	 <p>Contrast: 80.21 CIF: 5.57</p>
 <p>Contrast: 11.9</p>	 <p>Contrast: 65.43 CIF: 5.50</p>
 <p>Contrast: 16.9</p>	 <p>Contrast: 93.65 CIF: 5.54</p>
 <p>Contrast: 16.1</p>	 <p>Contrast: 88.78 CIF: 5.51</p>
 <p>Contrast: 16.8</p>	 <p>Contrast: 92.87 CIF: 5.53</p>

APPENDIX C

LISTS OF PUBLICATIONS AND EXHIBITIONS

Conferences:

1. F. M. Hani, T. Ahmed Soomro, H. Nugroho, and H. A. Nugroho, "**Enhancement of colour fundus image and FFA image using RETICA,**" in *Biomedical Engineering and Sciences (IECBES), 2012 IEEE EMBS Conference on*, 2012, pp. 831-836.
2. Ahmad Fadzil M Hani, Toufique. A. S, Ibrahima Faye, Nidal Kamel,Norashikin Yahya, "**Identification of Noise in the Fundus Images,**" IEEE International Conference on Control System, Computing and Engineering, 2013.
3. Ahmad Fadzil M Hani, Toufique. A. S, Ibrahima Faye, "**Non-Invasive Contrast Enhancement for Retinal Fundus Imaging**" IEEE International Conference on Control System, Computing and Engineering, 2013.
4. Ahmad Fadzil M Hani, Toufique. A. S, Ibrahima Faye, Nidal Kamel,Norashikin Yahya "**Denoising Methods for Retinal Fundus Images**" The 5th International Conference on Intelligent and Advance System, 3rd – 5th June 2014, Kuala Lumpur Convention Centre Malaysia

Exhibitions:

1. **Silver Medal** in Academic and Research Exhibition (**ACADREX 2012**), 19th -21st October 2012, Universiti Teknologi PETRONAS.
2. **Silver Medal** in Science and Engineering Design Exhibition 31 (**SEDEX 31**), 21st -22nd August 2013, Universiti Teknologi PETRONAS.
3. **Bronze Medal** in Science and Engineering Design Exhibition 32 (**SEDEX 32**), 11th -12th Dec 2013, Universiti Teknologi PETRONAS.

APPENDIX D

35-FUNDUS IMAGE AND FINDERS DATABASE

